STUDY OF A SMALL-SCALE COOLING SYSTEM BASED ON AN ICE-STORAGE AND A DC-POWERED VAPOUR COMPRESSION REFRIGERATION UNIT TO IMPLEMENT SOLAR ENERGY IN REMOTE AREAS

Muaz Bedru Hussen

UNIVERSITAT ROVIRA i VIRGILI

STUDY OF A SMALL-SCALE COOLING SYSTEM BASED ON AN ICE-STORAGE AND A DC-POWERED VAPOUR COMPRESSION REFRIGERATION UNIT TO IMPLEMENT SOLAR ENERGY IN REMOTE AREAS

MUAZ BEDRU HUSSEN

DOCTORAL THESIS
2020

STUDY OF A SMALL-SCALE COOLING SYSTEM BASED ON AN ICE-STORAGE AND A DC-POWERED VAPOUR COMPRESSION REFRIGERATION UNIT TO IMPLEMENT SOLAR ENERGY IN REMOTE AREAS

Muaz Bedru Hussen

Muaz Bedru Hussen

STUDY OF A SMALL-SCALE COOLING SYSTEM BASED ON AN ICE-STORAGE AND A DC-POWERED VAPOUR COMPRESSION REFRIGERATION UNIT TO IMPLEMENT SOLAR ENERGY IN REMOTE AREAS

DOCTORAL THESIS

Supervised by

Dr.Ing. - Demiss Alemu Amibe

School of Mechanical & Ind. Engineering

Prof. Alberto Coronas

Department of Mechanical Engineering

UNIVERSITAT ROVIRA i VIRGILI

Tarragona, 2020

STUDY OF A SMALL-SCALE COOLING SYSTEM BASED ON AN ICE-STORAGE AND A DC-POWERED VAPOUR COMPRESSION REFRIGERATION UNIT TO IMPLEMENT SOLAR ENERGY IN REMOTE AREAS

Muaz Bedru Hussen

UNIVERSITAT
ROVIRA i VIRGILI
DEPARTAMENT D'ENGINYERIA MECÀNICA
Escola Tècnica Superior d'Enginyeria Química (ETSEQ).
Avgda Paisos Catalans, 26; 43007 Tarragona (Spain)

Declaration

We STATE that the present thesis, entitled "Study of a small-scale cooling system based on an ice-storage and a DC-powered vapour compression refrigeration unit to implement solar energy in remote areas", presented by Muaz Bedru Hussen for the award of the degree of Doctor, has been carried out under our supervision at the CREVER research group in the Department of Mechanical Engineering of the Rovira i Virgili University, and that it fulfils all the requirements to be eligible for the International Doctorate Award.

Tarragona, October 3rd, 2020

Dr.Ing. Demiss Alemu Amibe

Prof. Alberto Coronas

STUDY OF A SMALL-SCALE COOLING SYSTEM BASED ON AN ICE-STORAGE AND A DC-POWERED VAPOUR COMPRESSION REFRIGERATION UNIT TO IMPLEMENT SOLAR ENERGY IN REMOTE AREAS

Muaz Bedru Hussen

Acknowledgements

I wish to express my deepest gratitude to my supervisor Prof. Dr Alberto Coronas, for allowing me to carry out my PhD studies at the University of Rovira i Virgili. I am very much thankful for his guidance, patience, unconditional support and encouragement during this study. I would like to extend my sincere appreciation to my co-supervisor Dr.Ing Demiss Alemu, who helped me so much throughout the doctoral program.

I would like to express my deepest appreciation and profound gratitude to Prof. Dr Joachim Müller and Dr Victor Torres-Toledo, for their help, discussions and valuable comments during my research stay in their group at the institute of agricultural engineering of the University of Hohenheim, Stuttgart, Germany. I am thankful to all staffs of Tropics and Subtropics research group for their friendly working environment and valuable inputs. I sincerely acknowledge Mrs Sabine Nugent, secretary of Prof. Müller, for her support and kindness. I also acknowledge all the members of solar cooling engineering-UG, a spin-off company of the University of Hohenheim; I had a great time with them developing systems, performing experiments and wonderful moments. Special thanks to Florian Männer, Julian Krüger, Farah Mrabet, Kilian Blumenthal, Ana Salvatera Rojas, Sonja Mettenleiter and Manuel Willahus for sharing ideas and their support on several experimental activities. My gratitude extends to the staff of the metal and wood workshop of the Institute of Agricultural Engineering for their assistance in fabrication of experimental systems.

I gratefully acknowledge the financial support received from Ethiopian Ministry Science and Higher Education and German Academic Exchange Service (DAAD) for funding my research stay in Germany. I also acknowledge the financial support from the Deutsche Gesellschaft für Internationale Zusammenarbeit (GIZ) GmbH during my research work at the Institute of Agricultural Engineering of the University of Hohenheim. My gratitude also extends to Efficiency for Access (EforA) Research and Development Fund from UK Aid and IKEA Foundation for the financial support. I thank Dr Dereje Ayou, all my Ethiopian friends both in Tarragona and in Stuttgart for all the good times we had together. I am also very grateful to my colleagues at Addis Ababa University, Dr Yilma Tadess and Mr. Getasew Ashagre, for all they have done to facilitate my research stay abroad.

My special gratitude goes to my family, my mother Muntaha Adem for her unconditional love and my father Bedru Hussen, for promoting my education. I would like to thank my brothers Mubarek, Fuad, Dr Kenzu, Amir, A.Fetah, and my sisters Amria and Semira. I

would like to thank also my family-in-law, Shemsu Seid, and Mehbuba Shamil for their continuous support and encouragement.

Finally, my special heartfelt thanks belong to my dear wife Kedija Shemsu, sweet children Firdews, Reyan and Muhammed who make me feel so special in my life.

Table of Contents

Acknowledgements iii
List of figures vii
List of tables xi
Summary xiii
Resumen xvii
CONTRIBUTIONS BY THE AUTHOR xxi
Articles in Sientific Journals xxi
Communications in Congresses, Conferences, Seminars, Workshops and Symposia xxi
Mobility/Internships xxi
Participation in projects xxii
Nomenclature xxiii
Chapter 1 Introduction, Objectives, Methodology and Structure of the Thesis 1
1.1 General introduction 1
1.2 Background 4
1.2.1 The ice-storage technology 4
1.2.2 Milk cooling 7
1.2.3 Prospects of the PV Technology 10
1.2.4 Research work on milk cooling in Hohenheim University 12
1.3 Objectives 16
1.4 Methodology and structure of the thesis 18
Chapter 2 Development and Fabrication of the Ice-Storage System 22
2.2 The vapour compression refrigeration unit 23
2.2.1 The heat load calculation for the cabinet and selection of insulation materials 24
2.2.2 Specifications of the cycle components 27
2.2.2.1 Compressor 27
2.2.2.2 Heat exchangers and the capillary tube 29
2.4 Fabrication of the refrigeration unit (the cooling unit) 29
2.5 Fabrication of the ice-storage system 30
2.6 Experimental optimization of the capillary tube length and refrigerant charge 31
2.6.1 Experimental setup 32
2.6.2 Capillary tube vs refrigerant charge 35
2.7 Conclusions 38
Chapter 3 Experimental Setups for Performance Characterizations 40

3.1 Introduction 40
3.2 The ice-making process 41
3.2.1 Measuring the evaporator surface temperature 43
3.2.2 Quantifying the ice mass and the energy stored 44
3.2.3 The DC power supply and energy demand prediction 44
3.2.4 Quantifying the overall system performance 45
3.2.5 Experimental uncertainty analysis 45
3.3 The lateral ice-slab thickness 47
3.3.1 Determining the cold side boundary condition 48
3.3.2 Evaluation of the vertical water temperature 48
3.3.3 The ice slab thickness measurement 49
3.4 The milk cooling and preservation 49
3.4.1 Recirculating water temperature 52
3.4.2 Milk cooling curves 52
3.4.3 Evaluating the milk-cooler preservation performance 52
3.4.4 Determination of milk to energy ratio based on actual and theoretical consumptions 52
3.4.5 Estimation of the milk cooling system capacity with respect to ambient condition and required milk temperatures 54
3.5 External-melt ice discharge with a fan-coil unit as an end-use device 54
3.6 Conclusions 57
Chapter 4 Results Analysis and Discussion 59
4.1 Introduction 59
4.2 Performance of the ice-storage system for varying operating points 60
4.2.1 Temperature distribution on the evaporator surface 60
4.2.2 Daily ice mass-produced and the energy stored 61
4.2.3 System energy demand 62
4.2.4 Coefficient of performance for the ice storage system 66
4.3 Water-ice phase change and ice thickness development 69
4.3.1 Phase front boundary condition temperature range 69
4.3.2 Effect of ambient temperature on sub-cooling before the phase transition 70
4.3.3 Cold side phase change boundary condition temperature range 72
4.3.4 Spatial ice slab temperature distribution indicating the lateral thickness change 75
4.3.5 Relevance of lateral thickness of with ice storage sizing and scale-up 78
4.4 Ice based milk cooling performance 79

4.4.1 Effect of WRR and PF on milk cooling curves 79
4.4.2 Milk-cooler preservation performance 83
4.4.3 Recirculating water temperature variation 84
4.4.4 Energy to milk ratio and the energy transfer effectiveness 86
4.4.5 The milk cooling system capacity range under varying parameters 87
4.4.5.1 Comparisons of experimental and theoretical energy demand of the milk 87
4.4.5.2 The milk cooler capacity variation with final milk temperatures 89
4.5 Ice discharge characteristics with fan-coil-unit as end-use device 90
4.5.1 Effect of fan speed on room air temperature variation 91
4.5.2 Effect of chilled water recirculation rate on FCU exit air temperature 92
4.5.3 Effect of chilled water recirculation rate on water temperature inside ice-storage 92
4.5.4 Effect of fan speed and WRR on water temperature across FCU 93
4.5.5 Overall ice-melting/discharge time 94
4.6 Highlights of major findings 95
4.7 Conclusions 99
Chapter 5 General Conclusions and Future Work 101
5.1 General conclusion 101
5.2 Future work 104
References 107

List of figures

Figure 1. 1 Number and percentage of the population without electricity (2016) [8] 2
Figure 1. 2 Ice lined freezer for cooling application using PV as energy source [9] 2
Figure 1. 3 The ice-maker configuration with four cooling circuits [22] 8
Figure 1. 4 a) PV direct-drive milk chiller array, b) PV-powered chiller using thermal ice storage and brine bags to chill evening milk [50] 9
Figure 1. 5 Schematic of milk chiller for the chilling process [51] 10
Figure 1. 6 Global power capacity by source [55] 11
Figure 1. 7 Refrigerator units operating in ice-making and cooling mode [56] 12
Figure 1. 8 Milk cooling by DC refrigerator to cool down 17 L milk at 4 °C employing 3 kg ice (a) temperature curve (b) current consumption at 12V for 30°C ambient [56] 13
Figure 1. 9 DC-freezer equipped with air circulation fan and 25 ice-cans for a total of 50 kg ice [57] 13

Figure 1. 10 Ice-compartment based milk cooling set-up (a) System components (b) Temperature distributions in an insulated can be loaded with 20 L milk and 8 kg ice [58]..... 14
Figure 1. 11 Configurations for the use of a refrigerator for small-scale milk cooling [58] 15
Figure 1. 12 Proposed schematic diagram of the small-scale cooling system including PV powered ice-storage and flow control loop..... 17

Figure 2. 1 Schematic diagram of the vapour compression refrigeration cycle unit with the insulated box as ice production and storage compartment 22
Figure 2. 2 Schematic and T-s diagram for actual vapour compression refrigeration cycle [60]. 23
Figure 2. 3 The refrigeration cycle unit configuration with insulated compartment 24
Figure 2. 4 Cabinet heat loss vs insulation materials..... 25
Figure 2. 5 Cabinet heat loss vs insulation materials showing equivalence of thickness..... 26
Figure 2. 6 Compressor capacity variations with the maximum run time 28
Figure 2. 7 Picture showing the basic components of the refrigeration cycle unit fabricated..... 30
Figure 2. 8 Pictures from fabrication process in the workshop (a) Cutting, bending and welding of the metal box (b) Fixing insulation to the metal box (c) Assembling VCRC unit with insulated box (d) Functionality testing in a climate chamber..... 31
Figure 2. 9 Schematic of the refrigeration unit showing varying capillary tube lengths and refrigerant charge 33
Figure 2. 10 Pictures of refrigeration units manufactured for testing and evaluation purpose..... 34
Figure 2. 11 Experimental set-up for VCRC unit optimization test 35
Figure 2. 12 Effects of refrigerant charge and capillary tube length on COP 36
Figure 2. 13 Effects of refrigerant charge and capillary tube length on suction line temperature 36
Figure 2. 14 Suction frost observed at evaporator exit and compressor inlet lines for three of the seven scenarios..... 37

Figure 3. 1 Schematic representation of the experimental ice-storage system 41
Figure 3. 2 Pictures of the experimental platform (a) cooling unit showing refrigerant flow pattern and sensor locations on evaporator plate (b) the insulated box filled with water after fixing cooling unit and sensors (c) initiation of the phase change (d) ice formation at the end of daily operation 43
Figure 3. 3 Experimental set up for ice-storage system performance evaluation..... 44

Figure 3. 4 Pictures of ice-storage showing effects of lateral thickness and storage size on ice growth: a) Single evaporator with narrow ice-storage width b) Multiple evaporators with narrower spacing between them..... 47
Figure 3. 5 Schematic of the experimental set-up for phase-change model (sectional view of the ice storage)..... 49
Figure 3. 6 Proposed solar milk cooling schematic..... 50
Figure 3. 7 Schematic of milk cooling experimental setup..... 51
Figure 3. 8 Schematic of ice-storage as applied to cold room/pick load application..... 54
Figure 3. 9 Enthalpy-Temperature relationship graph [66]..... 55
Figure 3. 10 Schematic of the experimental set-up of ice-storage for cold room application..... 57
Figure 3. 11 Pictures from the experiment (a) Ice-storage FCU assembly (b) Internal part of ice-storage (c) Internal section of FCU (d) Representative air temperature profile taken by the infrared camera..... 57

Figure 4. 1 Evaporator surface temperatures vs time at representative locations for lower compressor speed and different ambient temperatures..... 61
Figure 4. 2 Effect of ambient temperatures on evaporator surface temperatures at representative locations at higher compressor speed..... 61
Figure 4. 3 Picture of ice profile on the evaporator surface at different ambient temperatures and compressor speeds at the end of the daily operation..... 62
Figure 4. 4 Typical system power consumption for corresponding compressor speeds..... 63
Figure 4. 5 Effect of ambient temperature and compressor speed on the system power requirement..... 64
Figure 4. 6 Daily energy demands vs ambient temperature..... 65
Figure 4. 7 Ice-storage system performance summaries..... 67
Figure 4. 8 Vertical water temperature (Sub-cooling and phase front boundary condition) vs time in the ice storage for lower compressor speed and different ambient temperatures..... 70
Figure 4. 9 Vertical water temperature (Super-cooling and phase front boundary condition) vs time in ice storage for higher compressor speed and different ambient temperatures..... 72
Figure 4. 10 Cold side surface temperature variations vs time for different ambient temperatures (a) lower compressor speed (b) higher compressor speed..... 74
Figure 4. 11 Temperature distributions across the ice block vs time for different ambient temperatures and lower compressor speed showing ice thickness on the evaporator surface..... 76

Figure 4. 12 Temperature distributions across the ice block vs time for different ambient temperatures and higher compressor speed showing ice thickness on the evaporator surface..... 77
Figure 4. 13 Proposed Schematic of evaporator configuration inside ice storage for scalability concept 78
Figure 4. 14 Picture of ice formed showing complete freezing in a 100-litter capacity insulated box and a single modular unit 79
Figure 4. 15 Transient temperature distribution of milk along vertical axis at milk-can center for different packing factors and chilled water recirculation rates 80
Figure 4. 16 Effect of packing factor and chilled water recirculation rate on average milk temperatures 81
Figure 4. 17 Milk cooling time taken for a fixed packing factor and varying chilled water recirculation rate 82
Figure 4. 18 Milk cooling and preservation characteristics for different packing factors and chilled water recirculation rates 83
Figure 4. 19 Recirculating water temperature variations at the ice-storage and milk-cooler exit points 84
Figure 4. 20 Cumulative energy transferred to the milk-cooler vs recirculation time..... 87
Figure 4. 21 Range of air temperature drop across FCU showing the effect of varying fan speed 91
Figure 4. 22 Effect of chilled water recirculation rate on air temperature drop across FCU..... 92
Figure 4. 23 Effect of chilled water recirculation rate on water-bath temperature in the ice-storage 93
Figure 4. 24 Water temperature variations across FCU during ice discharge 94
Figure 4. 25 Ice and water temperature variations inside ice-storage during discharge..... 95
Figure 4. 26 Pictures from experimental campaign (a) Experimental ice storage system developed (b) DC-powered refrigeration cycle unit fabricated 96
Figure 4. 27 Scaled up ice storage system (a) Arrangement of multiple units in parallel (b) Ice profile on a single evaporator surface within the ice storage..... 97
Figure 4. 28 Application setup of the PV powered ice storage system (a) Milk cooling by chilled water recirculation (b) FCU as end-use device for cold room..... 98

List of tables

Table 1. 1 Comparison of compressor types under various batch sizes [51]..... 10
Table 1. 2 Amount of ice needed to cool down different volumes of milk at 25 °C and 35 °C ambient temperature (based on simulation results) [45]..... 14
Table 1. 3 Overview of small-scale off-grid solutions for on-farm milk cooling..... 15

Table 2. 1 Percentage improvement in transmission heat loss with insulation thickness..... 26
Table 2. 2 Technical data of the components of vapour compression refrigeration cycle unit 29
Table 2. 3 The refrigerant charge and capillary tube lengths considered for experimental optimization 33
Table 2. 4 No-load evaporating temperature limit of the VCRC unit fabricated for varying capillary tube length and refrigerant charge 38

Table 3. 1 Instrument parameters and measurement uncertainty 46

Table 4. 1 Effect of ambient temperature on daily energy demand..... 65
Table 4. 2 Monthly and annual energy demand of the ice-storage system..... 65
Table 4. 3 Monthly and annual energy storage capacity in the form of ice under different operation 66
Table 4. 4 Refrigeration effect under the different operation modes..... 66
Table 4. 5 Performance drop with changing ambient temperature operating point..... 67
Table 4. 6 COP vs useful energy for compressor speed operating point change at a fixed ambient temperature..... 68
Table 4. 7 Final milk Temperatures at different packing factor and recirculation rate 82
Table 4. 8 Experimental and theoretical milk cooling and preservation energy demand..... 88
Table 4. 9 The milk volume per energy input with respect to final temperature requirements.... 89
Table 4. 10 Daily energy output under varying climatic conditions..... 89
Table 4. 11 Milk cooler capacity based on theoretical energy demand..... 90
Table 4. 12 Milk cooler capacity based on experimental energy input 90

Summary

Refrigeration and cooling in a food value chain play an important role by maintaining the sensory quality of the product and minimizing the loss. However, remote areas of the developing countries were mainly characterized by low levels of technology, limited access to modern energy and dominancy of smallholder farms as a challenge to improve the cold value chain. Even though small scale cooling technologies are available in the market, technical and economic barriers are still challenging to implement in rural areas. Besides this, an improvement in PV technology both in terms of cost and efficiency is an opportunity to consider a vapour compression refrigeration system as a feasible candidate.

In this context, a cooling system integrated with ice storage has been developed to fulfil the diverse application requirements in remote and grid isolated areas. The main objective of this thesis is to develop and characterize a modular-multipurpose cooling system based on an ice-storage for small-scale applications in remote areas.

The Agricultural Engineering Institute of Hohenheim University in Germany implemented a commercial DC freezer as smart ice-maker for on-farm milk cooling technology that uses PV as a source of electrical energy. However, further research is required to improve the ice production technique and milk cooling performance. So that developing an ice-storage system with a flow controlled cooling loop is a key factor to make small scale ice-based cooling technology more diverse and competitive. Two possible solutions have been proposed in this thesis to improve the technique of ice-based cooling technology using solar PV as a source of electrical energy.

The first solution was on ice production technique which aims at the development of a general-purpose ice-storage system by using evaporators in water-bath configuration. The use of roll- bonded plate evaporators directly in water-bath reduces the thermal resistance between the refrigerant and the water by avoiding the air medium as used in a conventional freezer. Using ice-on-surface approach would also improve the thermodynamic cycle performance by increasing the evaporating temperature of the refrigerant. The proposed approach also provides an opportunity to scale-up the ice production capacity by connecting modular units in parallel to satisfy the demand-driven cooling load. The second solution proposed was the introduction of a hydraulic circuit between the ice-storage and the product

to be cooled. This mechanism has the advantage of controlling the product temperature as required as well as suitable for the diversified application.

The initial step was the development and fabrication of the ice storage system with a compressor power requirement in the range of 40 to 70 W. The system development process starts from refrigeration system capacity definition followed by components specifications, fabrication and testing. The average ice production per day, as well as the cabinet volume, was defined. Effects of insulation materials on transmission heat gain were analyzed from which a suitable insulation material and thickness were identified. Based on a calculated heat load for the cabinet, a DC compressor, heat exchangers and other standard components were specified for vapour compression refrigeration cycle considered. The refrigerant charge and the capillary tube dimensions were experimentally optimized for best operating point to maximize performance and avoid suction temperature drop. The result indicated that refrigerant overcharge could cause condensation and corresponding frost formation at the compressor suction line.

Next, the performance of the ice-storage system was experimentally evaluated in a controlled climate chamber by varying condensing temperature and compressor power input. Two compressor speeds of 2000 rpm and 3500 rpm and three ambient temperatures of 25℃, 35℃, and 45℃ were implemented as operational variables. A daily ice mass production rate from 13.96 kg to 26.28 kg was obtained for the compressor speeds, and ambient temperature ranges studied. The compressor energy consumption ranged from 0.83kWh to 1.71kWh, and the COP values varied between 1.5 and 2.63. The COP drop of 3.4% observed for operating point change from 25 ℃ to 35 ℃ at 3500 rpm suggests that best operating point for the ice storage system developed was at maximum compressor speed and ambient temperatures below 35℃. The COP of the smart-ice maker with conventional freezer configuration used as a baseline for this research was between 1.15 and 1.63. The monthly and annual energy demand of the system was also predicted based on the experimental data. Improvement of the ice production technique and corresponding experimental performance parameters obtained were the main contributions of this research regarding the ice-storage system.

Following this step, the water-ice phase change process was characterized with the objective of determining the maximum lateral thickness on evaporator surface for a daily operation as a modular spacing parameter for multiple vapour compression system unit arrangements in parallel. A lateral thickness in the range of 7-12.6 cm was obtained on both sides of an

evaporator. Impact of varying operational parameters on phase change boundary temperature curves and degree of sub-cooling were also evaluated.

The subsequent step was on ice discharge characterization using a chilled water recirculation loop for which the study was divided into two parts: the milk cooling and cold room applications. For the first part, an 80 L capacity milk cooler was manufactured by using conventional milk-cans and an insulated metal box to test cooling rate and preservation performance. A forced recirculation of chilled water at flow rates of 300 and 600 Lh^{-1} from external melt ice-on-evaporator surface configuration was an energy transfer approach used to cool an 80 L of milk from 35 to 4℃ in less than 4 hours. The effect of energy density variation in the ice-storage on milk cooling rate was also analyzed. The result showed that decreasing the recirculation rate introduces a time lag on cooling rate, whereas varying the packing factor (PF) mainly affects the minimum attainable milk temperature at a given time. The result also indicated that more energy input per litre of milk is required to get a lower milk temperature in the range of 4℃.

An ice discharge performance for cold room application was carried out by using a heat simulated room and a variable speed fan-coil unit as a load side parameters. For the external melt ice-in-water-bath configuration, the chilled water recirculation rate was varied together with a fan-coil-unit load to characterize the ice discharge performance. The effects of varying operational parameters both on the ice discharge rate and the range of air temperature drop across a fan-coil unit were analyzed.

In general, the research work performed in this thesis contributes more knowledge on the development of low-carbon cooling technologies suitable for developing countries. The research output has been promoted and applied by the solar cooling engineering Company in Germany that distributes key components to facilitate the local production of the solar cooling system with a modular design. Therefore, piloting and field testing of the technology are among the major recommendations for future work.

Resumen

La refrigeración y el enfriamiento en una cadena de valor alimentaria juegan un papel importante al mantener la calidad sensorial del producto y minimizar la pérdida. Sin embargo, las zonas remotas de los países en desarrollo se caracterizan principalmente por bajos niveles de tecnología, acceso limitado a energía eléctrica y predominio de pequeñas explotaciones agrícolas como desafío para mejorar la cadena de valor del frío. Aunque las tecnologías de refrigeración a pequeña escala están disponibles en el mercado, las barreras técnicas y económicas siguen siendo un desafío para implementarse en las áreas rurales. La mejora en la tecnología fotovoltaica tanto en términos de coste como de eficiencia es una oportunidad para considerar los sistemas de refrigeración por compresión de vapor como solución factible.

En este contexto, se ha desarrollado un sistema de refrigeración integrado con almacenamiento de hielo para cumplir con los diversos requisitos de aplicación en áreas remotas y aisladas de la red. El objetivo principal de esta tesis es desarrollar y caracterizar un sistema de refrigeración modular polivalente basado en el almacenamiento de hielo para aplicaciones de pequeña escala en zonas remotas.

El Instituto de Ingeniería Agrícola de la Universidad de Hohenheim en Alemania implementó un congelador de corriente continua comercial para fabricar hielo y uilizarlo para enfriar leche en granjas utilizando energía fotovoltaica. Sin embargo, se requiere continuar investigando para mejorar la eficiencia de producción de hielo y reducir el coste total del sistema de enfriamiento de leche original. Con esta finalidad, se propone el desarrollo de un nuevo sistema de almacenamiento de hielo con un circuito de enfriamiento controlado por flujo como factor clave para hacer que la tecnología de enfriamiento sea más modular y competitiva. En esta tesis se han propuesto un método para mejorar este sistema de refrigeración solar de leche el cual consta de dos partes principales.

La primera parte del sistema corresponde a un sistema de almacenamiento de hielo de uso general mediante evaporadores en configuración de baño de agua. El uso de evaporadores de placas inmersas directamente en baño de agua reduce la resistencia térmica entre el refrigerante y el agua al evitar el medio de aire como se usa en un congelador convencional. El sistema de producción de hielo en la superficie también mejoraría el rendimiento del ciclo termodinámico al aumentar la temperatura de evaporación del refrigerante. El metodo

propuesto también brinda la oportunidad de aumentar la capacidad de producción de hielo conectando unidades modulares en paralelo para satisfacer la demanda de una mayor carga de enfriamiento. La segunda parte del sistema corresponde a la implantación de un circuito hidráulico entre el depósito de hielo y el producto a enfriar. Este mecanismo tiene la ventaja de controlar la temperatura del producto según se requiera, además de ser adecuado para distintas aplicaciones.

En primer lugar se desarrolló y construyó el sistema de almacenamiento de hielo con un requerimiento de potencia del compresor en el rango de 40 a 70 W. El proceso de desarrollo del sistema se basa en la definición de la capacidad de refrigeración seguido de las especificaciones, fabricación y pruebas de los distintos componentes. Se determinó la producción de hielo promedio por día, así como el volumen máximo de leche a enfriar, y se analizaron los efectos de los materiales aislantes sobre las pérdidas de calor por transmisión, a partir de los cuales se identificó el material para el aislamiento y su espesor. En base a la demanda térmica calculada para el sistema de producción de hielo, se especificó un compresor de corriente continua, intercambiadores de calor y otros componentes estándar para el ciclo de refrigeración por compresión de vapor considerado. La carga de refrigerante y las dimensiones del tubo capilar se optimizaron experimentalmente para obtener el mejor punto de funcionamiento para maximizar el rendimiento y evitar una baja temperatura de succión. Los resultados obtenidos indicaron que la sobrecarga de refrigerante podría causar evaporacion parcial y la correspondiente formación de escarcha en la línea de succión del compresor.

A continuación, se evaluó experimentalmente el rendimiento del sistema de almacenamiento de hielo en una cámara climatica variando la temperatura de condensación y la potencia del compresor. Se implementaron como variables operativas dos velocidades del compresor de 2000 rpm y 3500 rpm y tres temperaturas ambiente de 25 °C, 35 °C y 45 °C. Se obtuvieron tasas de producción de hielo diaria entre 13.96 kg y 26.28 kg para las velocidades del compresor y los rangos de temperatura ambiente estudiados. El consumo de energía del compresor osciló entre 0.83 kWh y 1.71 kWh, mientras que los valores de COP variaron entre 1.5 y 2.6. La caída del COP de 3.4% observada por el cambio del punto de operación de 25 ℃ a 35 ℃ a 3500 rpm sugiere que el mejor punto de operación para el sistema de almacenamiento de hielo desarrollado es a la velocidad máxima del compresor y temperatura ambiente por debajo de 35 ℃. El COP del equipo de fabricción de hielo con la configuración

de congelador convencional utilizada como base para esta investigación está entre 1.15 y 1.63. La demanda de energía mensual y anual del sistema también se calculó en base a los datos experimentales. La mejora del sistema de producción de hielo y los correspondientes parámetros de funcionamiento experimental obtenidos fueron las principales contribuciones de esta investigación en relación al sistema de almacenamiento de hielo.

Después de este paso, se caracterizó el proceso de cambio de fase hielo/agua con el objetivo de determinar el espesor lateral máximo en la superficie del evaporador para una operación diaria como parámetro de espaciado modular de unidades de sistemas de compresión de vapor múltiples en paralelo. Se obtuvo un espesor lateral en el rango de 7-12.6 cm en ambos lados de un evaporador. También se evaluó el impacto de los parámetros operativos variables en las curvas de temperatura límite de cambio de fase y el grado de subenfriamiento.

El paso siguiente consistió en la caracterización de la descarga de hielo utilizando un circuito de recirculación de agua fría, para lo cual el estudio se dividió en dos aplicaciones: la de refrigeración de la leche, y el uso del mismo sistema para cámaras frigoríficas. Para la primera parte, se fabricó un recipiente aislado para enfriar 80 litros de leche utilizando cántaras convencionales en baño de agua con el objetivo de determinar la velocidad de enfriamiento. La circulación forzada de agua fría con caudales de 300 y 600 l/h entre el acumulador de hielo y el recipiente aislado fue suficiente para enfriar 80 litros de leche de 35 a 4 °C en menos de 4 horas. También se analizó el efecto de la variación de la densidad energética en el almacenamiento de hielo sobre la velocidad de enfriamiento de la leche. El resultado mostró que disminuir la tasa de recirculación introduce un retraso en la tasa de enfriamiento, mientras que variar el factor de empaque afecta principalmente a la temperatura mínima alcanzable de la leche en un momento dado. El resultado también indicó que se requiere un mayor consumo de energía por litro de leche para obtener una temperatura de la leche más baja en el rango de 4 °C.

Se determinó así mismo el rendimiento de descarga de hielo para la aplicación de climatización, se usó una cámara aislada y una unidad *fan-coil* de velocidad variable. Para esta aplicación del acumulador de hielo con la cámara frigorífica, se varió la velocidad de recirculación del agua fría junto con la carga térmica de la unidad fan-coil para caracterizar el rendimiento de la descarga de hielo. Se analizaron los efectos de la variación de los parámetros operativos tanto en la tasa de descarga de hielo como en el rango de caída de la temperatura del aire en una unidad *fan-coil*.

En general, el trabajo de investigación realizado en esta tesis aporta un mayor conocimiento sobre el desarrollo de tecnologías de refrigeración para aplicaciones con energía solar. El resultado de la investigación ha sido promovido y aplicado por una empresa de ingeniería de refrigeración solar en Alemania que distribuye componentes para facilitar la producción local de los sistemas presentados con un diseño modular. Por lo tanto, las pruebas de campo de los sistemas estudiados, se encuentran entre las principales recomendaciones para futuros trabajos.

.

CONTRIBUTIONS BY THE AUTHOR

Articles in Scientific Journals

Muaz Bedru Hussen, Victor Torres-Toledo, Joachim Müller, Demiss Alemu, Alberto Coronas, Experimental study of the performance of small-scale refrigeration system with ice-storage for milk cooling application, International Journal of Refrigeration (in preparation).

Communications in Congresses, Conferences, Seminars, Workshops and Symposia

Muaz Bedru Hussen, Alberto Coronas, Demiss Alemu, small scale milk processing and preservation in developing countries: the case of Ethiopia; a review, CYTEF 2016 − VIII Iberian Congress | VI Ibero-American Refrigeration Sciences and Technologies Coimbra-Portugal, 3-6 May, 2016. (Oral presentation). ISBN:978-989-99080-4-8

Muaz Bedru Hussen, Victor Torres-Toledo, Joachim Müller, Demiss Alemu, Alberto Coronas, performance characterization of an ice-storage system for small scale cooling applications, CYTEF 2020 − X Congreso Ibérico | VIII Congreso Iberoamericano de las Ciencias y Técnicas del Frío Pamplona, España, 11-12 Noviembre, 2020. (Oral presentation). ISBN: 978-2-36215-043-2

Victor Torres-Toledo, **Muaz Bedru Hussen**, Alberto Coronas, solar ice-storage for cold room applications, Technical training on DIY Solar Cooling Systems, Strathmore Energy Research Centre, Nairobi, KENYA, 18-21 March 2019. (Oral presentation).

Victor Torres-Toledo, **Muaz Bedru Hussen**, Alberto Coronas, solar cooling systems prototype, Off-Grid Experts Workshop, University of Hohenheim, Stuttgart, Germany, 23-25 September 2019. (Oral presentation)

Muaz Bedru Hussen, Victor Torres-Toledo, Alberto Coronas, current research status and outlook for solar water chillers, Technical training and workshop on DIY Solar Cooling Systems, University of Hohenheim, Stuttgart, Germany, 27-29 November 2019. (Oral presentation).

Mobility/Internships

Universität Hohenheim, Institute of Agricultural Engineering, Tropics and Subtropics group, solar cooling engineering team, (Germany)

Advisor: Prof. Dr. Joachim Müller

Period: The research stay took place for eighteen months in a three consecutive year's period:

First round: October 01, 2017, to March 31, 2018

Second round: October 01, 2018, to March 31, 2019

Third round: October 01, 2019, to March 31, 2020

Topic: Performance study of solar ice-storage for cooling applications

Grant: Ethiopian Ministry of Science and Higher Education in collaboration with DAAD. EECBP Home Grown PhD Scholarship Programme, 2017 (57375975)

Activities:

1) Participation in different projects in the solar cooling engineering team of Tropics and Subtropics research group;

2) Participation and presentation in workshops and scientific seminars;

3) Manufacturing and testing of the ice-storage system with solar cooling units

4) Various experimental works on ice-storage for milk cooling and cold room applications

5) Internationalization activities related to the work developed by the research groups under the institute of agricultural engineering

Participation in projects

Promotion of solar refrigeration for agricultural value-chains (Kenya and Mali), funded by Sustainable Energy for Food – Powering Agriculture (GIZ grant number 18.6251.5-002.00) of the Deutsche Gesellschaft für Internationale Zusammenarbeit (GIZ), Institute of Agricultural Engineering of the University of Hohenheim, Stuttgart, Germany 01.10.2018-31.12.2020

Development of key cooling components and engineering for improved access to refrigeration, Efficiency for Access (EforA) Research and Development Fund from UK Aid and IKEA Foundation, Solar Cooling Engineering UG- a spinoff company of the Institute of Agricultural Engineering of the University of Hohenheim, Stuttgart, Germany, 15.12.2019-30.04.2020

Nomenclature

A	Area (m^2)
C_p	Specific heat capacity (J $kg^{-1}K^{-1}$)
D	Depth, width (m)
d	Day
dm	Differential mass (kg)
dQ	Differential heat energy (J)
dt	Differential time (s)
E	Energy consumption (kWh)
$\dot{E}$	Compressor power (W)
H	Height (m)
h	Specific enthalpy (J kg^{-1}), hour
I	Current (Ampere)
k	Thermal conductivity (W $m^{-1}K^{-1}$)
L	Length (m), Liter
m	Mass (kg)
$\dot{m}$	Mass flow rate (kg s^{-1})
N	Compressor speed (rpm)
P	Power (W), Perimeter (m)
Q	Heat (J)
q	Heat flux (W m^{-2})
T	Temperature (°C)
t	Time (s), heat exchanger wall thickness
x	Lateral thickness of ice
U	Overall heat transfer coefficient (W m^{-2} K^{-1})
V	Voltage (V)

Abbreviations

AT	total heat transfer area
CFCs	chlorofluorocarbons
COP	coefficient of performance
CTES	cold thermal energy storage systems
DC	direct current
FAO	Food and Agriculture Organization of the United Nations
FCU	fan-coil-unit
Gt	Giga tone
HCFCs	hydro-chlorofluorocarbon
HFCs	hydro-fluorocarbon
HTF	heat transfer fluid
LHTS	latent heat storage systems
Min	minute
PC	personal computer

PCM	phase change material
PF	Ice to water fraction (Packing factor)
PV	photovoltaic
rpm	number of revolutions per minute
SHS	sensible heat storage systems
SLHX	suction line heat exchanger
TI	temperature of ice
TW	temperature of water
VCRS	vapor compression refrigeration system
VRF	variable refrigerant flow
WHO	world health organization
WRR	chilled water recirculation rate
ZT	Total heat transfer efficiency

Subscripts

amb	Climate chamber temperature
∞	Surrounding environment
$comp$	Compressor
ev	Evaporator
f	Liquid, friction factor
g	Gas
i	Fluid flow direction
ice	Water in solid phase
j	Fluid to fluid separating wall
ji	Wall cell j to fluid cell i
l	Liquid
ni	Number of wall cells
ref	Refrigerant, Reference temperature
s	Solid
sat	Saturated
$offset$	Error in temperature reading
storage	Insulated container for ice and water
wb	Water-bath

Greek letters

Δ	Difference
ρ	Density (kgm^{-3})
ε	Epsilon
φ	Body cooling or heating term
∂	Partial differential operator
ξ	Compressor heat losses
α	Void fraction
Φ_f^2	Two-phase friction multiplier

Chapter 1
Introduction, Objectives, Methodology and Structure of the Thesis

1.1 General introduction

The role of refrigeration and cooling in a food value chain is vital to maintain the sensory quality and minimize the loss. Spoilage reduction is an important aspect of preserving the quality of perishable foodstuffs of both animal and plant origin. Bacterial contamination, survival and growth are common in poorly preserved food products. The global average loss of perishable foods through a lack of refrigeration accounts for 20%, whereas it accounts for up to 23% for developing countries [1]. This food loss figure reaches 40% for the case of fruits and vegetables in developing countries. Thus, the use of refrigeration substantially reduces bacterial growth as well as the rate of undesirable chemical and physiological reactions that reduce quality in foods. Refrigeration is even more vital in hot countries, where bacterial growth takes place faster because of high temperatures [2]. According to FAO (2011) [3], one-third of food produced for human consumption is lost or wasted globally. The remoteness of production site from consumers market, seasonality of agricultural products and level of infrastructure development are among factors affecting the food quantity loss [4].

Introduction of cold chain network between producers and consumers have a positive impact on improving the food value chain. The dominance of smallholder farms (large population, small quantities), lack of access to modern energy, and low levels of technology are among challenges to address in improving cold value chain in developing countries [4]–[6]. Moreover, the cooling technology available in the market is mostly large scale and not suitable for small scale farmers in developing countries. Low cost, low-carbon cooling technologies suitable for developing countries are among the recent areas of research undergoing to improve the cold value chain. As shown in Fig.1.1, more than 600 million people live without electricity in sub-Saharan African alone. Access to grid electricity is also a challenge in many developing regions as well. Moreover, about 37 % of the 4.14Gt CO_2eq emission from the refrigeration sector is due to direct

emissions (leakage) of fluorinated refrigerants (CFCs, HCFCs and HFCs) [7]. Hence, Off-grid cooling with natural refrigerants offers an environmentally friendly solution contributing to a reduction in the global warming effect.

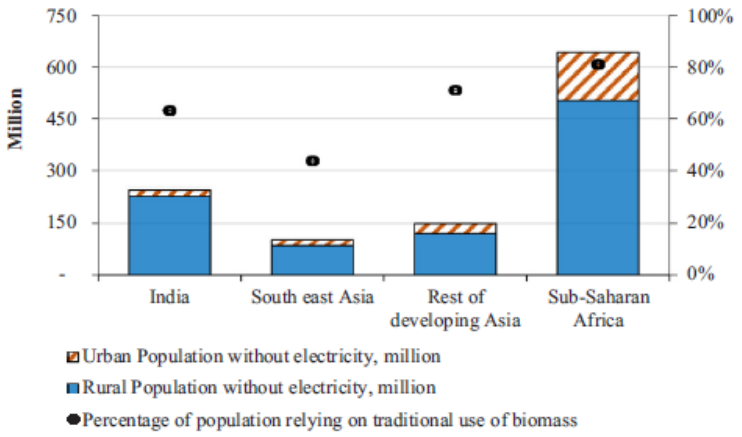

Figure 1. 1 Number and percentage of the population without electricity (2016) [8]

Energy storage is an important aspect when dealing with small scale cooling when the focus is on the areas of the world without access to grid electricity. Industrial ice-based cooling technology is a matured technology where sufficient data can be obtained from the literature regarding design, operation and performance. With the advancement of compressor technology, a direct drive variable speed compressors having low stating torque paved the way for many researchers to use ice packs as a means of energy storage in small scale cooling applications.

Figure 1. 2 Ice lined freezer for cooling application using PV as energy source [9]

Ivan Katic et al. [9]of the Danish technological institute used "standard chest-type refrigerator" to develop a grid-independent cold storage system. The researchers used ice packs to minimize required battery size and ensure faster cooling of products like milk to fulfil WHO requirements in their 150 $L.day^{-1}$ capacity milk cooler. The freezer was also designed to cool other perishable products, serving as small scale cold storage. In a similar concept, a German-based solar consulting company [10] used conventional STECA (PF 240 freezer) with ice packs around the freezer cabinet to cool 40 $L.day^{-1}$ milk using energy from solar PV. Poor energy performance and limited product storage volume are drawbacks reported on the ice-based cooling system using conventional freezers shown in Fig.1.2. Various research works for vaccine cooling also adapted the conventional refrigerator with PCM as energy storage medium. Jensen et al. [11] investigated factors that affect the autonomy of a stand-alone refrigerator for vaccine cooling. Through modelling and experimental work, the researchers concluded that the mass of ice in the storage was the most promising parameter to consider for prolonging the autonomy time. Dinesh Chawla et al. [12] presented some PV driven refrigeration system configurations as applied to small scale cooling systems. Performance of a 50 L capacity DC-driven vapor compression refrigeration system investigated by Asmaa Ahmed et al. [13] reported the effect of PCM on energy efficiency.

Energy efficiency, application diversification and modularity are among important aspects of small scale cooling with ice storage considered in this research. The challenge of energy efficiency improvement was addressed by devising the ice production technique improvement from conventional freezer applications. The solution on ice production technique improvement aims at the development of a general-purpose ice-storage system by using evaporators in water-bath configuration. The use of roll-bond plate evaporator directly in water-bath reduces the thermal resistance between the refrigerant and the water by avoiding the air medium as used in a conventional freezer. This approach would also improve the thermodynamic cycle performance by increasing the evaporating temperature of the refrigerant. The proposed method also provides an opportunity to scale-up the ice production capacity by connecting modular units in parallel to satisfy the demand-driven cooling load. For product diversification and control, a hydraulic circuit was introduced between the ice-storage and the product to be cooled. This mechanism has the advantage of controlling the product temperature as required as well as suitable for diversified application. Finally, a cooling system based on ice storage using a DC-powered

vapour compression refrigeration cycle was developed, fabricated and experimentally evaluated to fulfil the application requirements.

1.2 Background

1.2.1 The ice-storage technology

Energy storage can be in the form of sensible heat in a liquid or solid medium, as heat of fusion (latent heat), or as chemical energy or products in a reversible chemical reaction. In comparison with sensible heat storage (SHS), latent heat thermal storage (LHTS) is attracting increasing interest among other reasons because of the high volumetric capacity and low heat transfer losses [14], [15]. A review of the development of latent heat thermal energy storage systems detailing various phase change materials (PCMs) was performed by Agyenim et al. [14]. In the review, the researchers considered issues of the heat transfer enhancement techniques employed in PCMs to effectively charge and discharge latent heat energy and the formulation of the phase change problem. This review work put the absence of a standard method to test PCMs, making it difficult for comparison to be made to assess the suitability of PCMs to a particular application as an important remark.

The ice-storage technology was a suitable candidate to shift small capacity continuous load to larger capacity instantaneous thermal load for a quick cooling requirement. The technology plays a great role in using renewable energy, shifting peak load to off-peak [16], improving grid load rate and other aspects. Since the research focuses on small-scale cooling, commercially available large scale ice machines were not discussed here. Due to its higher economic efficiency, wider range of application and greater market advantages [17], static direct cool thermal storage system with an external ice-on-coil building/melting was considered in this research. Even though the ice-on-coil system is simple in concept requiring very little maintenance, the attempts to predict the behaviour of such systems through numerical and analytical modelling can prove difficult [18]. Several active research work was being undertaken on ice-storage systems for air-conditioning application as partial and pick load supplement. Use of ice-storage as baseload for small-scale cooling application is the state of the art research area that needs further investigation.

Researchers [15, 19, 20] studied coil pipe cool storage system experimentally and numerically for several applications. The basic set-up in all such cases is that the cooling coils with heat transfer fluid (HTF) flowing inside the cold storage are used to produce ice on the external surface of coils. As all these set-ups use an indirect type of cooling, they need a secondary circuit for HTF cycle which adds cost and complexity for cold thermal storage systems (CTES). The research work on hourly simulation and performance of solar electric-vapour compression refrigeration system by Bilgili [21] revealed that the COP of a refrigerator decreases with decreasing evaporating temperature. The work also showed that by controlling the evaporator temperature appropriately, the COP could be improved. One way of controlling the evaporator temperature is to use it for direct heat exchange in a water-bath configuration. Axaopoulos et al. [22] performed experimental work to use multiple compressors of variable speed to avoid batteries in a solar PV system and employ a new control device to monitor compressor operation. The possibility of using ice as a storage medium instead of batteries in the solar cooling application was successfully demonstrated.

Effect of natural convection on the melting performance of a latent heat thermal storage was investigated by Cheng Yu et al. [23]. The researchers reported a significant improvement of the melting rate for the system with natural convection when compared with the case without natural convection. Huang et al. [24] optimized the performance of a finned shell-and-tube ice storage unit by varying the number of fins around the tube. The thermal conduction enhancement due to the addition of fins improved the energy discharge performance of the shell-and-tube ice storage unit, according to the finding. Wang et al. [25] analyzed the discharging performance of a forced-circulation ice thermal storage system for a permanent refuge chamber in an underground mine. The minimum required velocity and the effective working time of the ice storage were among the main findings of the research work.

The effects of the inlet temperature and the flow rate of the heat transfer fluid (HTF) on discharge characteristics of cold thermal storage was analyzed by Wu et al. [26]. For organic phase change material (PCM) A164 and a thermic oil HTF, the energy released and discharging efficiency increase with increasing mass flow rate and with decreasing inlet HTF temperature [27]. In paraffin latent heat storage, higher HTF inlet temperature was the dominant discharge factor while mass flow dominates the discharge performance at lower HTF inlet temperature

[28]. Khan et al. [29] used water as an HTF in a paraffin-based novel shell and tube latent heat storage. The researchers performed a discharge experiment for HTF flow rate in the range of 1.5 to 3 L min^{-1} and inlet temperature varying from 5-15℃. In his case as well, an increase in the mean discharge power was reported for the case of lower HTF inlet temperature and higher flow rate.

The effects of air velocity and inlet air temperature on the performance of the thermal storage with calcium chloride hexahydrate PCM were analyzed by Mosaffa et al. [30]. In this configuration, the air was used as an HTF passing through the tube with external fins. It was reported that the outlet air temperature was more affected by the air inlet temperature than the air velocity. Several works of literature [37, 45] have been published on ice-water phase change modelling both experimentally and numerically. However, it is still challenging to get a single rule of thumb or numerical expression to design ice storage. Hence, the experimental approach is still among the effective ways to characterize the ice formation on the surface of non-uniformly varying boundary temperatures to obtain ice-storage design parameters.

The heat transfer involving phase change is a transient and nonlinear process with a moving boundary. During a phase change process by absorbing latent heat of fusion for ice formation, a boundary called solid-liquid interface coexists. In practical problems, the phase transition within PCM takes place over a temperature range in which the enthalpy is a complex function of temperature [40]. Existing analytical solutions deal with 1-D geometries with limited boundary conditions and cannot be used for problems of varying boundary conditions and complex geometries. Practical solidification and melting problems are rarely one dimensional, initial and boundary conditions are always complex, thermo-physical properties can vary with phases, temperatures and concentration, and various transport mechanisms (for example, convection, conduction, diffusion and radiation) can happen simultaneously [41].

Thus, many numerical schemes have been proposed to study transient heat conduction problems with phase change in one, two and three dimensions [42]. The unsteady ice layer growth around the cylindrical geometry subjected to free convection was studied theoretically by Lipnicki et al. [43], and the approximate solution for ice layer thickness was obtained. This analysis considers the temperature distribution around the cylinders to be uniform, the situation which is difficult to

attain in a direct cooling in water bath application for ice formation. In all discussions, there is no single general formula to calculate the thickness of the ice developed on a surface with varying boundary conditions. It is, however, possible to get an approximate solution using a numerical approach. Nevertheless, a numerical method itself needs a defined boundary condition that was yet to be known from the experiment for a specific application. Hence, experimental ice-thickness and the boundary temperature evaluated in this research could serve as an input for numerical solution methods.

1.2.2 Milk cooling

Milk is a valuable nutritious food that has a short shelf life and highly perishable because it is an excellent medium for the growth of microorganisms. Temperature is one of the most important factors influencing the growth of naturally occurring bacteria in milk. The role of refrigeration and the cold chain in maintaining the quality and safety of both raw and pasteurized milk is well recognized [44]. Unless rapidly cooled from its initial temperature of 37 °C to 4 °C, raw milk can exceed the maximum bacterial count allowed by food safety laws after 2 to 5 h [45]. Cooling the milk to 4 °C within three to four hours after milking maintains the original quality of the milk and is the method of choice for ensuring good-quality dairy for processing and consumption. Storing the milk at 20°C and 15°C limits bacteria growth not to exceed 1 million per ml for 6 and 12 hours respectively [46].

The ice-making capability of evaporators immersed in a water bath for PV application was evaluated by Axaopoulos et al. [22]. The researchers reported a daily ice mass in the range of 4.5-17 kg using 440 W_p solar panel by operating four small DC compressors of similar capacity at a time. The developed system was proposed to cool 25-litre milk at a time by directly putting the milk-can inside the ice-storage shown in Fig.1.3. A control strategy designed for the operation of multiple compressors sequentially based on the availability of solar energy to avoid battery storage was an important contribution of the work mentioned. However, putting the milk-can directly into the ice-storage has a drawback of milk temperature control which is a sensitive parameter to maintain the milk quality. Moreover, making the ice-storage and milk-cooler to operate independently as proposed in this research adds flexibility on diversification of application and scalability.

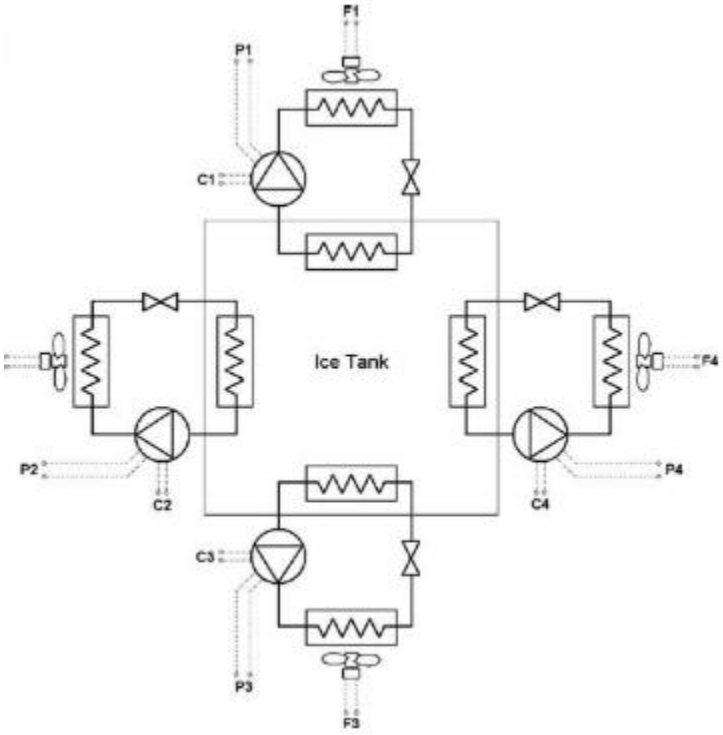

Figure 1. 3 The ice-maker configuration with four cooling circuits [22]

Although large scale milk processing and preservation is a matured technology, there are few successful and promising works so far on milk preservation at the smallholder level. By using the lactoperoxidase (LP) enzyme system, milk can be preserved for about 7-8 hours after milking at a temperature of 30-35 °C [44]. However, lowering the raw milk temperature increases the spoilage free storage life significantly. Thus, concerning prevention of spoilage of raw milk, the LP-s can be complementary to refrigeration. Such a system of milk preservation is helpful for farmers to preserve their milk for hours required to transport the milk to nearby markets or chilling centers. In an attempt to reduce the loss of evening milk in sub-Saharan countries, the performance of 15.5 litter adsorption evaporative cooler using biogas as the heat source for regeneration was assessed by Ndyabawe et al. [47]. The assessment result showed that preservation of milk for 24 hours is achieved. Thermal performance of chilling milk units in remote villages working with the combination of biomass, biogas and solar energies was evaluated by Edwin et al. [48]. The researchers estimated to find suitable proportions of biomass, biogas and gobar gas as the main energy source and solar energy as a complementary source to drive absorption-chilling plant. Considering the limited access to electricity in rural areas,

especially in Sub-Saharan Africa [49], the implementation of solar energy-based cooling systems has a long term impact on the improvement of product quality and the reduction of food losses.

A field study carried out by Foster et al. [50] demonstrated the direct-drive PV application for small scale milk cooling. The system shown in Fig. 1.4 was able to cool 20 L of milk per day by using ice and brine as a thermal energy storage medium. Such systems are the latest innovations even though PV powered direct drive refrigerators were used for vaccine preservation in remote clinics for several years. The control of variable milk volume and the possibility for product diversification could be the main constraint of the PV based milk cooling system used in this case.

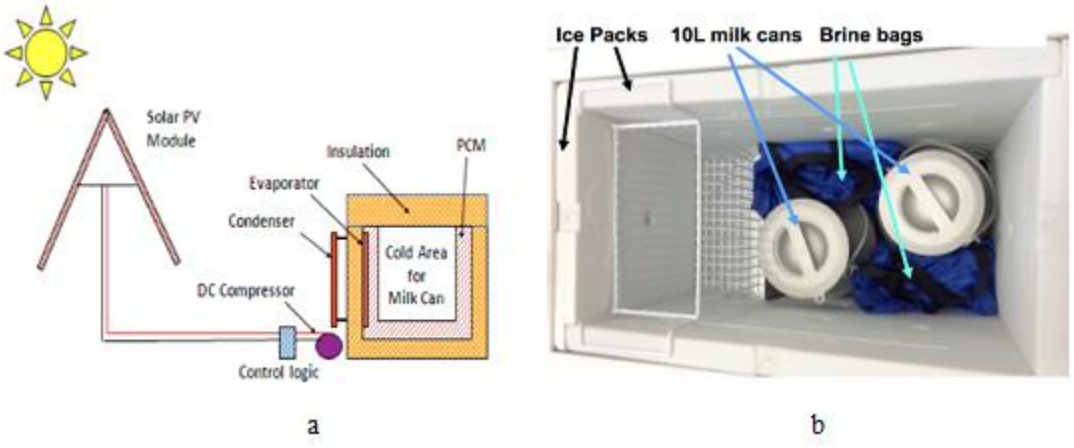

Figure 1. 4 a) PV direct-drive milk chiller array, b) PV-powered chiller using thermal ice storage and brine bags to chill evening milk [50]

Khan et al. [51] developed a 200 L capacity milk cooling system that implements a PV powered vapour compression system with VRF. This research compared the power requirement of different compressors and obtained varying energy consumption for a similar load applied, as shown in Table 1.1. Besides this, the compressor powers of 1.8kW, 1.2kW, and 0.8kW were experimentally observed for reciprocating, rotary with capacitor and rotary with VRF configurations respectively. With this finding, the researchers concluded that employing VRF technology could improve system energy efficiency by reducing the torque load. Even though the energy efficiency improvement was realized through VRF application, this system was designed to satisfy the instantaneous requirement of one tonne of refrigeration directly from PV to cool a 200 L of milk in 2 h time with the configuration shown in Fig.1.5. Hence, a system with smaller compressor power requirement incorporated with energy storage to cool larger product

volume at a time would be another option to consider for PV based cooling application considering the scale of investment.

Table 1. 1 Comparison of compressor types under various batch sizes [51]

Batch size	Compressor type	Chilling time (h)	Energy used (kWh)	Standard errors
50 L	Reciprocating	0.39	1.15	
	Rotary	0.41	0.91	0.014
	Rotary with inverter	0.62	0.82	
100 L	Reciprocating	0.75	1.65	
	Rotary	0.82	1.38	0.011
	Rotary with inverter	1.10	1.29	
150 L	Reciprocating	1.15	1.92	
	Rotary	1.31	1.67	0.019
	Rotary with inverter	1.58	1.65	
200 L	Reciprocating	1.17	2.4	
	Rotary	1.86	1.92	0.012
	Rotary with inverter	1.88	1.86	

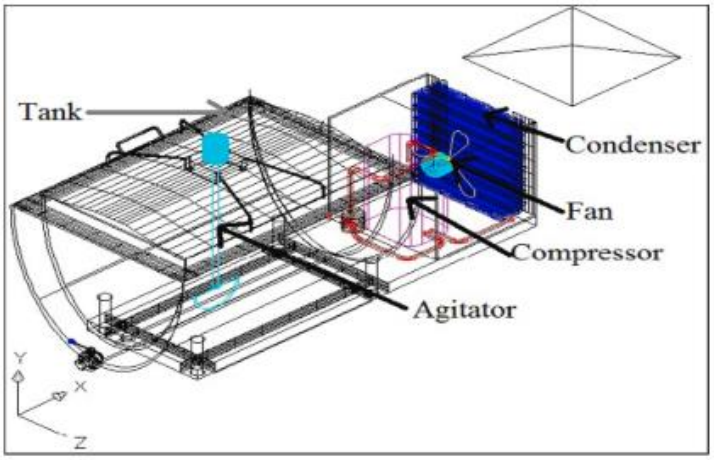

Figure 1. 5 Schematic of milk chiller for the chilling process [51]

1.2.3 Prospects of the PV Technology

The recently increasing concern on environmental pollution and limited nature of non-renewable energy sources paves the way to research and development on renewable energy sources. Solar energy is among the form of clean energies that can be utilized without environmental pollution. Several applications of solar energy were realized with rapid improvement in efficiency and cost, thanks to research and development in the field. In a broader context, solar energy was used to heat and cool buildings (both actively and passively), heat water for domestic and industrial uses, heat swimming pools, power refrigerators, operate engines and pumps, desalinate water for drinking purposes, generate electricity, for chemistry applications, and many more operations [52].

In 2018, the global solar PV share among the solar conversion technologies accounted for more than half of the energy generation from solar source. According to IEA (2019) report [53] the solar PV share for the year 2018 was 58.8 % (585TWh), the solar thermal heat generation was 39.8 % (396TWh) and solar thermal electricity generation accounted only 1.3 % (13.4TWh). The report also indicated that the worldwide solar conversion technology trend showed a dramatic increase in PV electric generation in a decade time. As a symbolic indication during the year 2008, the solar energy conversion proportion was 8.5% (12TWh), 90.4% (128TWh) and 0.6% (0.9TWh) for PV electric, solar thermal heat, and solar thermal electric respectively.

The continued effort on research and development on energy conversion systems that are based on renewable energy technologies brought a significant cost reduction in PV technology. According to the renewables global status report (2019) [54], the power production from PV shown in Fig.1.6 will continue increasing and can take major share from all the energy sources available. Hence, the use of vapour compression refrigeration system powered with PV energy would be a more relevant solution for cooling in remote locations with poor grid connection.

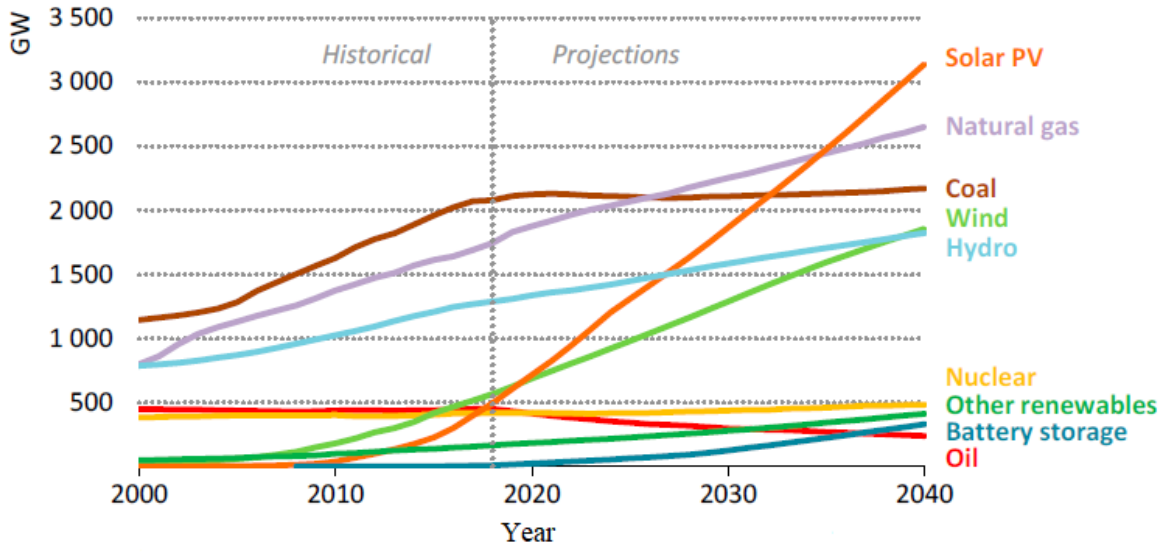

Figure 1. 6 Global power capacity by source [55]

1.2.4 Research work on milk cooling in Hohenheim University

The solar cooling team under Agricultural Engineering Institute of the Hohenheim University in Germany performed rigorous research work on small scale milk cooling since 2015. Torres et al. [56] characterized the transient performance of a small on-farm milk cooling system. The researchers proposed the use of two independent commercial DC refrigerators shown in Fig. 1.7 to operate at −10 °C and 4 °C for ice production and milk preservation, respectively.

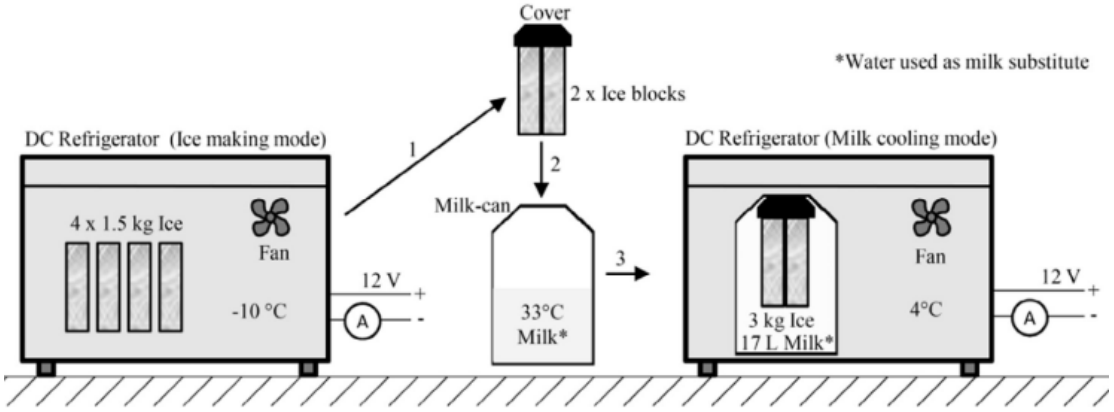

Figure 1. 7 Refrigerator units operating in ice-making and cooling mode [56]

The paper provided a strong background on the use of solar PV coupled with conventional vapour compression compressors based on a review of existing technology. The energy consumption of ice making mode was evaluated for the production of 6 kg ice per day at varying ambient temperatures and compressor speeds. By using a DC-refrigerator as an ice-assisted milk cooler, the researchers reported the cooling of 17 L milk from 33°C to 10°C in 2 hours. However, further cooling of the milk to 4°C took 8-10 hours as shown in Fig.1.8. Similarly, it takes 16 to 20 hours based on surrounding ambient temperatures to produce a 6 kg ice in the proposed set-up. The researchers reported a significant effect of ambient temperature on system COP and total specific energy consumption per litre of milk in the range of 30 Wh/L and 58 Wh/L for 20 °C and 40 °C ambient temperature.

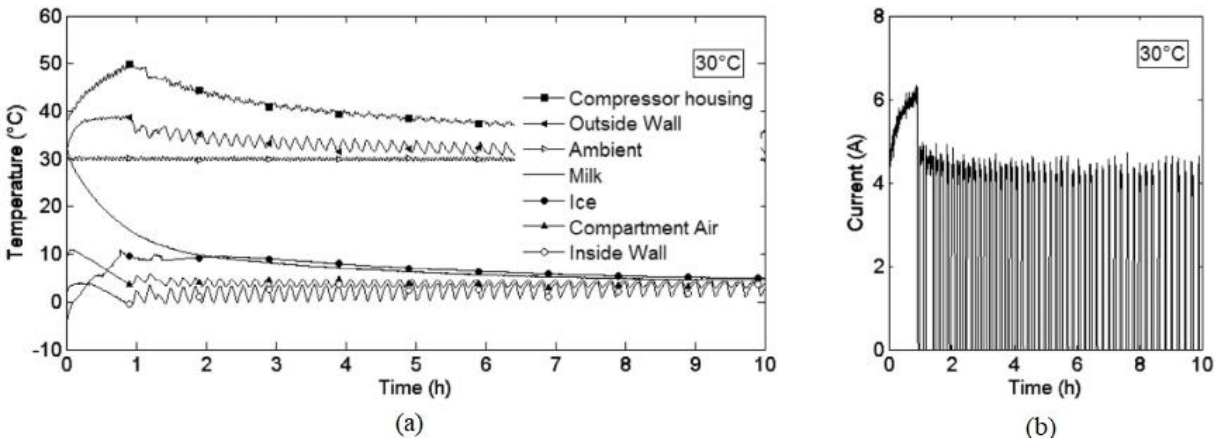

Figure 1. 8 Milk cooling by DC refrigerator to cool down 17 L milk at 4 °C employing 3 kg ice (a) temperature curve (b) current consumption at 12V for 30°C ambient [56]

With the introduction of a new adaptive control unit and a relatively powerful fan inside the DC freezer, Torres et al. [57] presented the modified version of the solar ice-maker based on a DC-freezer. The freezer holding a 50 litre of water in small canisters of 2 kg each as shown in Fig.1.9 has the capacity of producing 12 kg ice per day. Optimization for PV system sizing was performed, and the utilization of conventional freezers to make ice with solar energy was experimentally evaluated. For a DC-freezer producing 12 kg ice per day, a solar PV system of 600 Wp and 65 Ah at 24 V battery capacity provided a four-day autonomy in Sidi Bouzid of Tunisian weather

Figure 1. 9 DC-freezer equipped with air circulation fan and 25 ice-cans for a total of 50 kg ice [57]

Based on the field experience in Tunisia, another important modification on milk cooling mode was also proposed and implemented by the solar cooling engineering team of Hohenheim University. Torres et al. [45] presented the experimental and simulation result on milk cooling using an insulated-can with an integrated ice-compartment concept, as shown in Fig.1.10. The researchers developed a computational model based on experimental results to predict milk/ice ratio and summary the result is presented in Table 1.2.

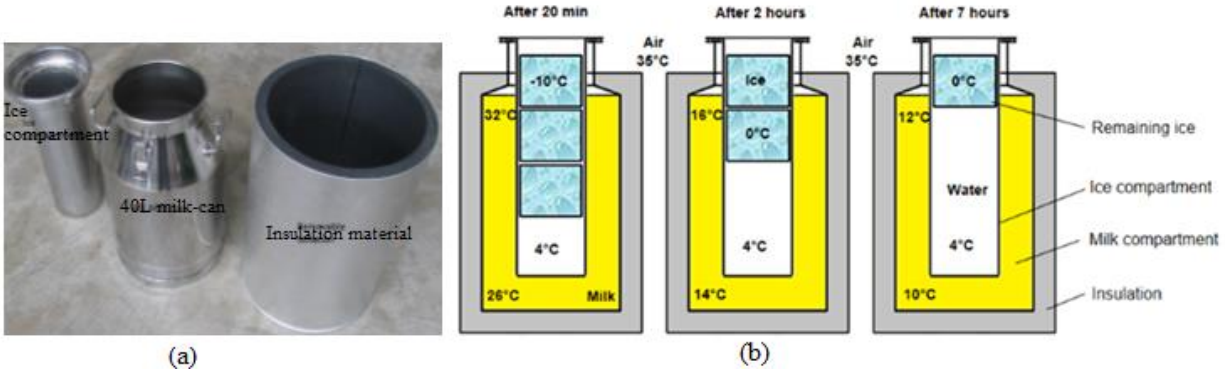

Figure 1. 10 Ice-compartment based milk cooling set-up (a) System components (b) Temperature distributions in an insulated can be loaded with 20 L milk and 8 kg ice [58]

Table 1. 2 Amount of ice needed to cool down different volumes of milk at 25 °C and 35 °C ambient temperature (based on simulation results) [45].

Ambient temperature		25°C		35°C	
Cooling time		6 h	12 h	6 h	12 h
Cooling temperature		<19°C	<13°C	<19°C	<13°C
Milk volume	**10 L**	1.9 kg	3.4 kg	2.4 kg	4.5 kg
	15 L	2.7 kg	4.8 kg	3.2 kg	5.8 kg
	20 L	3.6 kg	6.2 kg	4.1 kg	8.1 kg
	25 L	4.6 kg	8.6 kg	5.0 kg	9.7 kg
	30 L	5.5 kg	10.0 kg	5.9 kg	11.2 kg

The systems were also installed in several locations in Kenya, Tunisia and Colombia. The existing system was able to cool a maximum of 30 L to 15 ℃ and 20 litres of milk to 8 ℃ at a time as discussed in earlier sections. It was also realized through field testing that there is a demand for cooling down a larger volume of milk at a time to a standard temperature of 4℃ to promote a cooperative business in rural areas. Diversifying the application ice-based cooling to several agricultural products and the possible use of the solar ice-maker for pick load supplement

in building Air-Conditioning are among current demanding areas to perform further research in this field.

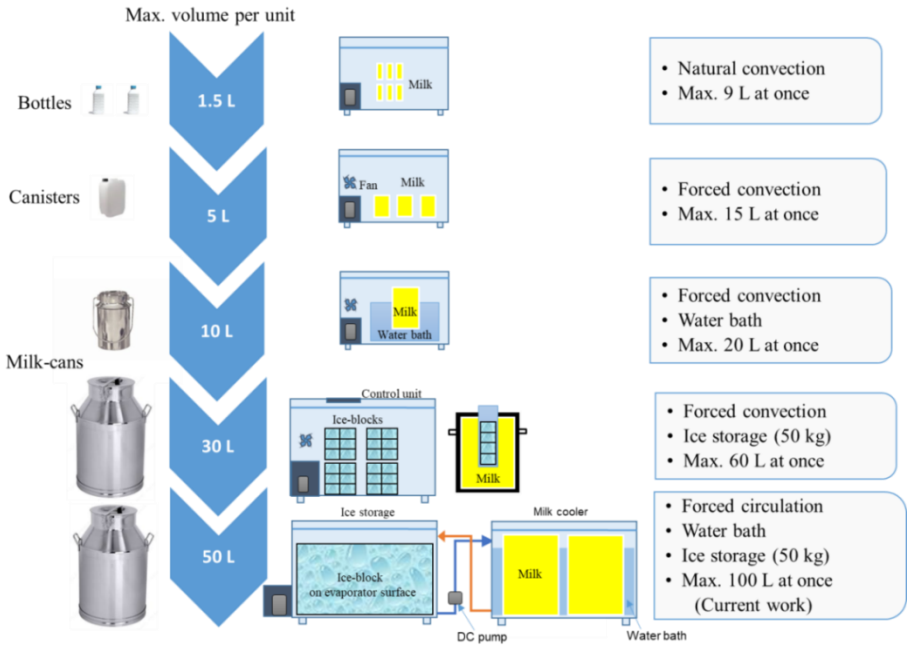

Figure 1. 11 Configurations for the use of a refrigerator for small-scale milk cooling [58]

Table 1. 3 Overview of small-scale off-grid solutions for on-farm milk cooling

	University of Georgia [47]	SimGas B.V. [59]	SunDanzerInc. [50]	University of Hohenheim [58]	University of Hohenheim (Current work)
Energy source	Biogas to regenerate a desiccant	Biogas	Photovoltaic battery-free	Photovoltaic	Photovoltaic
Refrigeration technology	Evaporative cooling	Absorption refrigeration	Vapour compression refrigeration	Vapour compression refrigeration	Vapour compression refrigeration
Energy storage	Desiccant materials	Water bath	Phase change materials	Ice blocks	Ice and water bath
Cooling medium	Insulated milk can with a compartment for a desiccant	Milk-cans submerged in a water bath inside the refrigerator	Water bags and milk cans inside the refrigerator	Ice produced inside the refrigerator and placed in ice compartments	Ice produced inside ice-storage and chilled water recirculates through milk-cooler where milk cans are submerged in water-bath
Milk canister	15.5 L	5 L milk-cans	10 L milk-cans	30 L insulated	40-50 L milk-

	insulated milk-cans			milk-cans	cans
Capacity	15.5 L/milk-can	10 L/day/system	20 L/day/system	60 L/day/system	80-100 L/day/system

The use of a commercial refrigerator for small scale milk cooling was presented in Fig.1.11. In all configurations, the commercially available household refrigerator was used as a milk-cooling device but as icemaker in the last two options. The result showed that the fridge was able to cool only a small volume of milk at a time to a standard temperature. Moreover, the ice-storage concept gives flexibility in terms of milk volume to handle and minimum temperature control as seen from Fig.1.11. An overview of small scale off-grid on-farm milk cooling solution was also presented in Table 1.3. Ndyabawe et al [47] developed a 15.5 L/day capacity milk cooling system using insulated milk-can with a compartment for a desiccant for evaporative cooling. They used biogas as a heat source for the removal of moisture from zeolite (regeneration) purpose. Even if this off-grid solution is an important technology for the improvement of milk quality at farm level, the researchers proposed a system in the range of 50-100 L capacity to be more suitable for the rural society. Poelhekke [59] used absorption cooling technology to develop a 10 L/day milk cooling system tailored to the needs of small-scale dairy farmers using biogas as an energy source. Thus, based on the small scale milk cooling solution discussed and considering the requirement for diversification and scalability, the use of a small capacity vapour compression cycle unit to produce ice as a cold source for the multipurpose cooling application was proposed in this research.

1.3 Objectives

Controlling the temperature of the product in a food value chain saves the nutritional value and minimizes loss both in production and consumption levels. Energy and means of preservation is the main challenge in smallholder farming dominated remote areas of developing nations. As discussed in the general background section, the Agricultural Engineering Institute of Hohenheim University in Germany is working on farm level small scale solar milk cooling technology that implements PV as the source of electrical energy. Through the continuous improvement in the design of the control unit, and enhancement of the heat transfer mechanism in the freezer compartment, improvement in the daily output of stored thermal energy was realized. The field experience also shows that there is a need to diversify and scale up the

application of the solar ice-based cooling, enhance the system performance and improve the milk cooling approach.

The smart ice-maker in the system produces ice in conventional freezing approach where the air is a heat transfer medium between the evaporator and the ice-blocks. On the other hand, if the evaporator surface is made to operate directly in a water bath, the thermal resistance due to air will be reduced, and the refrigerant evaporating temperature will also increase. This in turn will have a net effect on the improvement of the system's COP and daily ice production rate. The manual ice harvesting and use of ice-compartments inside the milk-can also presents a challenge on maintaining the milk quality during cooling due to possible contaminations.

Moreover, the geometric limitations on heat transfer area of the ice-compartments in milk-can pose a restriction on minimum attainable milk temperature at the end of cooling. Hence, a milk-can in water bath approach with chilled water recirculation across the milk-cooler will avoid problems of both the final milk temperature limit and minimize the risk of contaminations. So that developing an ice-storage system with flow controlled cooling loop, as shown in Fig. 1.12 is among suitable solutions to make small scale ice-based cooling technology more diverse and competitive.

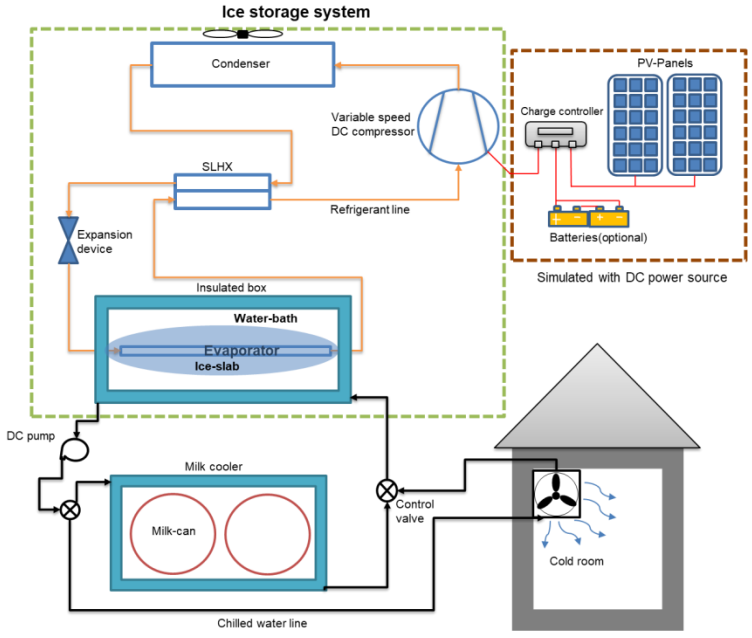

Figure 1. 12 Proposed schematic diagram of the small-scale cooling system including PV powered ice-storage and flow control loop

Therefore, the main objective of this research is to develop and characterize a cooling system based on an ice-storage with improved performance for small-scale milk cooling and cold room applications.

Specific objectives

1 Develop and fabricate an ice storage system with the evaporator in water-bath configuration powered by a variable speed DC compressor suitable for PV application.
2 Evaluate the performance of the ice storage system developed with respect to varying compressor power input and the surrounding ambient.
3 Characterize the ice thickness development on the evaporator surface to set a limit on the spacing of multiple units in parallel in order to scale up the ice storage capacity.
4 Develop milk cooler with a capacity of 80-100 litres using conventional milk-cans integrated with chilled water circuit from ice storage, evaluate its performance with respect to cooling milk from 35 to 4°C within four hours and preserve it for one day.
5 Analyze the external melting of ice in the water bath by implementing the fan coil unit as a load-side end-user device with the aim of using the ice storage for cold room application.

1.4 Methodology and structure of the thesis

The thesis is organized in five chapters with each chapters detailing specific issue related to the objectives of the research. The **first chapter** is dedicated to a general introduction, methodology and structure of the thesis. Here the general background of existing research work was discussed from which the current research is formulated. The research problem was identified, and the possible solution was proposed. The thesis objective outlining the intended outcome of the research work is also discussed in the first chapter. The section concludes by setting a methodological approach to the thesis work.

The storage of a continuous small-capacity thermal energy to satisfy an instantaneous load demand in remote locations is the central focus of this research. To this end, experimental system development and fabrication was one of the core activities to perform. Thus, **chapter two** is dedicated to ice storage system development and fabrication. In this chapter, the vapour compression refrigeration unit was analyzed to define the cooling capacity by considering transmission gain through the insulated wall and daily energy demand as the main source of heat

load. Effect of thermal conductivity and insulation thickness on transmission heat gain was evaluated from which insulation material is selected. For the defined cooling capacity, a variable speed compressor was specified using SECOP selection software. Conventional cool box components of a roll-bond plate evaporator and an air-cooled finned condenser were implemented for the heat exchanger part. Finally, the refrigeration cycle unit was fabricated and assembled with the insulated compartment (the ice storage box). A capillary tube length and refrigerant charge were experimentally optimized for best operating point. The ice storage system developed, which is the major output of this section is used as part of an experimental system for performance characterizations in subsequent chapters.

Chapter three focuses on experimental setup configuration for performance characterizations of the ice-storage system, the milk cooling and cold room applications. The experiment was carried out for the ice making process by varying the operating points of the ice storage system to compare operational efficiencies and evaluate the ice thickness on the evaporator. Milk cooling experiment was performed using 80 L capacity milk cooler to evaluate the milk cooling performance and identify milk to energy ratio. Ice discharge was also tested with a heat simulated room and an FCU to study melting rate. A controlled room (climate chamber) was configured to control ambient temperatures for all experimental campaigns. The measuring and control devices, as well as the experimental systems and the methodological approaches, were discussed. In addition to this, the appropriate scenarios and variables were defined for each set up together with the measurement data points. The energy balance equations and the material properties were specified for system performance evaluation purpose. In general, the experimental system setting, sequencing, and configurations were discussed in this chapter.

Chapter four is all about results, analysis and discussion on findings. The influence of varying compressor power input and surrounding ambient on ice storage performance was experimentally evaluated. The daily masses of ice produced for different scenario were presented together with the energy input for each case. The heat losses to the surrounding ambient were quantified using measured temperatures and cabinet material properties. The system COP was analyzed against the optimum operating range. Besides the operating performance characterization, the systems energy demand was predicted based on the experimental results. The result for the ice-thickness development rate on the evaporator surface was discussed using

phase change processes of the water-to-ice temperature profile. The milk (water as a milk substitute) and the heat transfer fluid temperatures at various representative locations were utilized to generate the milk cooling curves. Effects of recirculation rate and energy density on milk cooling, milk cooler preservation performance, and chilled water temperature variations were analyzed. A tabular relation was formulated that relates the range of milk volume to be cooled with the ice storage operating conditions. The external-melt-ice-on-surface discharge for cold room application was evaluated using a closed hydraulic circuit with a heat simulated room and a FCU.

General conclusions and recommendations on overall system development were addressed in **chapter five**. Here, the main findings, as well as future recommendations, were outlined.

Chapter 2
Development and Fabrication of the Ice-Storage System

2.1 Introduction

Ice is an excellent medium owing to its higher thermal capacity to store thermal energy to satisfy an instantaneous cooling load demand. The ice production technique can be either static or dynamic based on the system design. The thermal energy storage system where ice is stored on the evaporator surface until needed by the load is called the static ice-storage system. Thus both the ice production and storage is accomplished within a single system as opposed to a dynamic ice-storage system where a separate medium for storing ice is required. A direct expansion, static ice storage system shown in Fig.2.1 where refrigerant directly absorbs heat from the water to build ice on the evaporator surface was implemented in this research.

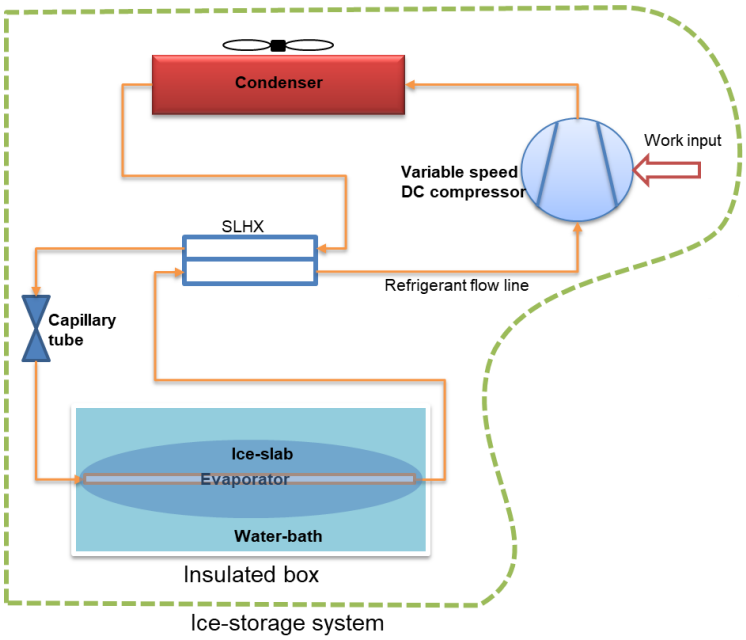

Figure 2. 1 Schematic diagram of the vapour compression refrigeration cycle unit with the insulated box as ice production and storage compartment

The system development process starts from refrigeration system capacity definition followed by components specifications, fabrication and testing. A 100 L capacity cabinet filled with water was assumed to produce on average a 20 kg of ice per day. Effects of insulation materials on transmission heat gain were analyzed from which a suitable insulation material and thickness

were identified. Based on a calculated heat load for the cabinet, a DC compressor and other standard components were specified for vapour compression refrigeration cycle considered. After several preliminary tests, the parameters for refrigerant charge optimization were defined, and the experiment was performed. Thus, the refrigerant charge and the capillary tube dimensions were optimized for the best operating point at 3500 rpm and 30 ℃ to maximize performance and avoid suction temperature drop. In this chapter, the ice storage system development and fabrication are covered.

2.2 The vapour compression refrigeration unit

The vapour compression refrigeration cycle unit is the main part of an ice storage system fabricated and tested in this research. This unit is composed of main components, namely compressor, evaporator, condenser and expansion device. The refrigerant flows through the cycle by removing heat from the space to be cooled (evaporator section) and rejects it through the condenser to the heat sink, as shown in Fig.2.2.

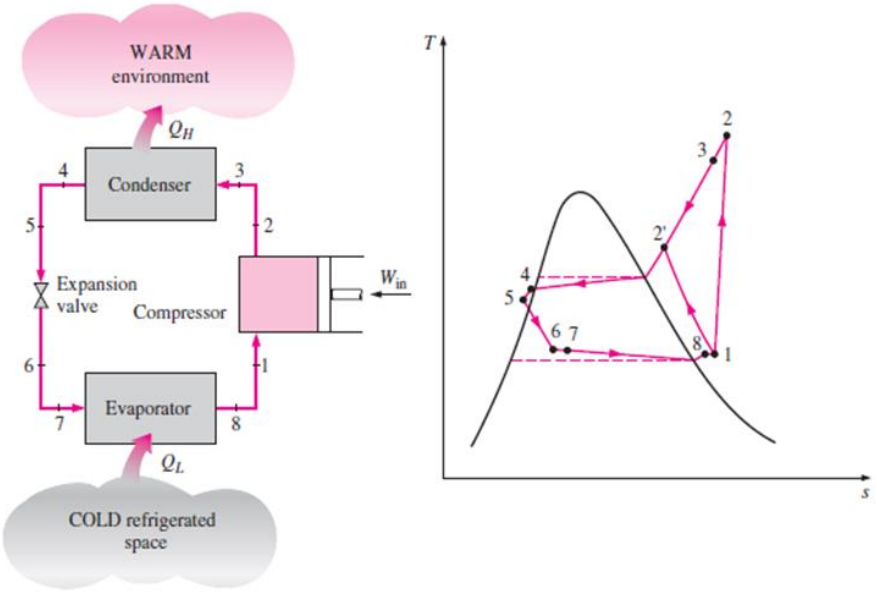

Figure 2. 2 Schematic and T-s diagram for actual vapour compression refrigeration cycle [60]

A compressor moves the refrigerant from low temperature, low-pressure region (evaporator) to high temperature, high-pressure region (condenser). The capillary tube reduces the condenser pressure to evaporator pressure without changing the refrigerant phase. It also regulates the refrigerant mass flow rate. The thermodynamic cycle continues as the refrigerant changes its

phase inside the evaporator by absorbing heat from its surrounding. The suction-line heat exchanger was included with the current system to superheat the refrigerant leaving the evaporator by subcooling the refrigerant leaving the condenser. In this section, the refrigeration load calculation and components specification were covered from which fabrication and testing follow.

2.2.1 The heat load calculation for the cabinet and selection of insulation materials

The refrigeration load mainly composed of product cool down, load due to fan and lighting, infiltration due to door openings, latent heat of fusion during ice formation and heat gain by conduction through the wall of the ice storage system shown in Fig.2.3.

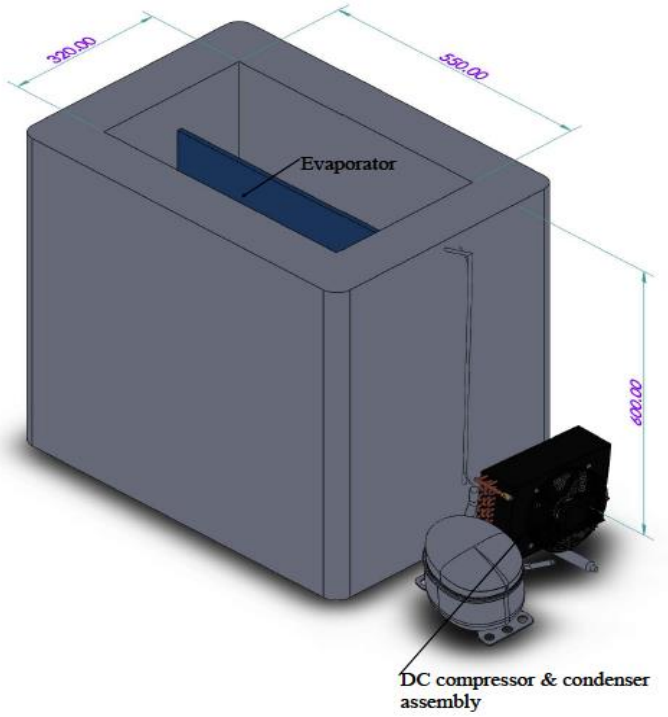

Figure 2. 3 The refrigeration cycle unit configuration with insulated compartment

The product cool download depends on the product mass, initial and final temperatures, and the required cooling time for the product. This load can be very high and will require a higher compressor capacity. Since sensible cooling of water is not recurring on a daily basis for the ice storage system considered, cool down was assumed to be negligible. There is no evaporator fan and lighting requirement for the system. The ice-storage operation would not demand frequent door opening. Also, air infiltration load would be negligible if any since cabinet would be filled

with water at 0℃ while in operation. The daily ice mass depends on system performance and other operating parameters like varying compressor speed and refrigerant charge so that it would be a required output. Thus, the small capacity unit is assumed to produce in average 20 kg ice per day which would be equivalent to 76 W under continuous operation. If 80% compressor operation time is considered, this load could be 90 W.

The rate of heat gain through the wall is governed by Fourier's law, as shown in Eq. (2.1).

$$Q = -\frac{kA\Delta T}{l} \tag{2.1}$$

The insulation thickness (l) and thermal conductivity (k) play an important role in heat load reduction through the area (A) due to a temperature difference (ΔT). For the internal cabinet dimension of (550mmx320mmx600mm), the calculated heat gain through the wall showing the comparison between different insulation types and thickness was presented in Fig.2.4.

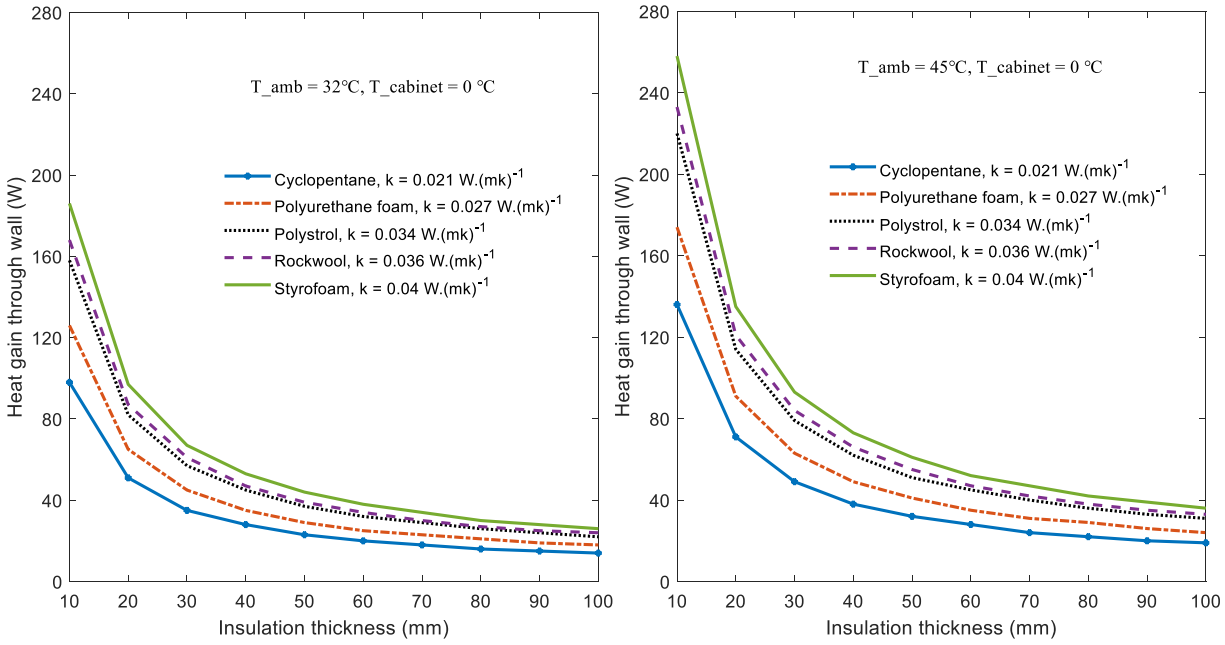

Figure 2. 4 Cabinet heat loss vs insulation materials

Five different insulation materials were evaluated for their effect on heat gain through the wall of the cabinet (insulated box). Operating temperatures of 32℃ and 45℃ were considered as representative ambient conditions. Smaller insulation thickness causes higher heat gain through

the transmission. For the same heat duty, it was also shown that insulation materials with lower thermal conductivity require less thickness compared with insulation materials with higher thermal conductivity.

By changing the operating ambient temperature from 32℃ to 45℃, the response of the cabinet with ambient was analysed. Besides the problem of higher transmission heat gains, smaller insulation thickness cause increased heat fluctuations with ambient temperature change as shown in Fig.2.5. A 13 ℃ change in ambient temperature resulted in 38 W and 72 W transmission heat gain changes respectively for cyclopentane and Stayrofoam both at 10 mm thickness. Increasing the insulation thickness to 40 mm, reduced the change in transmission heat gain to 10 W and 20 W, respectively. However, a 100 mm thick Styrofoam would be required to minimise the change in transmission heat gain to 10 W due to a 13 ℃ ambient change.

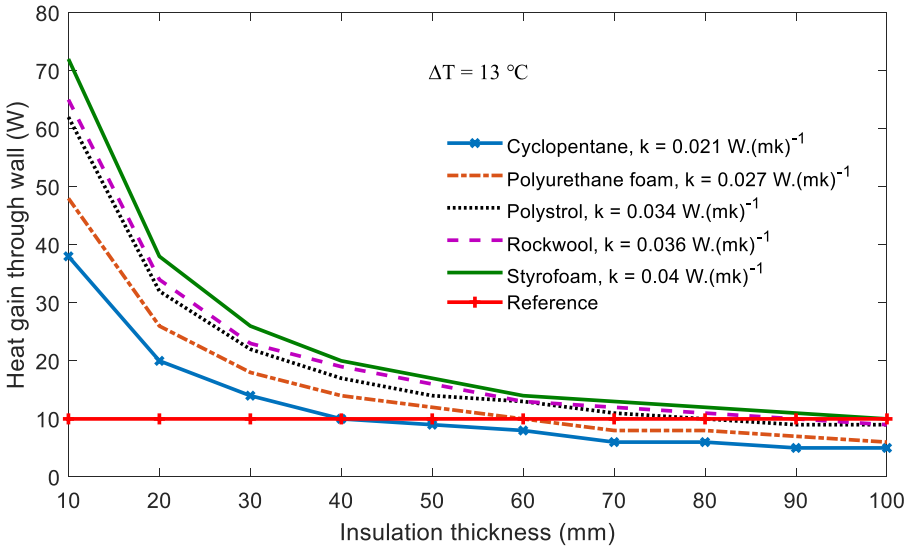

Figure 2. 5 Cabinet heat loss vs insulation materials showing equivalence of thickness

Even though the insulation material selection needs economic analysis besides several other requirements, for the cabinet considered in this case, a thickness above 50 mm provides relatively smaller improvements in transmission heat loss as shown in Table 2.1.

Table 2. 1 Percentage improvement in transmission heat loss with insulation thickness

Insulation thickness (mm)		20	30	40	50	60	70	80	90	100
Improvement in transmission loss (%)	k = 0.021 /m.K	48	31	21	17	14	11	12	7	7
	k = 0.04 W/m.K	48	31	20	18	13	10	11	6	7

Insulation materials with lower thermal conductivity will have a lower system size compared with ones with higher thermal conductivity. As presented previously, a 40 mm cyclopentane will have similar insulating effect with a 100 mm Styrofoam. However, because of availability, initial cost, and structural firmness, a 100 mm thick Styrofoam was selected in this research. With this selection, the transmission heat load could be 26 W for operation at 32℃ and 36 W for operation at 45℃ ambient temperatures. Thus the total refrigeration capacity would be in the range of 120 to 130 W.

2.2.2 Specifications of the cycle components

2.2.2.1 Compressor

In the refrigeration cycle unit used for the ice storage system, the compressor is an important component that compresses the refrigerant to the condenser pressure. It can usually be represented by three equations for refrigerant mass flow rate, power input, and enthalpy change across the compressor. The refrigerant mass flow rate ($\dot{m}$) is a product of density, volume flow rate and volumetric efficiency as shown in Eq.(2.2). Volumetric efficiency (η_v) indicates the ratio of compressor discharge volume against the suction volume. Because there is a clearance volume inside the reciprocating type compressor, the volumetric efficiency is associated with the compressor geometry. The refrigerant density (ρ_i) and volume flow rate ($\dot{V}_s$) needs to be specified at a given flow condition and state of refrigerant.

$$\dot{m} = \rho_i \dot{V}_s \eta_v \tag{2.2}$$

The governing equation for the compressor power input ($\dot{E}$) is formulated based on the isentropic work done ($h_{is} - h_i$) on the refrigerant to compress it from suction to discharge pressure and is given in Eq. (2.3). The compressor efficiency (η_c) can be provided from manufactures based on performance data.

$$\dot{E} = \frac{\dot{m}(h_{is} - h_i)}{\eta_c} \tag{2.3}$$

By linking the isentropic enthalpy change across the compressor with compressor efficiency and surrounding ambient the actual enthalpy (h_o) at the exit of the compressor can be evaluated, and it is shown in Eq.(2.4). The isentropic enthalpy (h_{is}), enthalpy at the inlet of the compressor (h_i),

and heat loss from the compressor to the surrounding ambient (ξ) are parameters to be specified at a given refrigerant flow condition and surrounding ambient.

$$h_o = h_i + \frac{h_{is} - h_i}{\eta_c}(1 - \xi) \quad (2.4)$$

Compressors are generally specified to satisfy a known cooling capacity and match the operating pressure range. *Secop* heat load calculation software [61] was used in this research to specify the compressor to satisfy a refrigeration load of 120 to 130 W capacity. Accordingly, the BD35K [Nidec] compressor [62] with HFC-free refrigerant (R600a) was specified. The variable speed ranging from 2000-3500 rpm and lower starting current makes this compressor suitable for off-grid applications with ice as the energy storage medium. The compressor run time also affects the compressor capacity and corresponding power input. This is demonstrated in Fig.2.6 by varying the compressor run time for a fixed cooling capacity using Secop heat load calculation software. The evaporating temperature was maintained at -10 ℃ while the *Styrofoam* insulation thickness was 100 mm for all calculations.

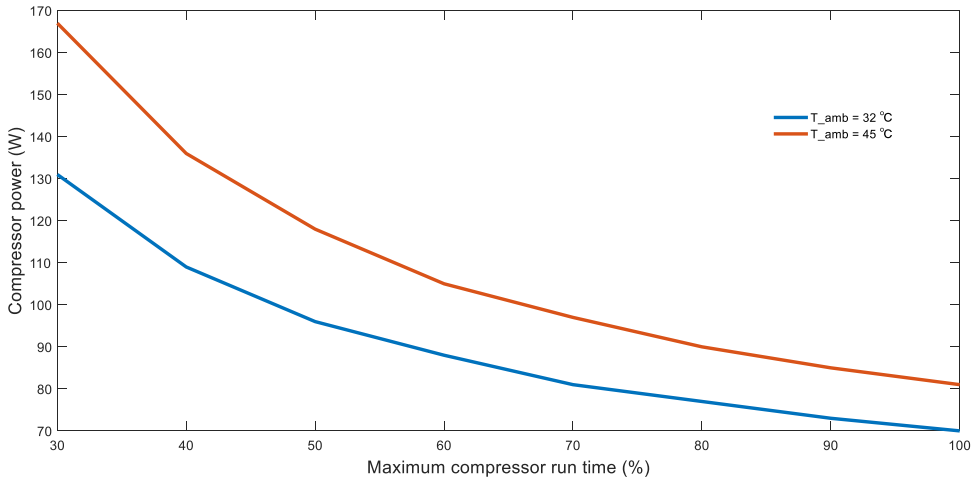

Figure 2. 6 Compressor capacity variations with the maximum run time

The figure shows that as the compressor run time increases, the required compressor capacity decreases. Lower run time results in a reduced cooling capacity in actual systems since the compressor is selected for a known capacity range. Considering the current ice storage system, maximum compressor run time above 85 % would be sufficient even though continuous operation could increase the daily output.

2.2.2.2 Heat exchangers and the capillary tube

Both the evaporator and condenser components are the major heat exchange devices in a refrigeration system. The roll-bonded plate evaporator and compact air-cooled condenser of a box cooler [63] were implemented for the proposed ice storage application. Hence, the technical specifications of the basic components of the vapour compression refrigeration cycle unit were presented in Table 2.2. The capillary tube length and the refrigerant charge were experimentally evaluated and will be explained in the next sections.

Table 2. 2 Technical data of the components of vapour compression refrigeration cycle unit

Dimensions			
Overall (Width, Depth, Height)			250 x 600 x 650 mm
Evaporator: Roll-bonded aluminum plate with U-pattern tube	Flat surface (W x H)		510 x 540 mm
	Tube channel length		9000 mm
	Tube channel diameter		6 mm
Condenser: Compact cross-flow, air-cooled, staggered tube arrangement, aluminum fins on copper tubes	Tube length		130 mm
	Number of rows		2
	Number of tubes per row		6
	Longitudinal tube spacing		15
	Transverse tube spacing		18
	Tube internal diameter		7 mm
	Heat exchanger width		960 mm
	Number of fins		33
	Fin size (WxH)		33 x 110 mm
	Fin thickness		0.1 mm
	Fin density		344 fins/m
	Fan capacity		3 Watt
Capillary tube:	Length		4 - 6m
Compressor: Danfoss hermetic system, manufactured by Secop-Nidec	*Secop* (BD35K)		Variable speed DC compressor
	Capacity: 40W at 2000 rpm (min speed) 70 W at 3500 rpm (max speed)		
Refrigerant	R600a, charge: Min. 20g, Max.120g		
Connected voltage:		12 V/DC	24 V/DC
Rated current:		6.2 A Max	3.1 A Max
Fuse:		15A	7.5A

2.4 Fabrication of the refrigeration unit (the cooling unit)

The refrigeration unit was fabricated using the basic dimensions specified and other accessories like pipes and filters with required standards. A specialized company (TM Technischer

Gerätebau GmbH | Böttgerstr. 13 | D-89231 Neu-Ulm) performed the assembling process, including welding and refrigerant filling. Fig.2.7 shows a picture of the unit developed for subsequent test and performance evaluation.

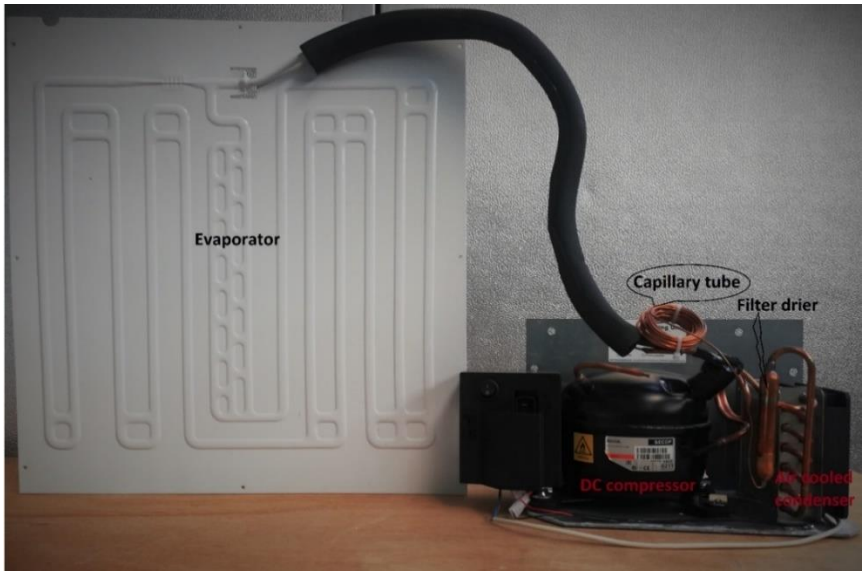

Figure 2. 7 Picture showing the basic components of the refrigeration cycle unit fabricated

Fabrication of the insulated compartment, assembling of the ice storage system and optimizing refrigerant charge and capillary tube length at the typical best operating point will be dealt in sections 2.5 and 2.6.

2.5 Fabrication of the ice-storage system

The ice storage system in this research is an assembly of the refrigeration cycle unit with an insulated compartment. This system was fabricated at the mechanical workshop of the Hohenheim University, Stuttgart using a modular refrigeration cycle unit and an insulated cabinet. The basic considerations in the fabrication of the insulated cabinet include waterproof, structural stability, good insulating characteristics, corrosion resistance, accessibility for cleaning and drainage, durability, maintainability, and mobility. The 1.5mm thick sheet metal was used for internal lining. Styrofoam insulation materials together with a wooden box as external structures were used to minimize transmission heat loss and provide structural stability.

The basic processes in the metal box fabrication include layout preparation, cutting, bending and welding. To avoid rust and other impurities on metal surface after welding, the welded surface

was cleaned with electrochemical welding method by using electrolytic fluids and a weak electrical current. Following this process, the metal box was externally insulated using glue to fix the foam with the metal surface. Finally, the refrigeration cycle unit was assembled with an insulated compartment, as shown in Fig.2.10 c. In this case, the evaporator was positioned at the center of the insulated box to avoid constrained growth of ice on the surface. The compact heat exchanger (condenser), compressor and capillary tube assembly were positioned at the external support structure of the insulated cabinet. The final step in the ice-storage system development and fabrication was the optimization of the unit for a given operating point. For this specific case, seven refrigeration units with varying parameters (different refrigerant charge and capillary tube lengths) were manufactured. A suitable refrigerant charge and capillary tube length were identified through experimental work and is covered in section 2.6.

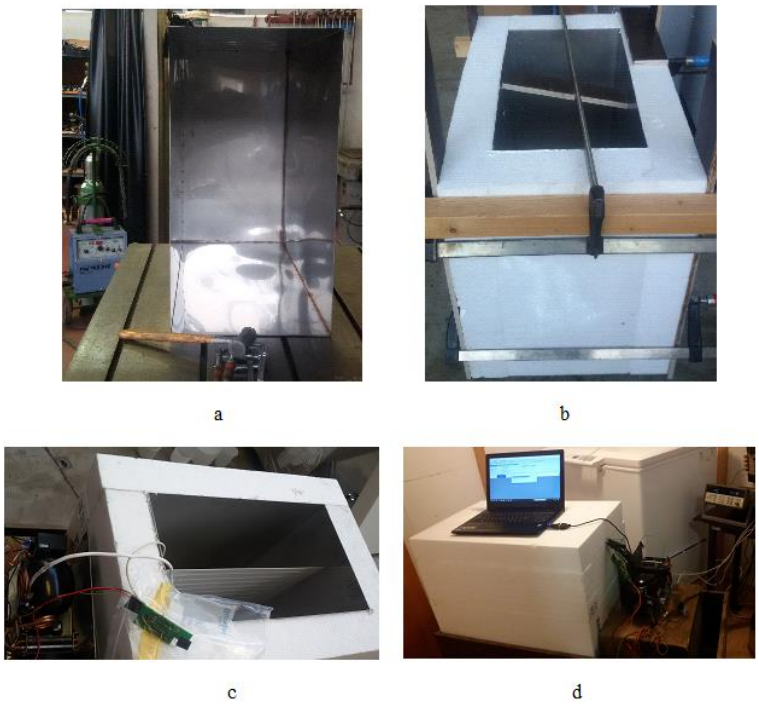

Figure 2. 8 Pictures from fabrication process in the workshop (a) Cutting, bending and welding of the metal box (b) Fixing insulation to the metal box (c) Assembling VCRC unit with insulated box (d) Functionality testing in a climate chamber

2.6 Experimental optimization of the capillary tube length and refrigerant charge

The refrigerant charge and capillary tube dimensions are important design parameters. The flow restriction by capillary tube depends on its diameter and length. At a given internal diameter, the

longer the capillary tube length, the slower the flow will be and vice versa. The capillary tube is usually selected without optimization process, but the refrigerant charge should be optimized to minimize energy consumption. However, an absolute reduction in energy consumption could be achieved if the capillary tube and refrigerant charge are modified at the same time [64]. Even though it is a costly option to consider, the experimental approach provides a practical range of system variables for operation in water-bath and hence capillary tube size and refrigerant charge variation was analyzed experimentally in this research. The system performance reduction could be due to both undercharged and overcharged systems. At the same, many combinations of refrigerant charge and capillary tube dimensions could give a similar performance value. Moreover, the refrigerant charge also affects the sub-cooling at condenser exit, and the evaporator superheating, which in turn affect the cooling capacity.

A preliminary experiment was carried out to identify a suitable range of refrigerant charge and capillary tube dimensions to consider. Accordingly, shorter lengths of 0.6 m to 1 m and internal diameters of 0.8 mm and 0.7mm were considered at refrigerant charges of 35 - 50 g. Due to poor performance in those ranges, higher capillary tube length case was chosen for optimization. Therefore, the capillary tube length varied from 4 to 6 m by keeping a fixed diameter of 0.7 mm for the current setup. The refrigerant charge was varied from 30 to 50 g. In addition to the refrigerant charge, the system performance is sensitive to ambient temperature. If the system is determined to be optimum at a given temperature, the performance will decrease if operated either at higher or lower ambient temperatures based on the refrigerant charge. An ambient temperature of 30 ℃, which is near to standard refrigerator test condition of 32 ℃, was used in this case. Since higher cooling capacity is the main priority, the compressor speed was fixed at its maximum value. Hence, an experiment was carried out to determine optimum capillary tube length and refrigerant charge for operation at a 3500 rpm and a 30 ℃ ambient temperature.

2.6.1 Experimental setup

Three different capillary tube lengths and five refrigerant charge amounts shown in Table 2.3 were considered. Type K thermocouples, data logger, a DC power source and a climate chamber for controlled ambient were among materials used. The schematic representation of the experimental setup with a single refrigeration cycle unit is shown in Fig.2.11. However, independent units with varying refrigerant charge and capillary tube length were used in this

research. For this purpose, a vapour compression refrigeration cycle units shown in Fig.2.12 with varying capillary tube and refrigerant charge combination were manufactured. Hence, an experimental test setup shown in Fig.2.13 was implemented to identify an optimum configuration among the units considered.

Table 2. 3 The refrigerant charge and capillary tube lengths considered for experimental optimization

Test unit code	Test unit serial no.	Refrigerant charge (g)	Capillary tube length (m)
1	TU-101181014581	50	4
2	TU-101181014584	45	4
3	TU-101181014585	40	4
4	TU-101181014588	35	4
5	TU-103181216423	35	5
6	TU-103181216425	35	6
7	TU-103181216426	30	4

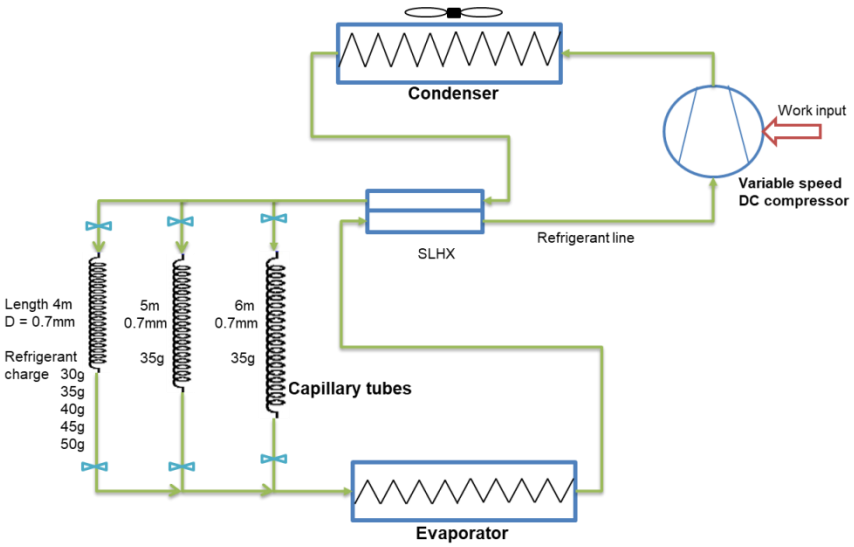

Figure 2. 9 Schematic of the refrigeration unit showing varying capillary tube lengths and refrigerant charge

Figure 2. 10 Pictures of refrigeration units manufactured for testing and evaluation purpose

The water temperature inside the insulated cabinet and the climate chamber temperature was measured and monitored. By measuring the current flow at a fixed voltage, the energy consumption of a DC compressor was evaluated.

Compressor suction line temperature was measured as an indicative parameter for suction line pressure drop. The cooling effect, the energy consumed, and corresponding system COP were evaluated using Eqs. (2.5), (2.6), and (2.7) respectively.

$$Q_{cooling-effect} = (m_{water}.C_{P-water}.\Delta T_{water} + UA.\Delta T_{ambient-water}\Delta t) \quad (2.5)$$

$$E_{comp} = \sum VI\Delta t \quad (2.6)$$

$$COP = \frac{Q_{cooling-effect}}{E_{comp}} \quad (2.7)$$

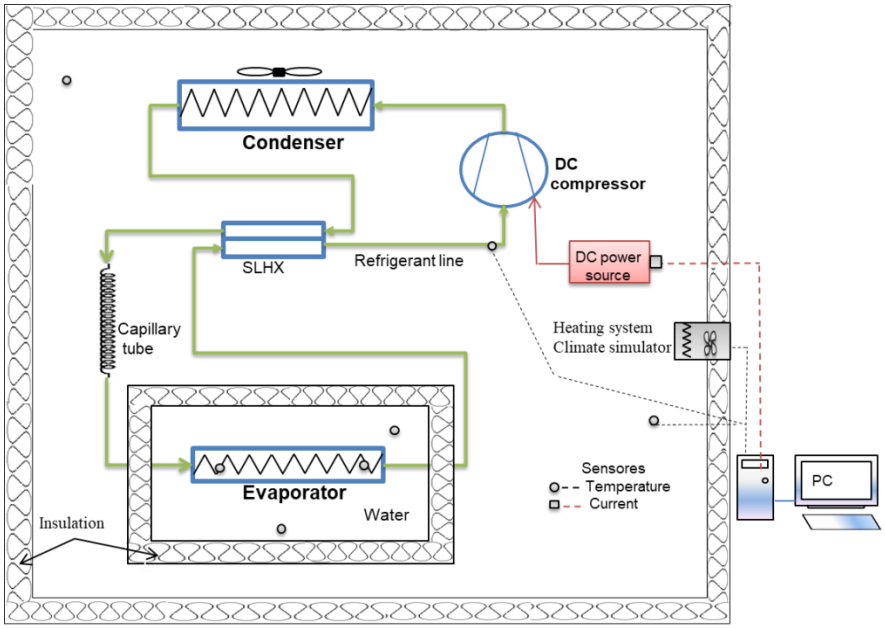

Figure 2. 11 Experimental set-up for VCRC unit optimization test

2.6.2 Capillary tube vs refrigerant charge

Fig.2.14 shows the effects of refrigerant charge and capillary tube length on system performance. For a given capillary tube length of 4 m, the maximum COP was obtained at a refrigerant mass of 35 g. For both refrigerant quantities below and above 35 g, the system COP obtained was relatively lower. The experimental result on the effect of varying capillary tube length at a fixed refrigerant mass of 35 g was also presented on Fig. 2.14. It was observed that the effect of capillary tube length was not significant as refrigerant charge even if the 4 m length gives relatively better performance over the 5 and 6 m values. In general, it was observed that increasing the refrigerant charge above 35 g for the same capillary tube geometry resulted in a decrease in system performance. The trend observed in Fig.2.14 agrees with the results of experimental and simulation work reported by Pisano et al. [64].

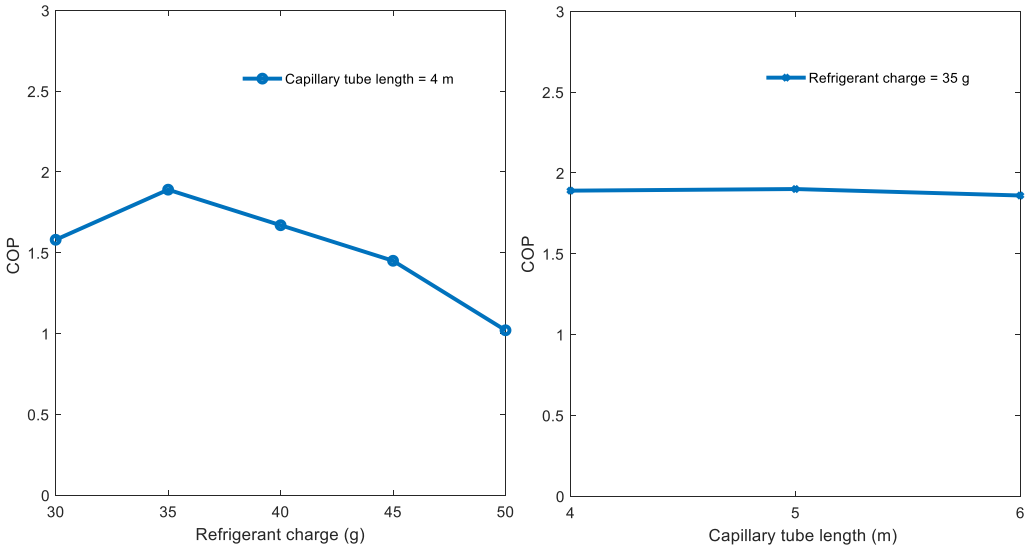

Figure 2. 12 Effects of refrigerant charge and capillary tube length on COP

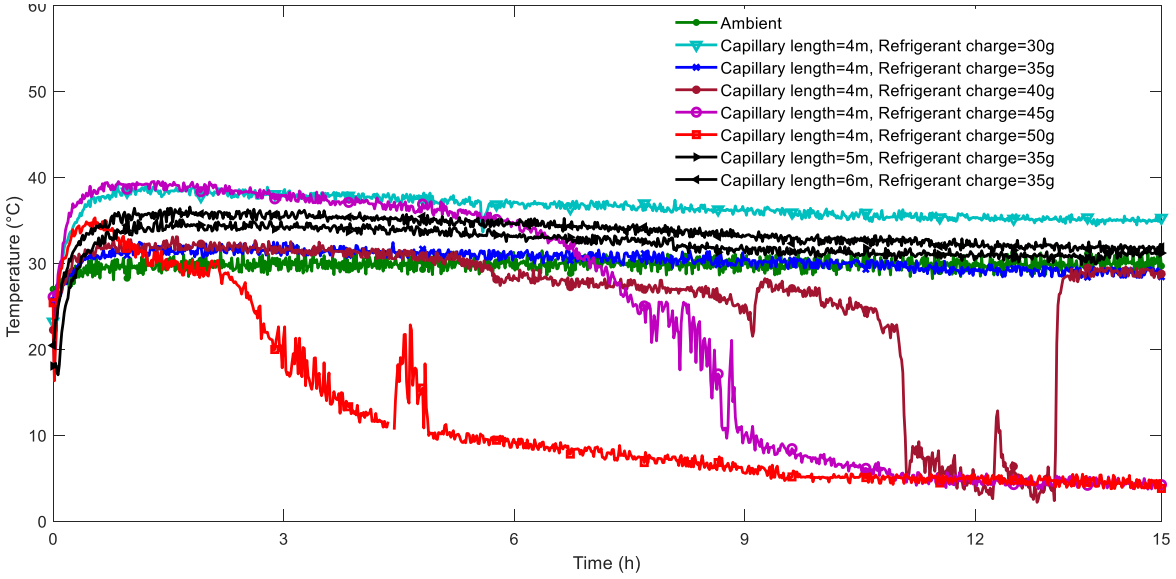

Figure 2. 13 Effects of refrigerant charge and capillary tube length on suction line temperature

Effects of refrigerant charge and capillary tube length on suction line temperature were shown in Fig.2.15. Theoretically, the suction line pressure should be slightly above the surrounding pressure, and the suction line temperature also indicates the state of the refrigerant entering the compressor. A refrigerant charge of 40, 45, and 50 g resulted in a suction line temperature drop below the surrounding ambient. Besides this, the suction temperatures were below the dew point

temperature at 30℃, causing the suction line frost as shown in Fig.2.16. Hence, it was possible to assume that there would be a liquid introduced into the refrigerant compressor at this low suction temperature condition. It is known that the liquid introduction to the compressor will damage the compressor blade through erosion and corrosion.

For a capillary tube length of 4, 5, and 6 m plus a refrigerant charge of 30 and 35 g, the suction line temperature was above the ambient temperature of 30℃. This implies that the objective of avoiding water condensation at the suction line is achieved at these operating conditions. But longer capillary tube length and lower refrigerant charge resulted in higher suction line temperatures which will, in turn, cause a decrease in COP. Hence, it was possible to conclude that a capillary tube length in the range of 4 - 6 m and a refrigerant charge of 30-35 g would be suitable for the small capacity refrigeration cycle unit considered. Besides these range of values, the combination of a 4 m long capillary tube and 35 g refrigerant charge could be taken as optimum values for operation at 3500 rpm and 30℃ ambient temperature.

Figure 2. 14 Suction frost observed at evaporator exit and compressor inlet lines for three of the seven scenarios

Besides the performance in water-bath, the minimum no-load evaporating temperature under air was evaluated at a fixed operating point, and the results were presented in Table 2.4. It was observed that a refrigerant charge of 35 g at 4 m capillary tube length achieved evaporating temperatures of -16.5 ℃. Moreover, the evaporating temperature increased with increase of the refrigerant charge.

Table 2. 4 No-load evaporating temperature limit of the VCRC unit fabricated for varying capillary tube length and refrigerant charge

Capillary tube length (m)	Refrigerant charge (g)	Minimum evaporator temperature in air (℃)
4	50	-6.5
	45	-7.5
	40	-10.5
	35	-16.5
	30	-17
5	35	-16
6	35	-17.5

2.7 Conclusions

In this chapter, the refrigeration system capacity was analyzed and used to specify the cycle components. Standard components (Compressor, condenser, evaporator, capillary tube and auxiliary pipes) were specified and used to manufacture the refrigeration cycle unit. An ice storage system with 40-70 W DC compressor capacity was developed and fabricated. An insulated compartment composed of stainless steel, Styrofoam, and wooden box was manufactured for use as a cabinet for the water-bath. Suitable refrigerant charge and capillary tube length were experimentally optimized for best operating point at 3500 rpm and 30 ℃ ambient temperature. A refrigerant charge both below and above 35 g resulted in a reduction of system performance while varying capillary tube length at a fixed refrigerant charge did not bring a significant change on system performance. A drop in suction line temperature occurs for a refrigerant charge above 35 g. Considering the system performance, suction line temperature and minimum no-load evaporating temperature, a capillary tube length of 4 m and a refrigerant charge of 35 g would be a suitable option for the refrigeration cycle unit developed in this research. Operations at best efficiency point and other off-design scenario will be covered in the subsequent chapters under ice making process. Experimental setups for performance characterization of the ice storage system together with the milk cooling and cold room applications will be discussed in chapter three.

Chapter 3
Experimental Setups for Performance Characterizations

3.1 Introduction

The development and fabrication of the ice storage system using a DC-powered vapour compression refrigeration cycle unit were covered in chapter two. The refrigeration cycle unit was optimized for a single best operating point of 3500 rpm and 30 ℃. However, the system should be characterized for different operating conditions to analyze best efficiency points and evaluate the off-design performances. Investigations of the ice storage system for milk cooling and cold room applications were also important aspects of being studied for the small scale cooling system proposed. In the ice-storage performance characterization, the effect of varying the compressor speed and surrounding ambient temperature on the amount of the daily ice production, the energy demand, the COP, and the temperature variation on evaporator surface were evaluated. This would provide original information and data on the system performance as a result of varying parameters.

The system scale-up and application diversification is another important aspect of the research work performed. A liquid solidification experiment in a rectangular space under the influence of free convection to evaluate the ice layer thickness on the evaporator surface under varying boundary conditions was performed. This helps to analyze the spacing of multiple modular units in the parallel arrangement within an insulated compartment for the ice storage capacity scale up. The application diversification was also demonstrated through the evaluation of the milk cooling, preservation and heat load simulated cold room performance using chilled water from the ice storage system. To this end, several materials, methods and experimental procedures were involved in addressing the objectives set for the research work. Hence, a detailed experimental approach utilized for the ice making process, water-ice phase change process, milk cooling and preservation, and ice discharge for cold room application were presented in this chapter.

3.2 The ice-making process

Here, we consider the refrigerant flows through a channel of roll-bond plate evaporator immersed in a pool of PCM, as illustrated in Fig. 3.1 and Fig.3.2. The PCM used for the current study is water. The refrigerant absorbs heat from the surrounding water by forming ice-slab on both sides of the evaporator surface, as shown in Fig.3.1. An ice layer starts to form after nucleation or phase transition state, the condition at which all the water mass inside the ice-storage is crystalized as seen in Fig.3.2c. Several factors affect the daily output of the system; however; the compressor power input and condenser pressure variation are the main factors among others. In this research, experimental studies were carried out to explore the effects of operating compressor speeds, and ambient temperatures on the energy consumption, evaporator surface temperature variation, and the daily ice production of a DC powered ice-storage system developed. The system COP, monthly and annual energy demands of an ice-storage system with a single cooling unit operation was also evaluated based on the experimental data. A DC power was supplied to the compressor instead of powers from PV for the test at the laboratory level.

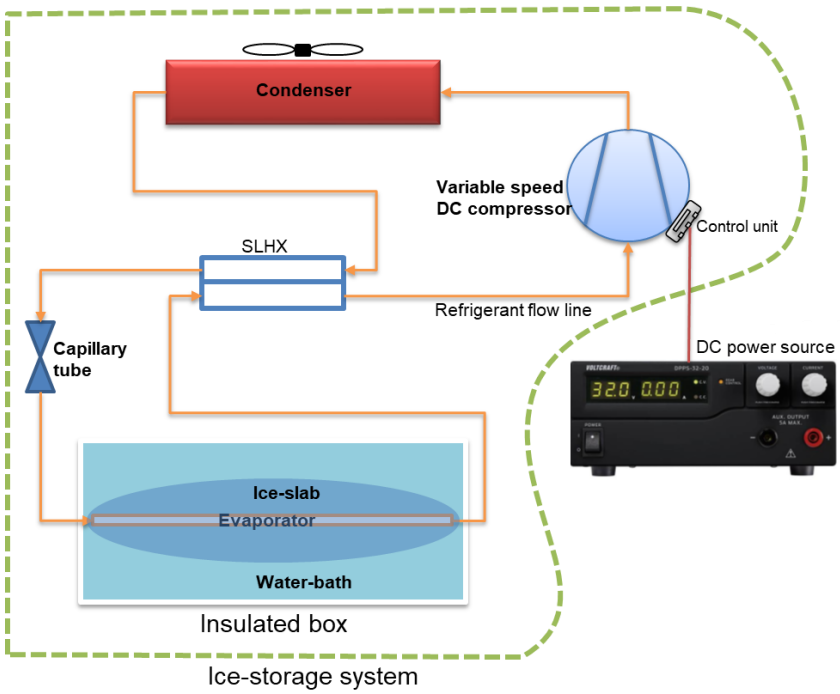

Figure 3. 1 Schematic representation of the experimental ice-storage system

This section of the set up mainly consists of a climate chamber, an insulated metal box with 100-litre capacity, a vapor compression refrigeration unit (Serial No. 103181216423, TM89293 Neu-

Ulm, Germany), a DC power source (DPPS-32-20, Voltcraft), a data logger (Agilent-34970A), thermocouples (Type-K), a digital measuring balance, a DC pump, a climate chamber controller and a PC. The insulated metal box made from stainless steel had a thickness of 1.5mm and dimensions of 55cmx32cmx60cm (LxDxH). The insulation material was made of Styrofoam with a thickness of 10 cm and a thermal conductivity of $0.04 W.m^{-1}K^{-1}$. The refrigerant R600a circulates through the evaporator coil of the cooling unit by absorbing heat directly from the water inside the insulated metal box.

The roll-bond plate evaporator measuring 51cm x 54cm (LxH) was positioned at the centre of the ice-storage, as shown in Figure 2b. BD solar compressor Secop (BD35K) with a voltage range of 10-45 V DC and maximum power consumption of 70W was used. The air-cooled condenser and capillary tube (4 m length and 0.7 mm-inner diameters) are integral parts of the cooling unit used. The climate chamber for this experiment is an insulated room designed to maintain the required temperature in the experimental laboratory.

The ice-storage system was filled with a 100-litre water after the evaporator, and all the thermocouples had been mounted in their respective positions. Setting the required compressor speed and climate chamber temperature are parts of the initial procedure to start the experiment. The compressor speeds in the experiments were set to 2000 and 3500 rpm sequentially. In addition, three constant ambient temperatures of 25℃, 35℃, and 45℃ were set in the climate chamber. The two compressor speeds and three constant temperatures comprised six different scenarios for analysis. Configurations for temperature logging, voltage, and current consumption measuring were tasks performed before starting the operation. The ice-storage system worked for 24 hours after initiation of the phase change process as shown in Fig.3.2c.

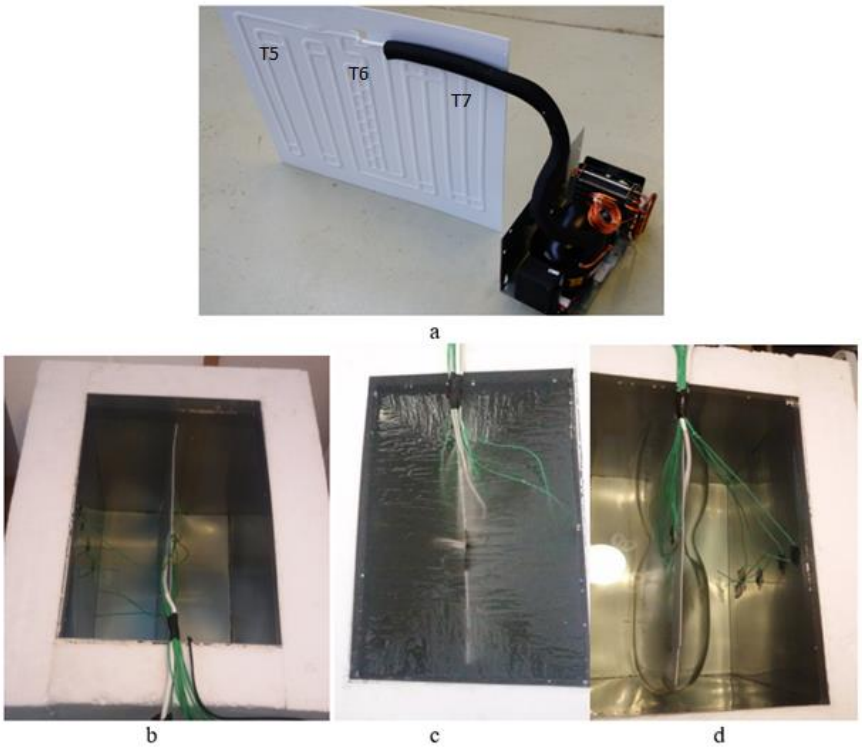

Figure 3. 2 Pictures of the experimental platform (a) cooling unit showing refrigerant flow pattern and sensor locations on evaporator plate (b) the insulated box filled with water after fixing cooling unit and sensors (c) initiation of the phase change (d) ice formation at the end of daily operation

3.2.1 Measuring the evaporator surface temperature

The uniformity of the temperature distribution on the evaporator surface depends on the geometry of the evaporator and the capillary tube, the amount of refrigerant in the system, the compressor speed and the surrounding ambient temperature [64]. The rate of the refrigerant flow through a capillary tube, on the other hand, always increases with an increase in inlet pressure [65] which corresponds to the condenser pressure. Increasing the compressor speed at the same evaporator geometry also increases the refrigerant flow rate. The aim here was to determine the temperature distribution on the evaporator surface at different working conditions. Therefore, three representative locations were identified so that temperature sensors were placed at the refrigerant inlet surface (T_5), the refrigerant exit surface (T_6), and the intermediate surface (T_7) as a representative points shown in Fig. 3.2a and Fig.3.3.

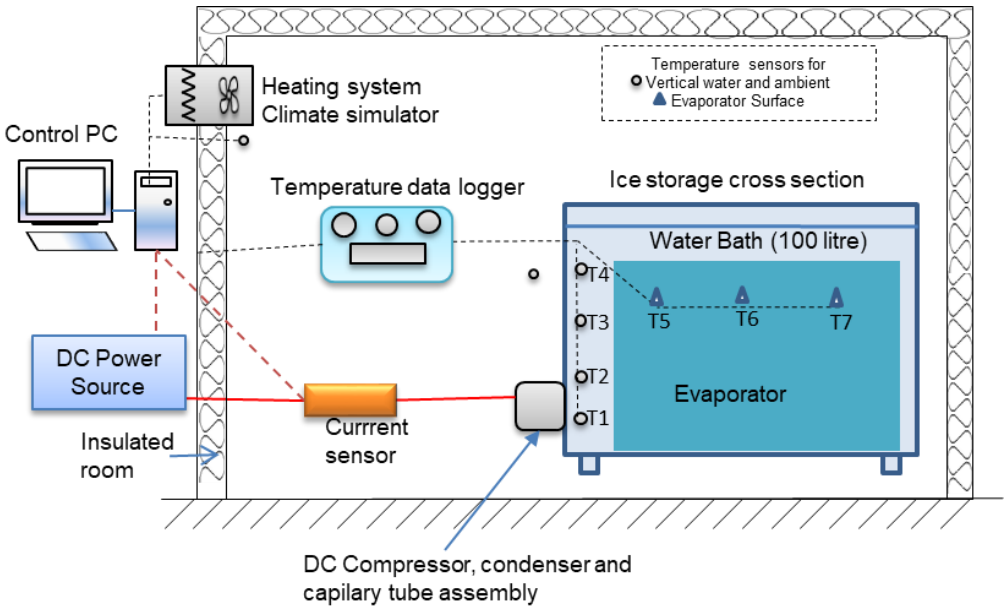

Figure 3. 3 Experimental set up for ice-storage system performance evaluation

3.2.2 Quantifying the ice mass and the energy stored

At the end of each experiment, water from the ice-storage was pumped to a container on a calibrated digital measuring balance to determine the amount of ice formed. The mass of ice was quantified by subtracting final water mass from initial water mass. Losses in the pump were also determined for each measurement by accounting the wet and dry weight difference of the pumping system. Hence, the daily amount of energy stored was evaluated using Eq.(3.1).

$$Q_{ice} = (m_{ice} * h_{fg-ice} + m_{ice} C_{P-ice} \Delta T_{ice}) \quad (3.1)$$

3.2.3 The DC power supply and energy demand prediction

A DC power source supplies the required electrical power for the ice-storage system as indicated in Fig.3.3 of experimental system configuration. The voltage was kept constant at 26 V for all experiments, and the current flow was measured every 50s to quantify the energy consumption. The instantaneous electrical power consumed by the compressor was evaluated using Eq. (3.2)

$$W_{comp} = V\ I \quad (3.2)$$

The daily energy consumption of the system was calculated using Eq. (3.3) based on measured values of voltage, current and time.

$$E_{daily} = \sum VI\Delta t \tag{3.3}$$

The monthly and yearly energy demands of the system were determined by using Eq.(3.4) and (3.5), respectively.

$$E_{monthly} = E_{daily} * 30 \frac{days}{month} \tag{3.4}$$

$$E_{annuall} = E_{daily} * 365 \frac{days}{year} \tag{3.5}$$

3.2.4 Quantifying the overall system performance

The ice keeps the internal temperature of the ice-storage at nearly 0℃, even if heat is gained from the surrounding external environment. Thus, the refrigeration effect was calculated by quantifying both the energy in the ice-storage and the corresponding heat gain from the surrounding ambient through the insulated surface. The steady-state heat gain through the insulation of an ice-storage system was evaluated using Eq. (3.6). The evaluation of the ice-storage system's coefficient of performance is finally performed using Eq. (3.7). Based on the ice-storage geometry and insulation material property, the UA value for this experiment was 0.56 $W.K^{-1}$. The internal dimension of the ice storage was used to evaluate the surface area and mainly the 10 cm thick Styrofoam with thermal conductivity of $0.04W.m^{-1}K^{-1}$ was considered to evaluate the U-value.

$$Q_{gain} = UA\ \Delta T\ \Delta t \tag{3.6}$$

$$COP = \frac{Q_{ice} + Q_{gain}}{E_{daily}} \tag{3.7}$$

3.2.5 Experimental uncertainty analysis

Evaluating the overall uncertainty of experimental results depends on the uncertainty of individual parameters measured. Let a given experimental result P be a function of independent variables $x_1, x_2, x_3, \ldots x_n$ shown in Eq.(3.8). For such a result, the uncertainty in the overall result (u_P) can be evaluated using Eq.(3.9).

Where $u_1, u_2, u_3, \ldots u_n$ are the uncertainties of the independent variables

$$P = P(x_1, x_2, x_3, \ldots x_n) \tag{3.8}$$

$$u_P = \left[\left(\frac{\partial P}{\partial x1}u_1\right)^2 + \left(\frac{\partial P}{\partial x2}u_2\right)^2 + \left(\frac{\partial P}{\partial x3}u_3\right)^2 + \cdots + \left(\frac{\partial P}{\partial n}u_n\right)^2\right]^{1/2} \quad (3.9)$$

$$COP = COP(m_{ice},\ h_{fg},\ C_{P-ice}, \Delta T_{ice},\ UA, \Delta T_{\infty-w}, I, V) \quad (3.10)$$

Table 3. 1 Instrument parameters and measurement uncertainty

Parameter	Instrument range	Value	Uncertainty	Remark
Mass of ice, m_{ice}	0-60kg	13.96 - 26.28 kg	2%	Uncertainty arises due to digital measuring balance and reading error
Temperature difference, $\Delta T_{\infty-w}$	-50℃ - 260℃	25℃ - 45℃	±2℃	Uncertainty arises due to climate chamber temperature distribution
Temperature difference, ΔT_{ice}	-50℃ - 260℃	-5℃ - 0.5℃	±0.5℃	Uncertainty arise due to thermocouple measurement
Latent heat, h_{fg}	----	333 (kJ kg^{-1})	±0.5%	Uncertainty arise due to thermos-physical property selection
Specific heat of ice	-----	2040($Jkg^{-1}.K^{-1}$)	±0.3%	Uncertainty arises due to thermos-physical property selection
UA	----	0.56 W K^{-1}	neglected	
Electrical current, I	0-10A	0-3.5 A	±1.5%	Uncertainty arise due to electronic data logging
Phase change process time taken, Δt	----	24 hour	±1%	Uncertainty arises due to reading of start and stop time
DC voltage, V	10-45 V	26 V	neglected	

The ice-storage system coefficient of performance (COP) is a function of several independent variables indicated in Eq.(3.10). Since the system voltage and UA value were fixed during experiment, their contribution to uncertainty was neglected. Hence, based on the individual measurement uncertainty shown in Table 3.1, the overall uncertainty in the experimental result for the ice-storage COP was 3.09%.

3.3 The lateral ice-slab thickness

The design of an ice-storage system requires appropriate system sizing based on end-use load demand and characteristics of the phase-change process within the storage. The end-use load demand defines the overall storage size requirement, while phase change characterization helps to determine the actual system sizing. A narrow width of an ice storage size would cause a 100 % solidification as shown in Fig.3.4a and creates a problem on an HTF (chilled water) circulation for external-melt ice-on-surface melting mechanism during an ice discharge. It will also cause performance loss if the operation continues after solidification since there would be only sensible cooling of solids. In order to avoid a constrained growth shown in Fig.3.4b of ice by using multiple evaporators in single ice-storage, the spacing between evaporators has to be sized appropriately. For known design parameters of a vapour compression refrigeration unit, varying the operation condition also affects the output amount and corresponding lateral thickness of the ice. The appropriate ice profile thickness must be defined for operation under varying conditions. Therefore, the aim of the experimental work was to evaluate the appropriate ice layer thickness on the evaporator surface under varying conditions of the evaporator surface temperature.

(a) (b)

Figure 3. 4 Pictures of ice-storage showing effects of lateral thickness and storage size on ice growth: a) Single evaporator with narrow ice-storage width b) Multiple evaporators with narrower spacing between them

The solidification process considered in this research uses an insulated rectangular box with the evaporator surface positioned at the centre of a phase change material (water). The evaporator surface was considered as a cold side temperature boundary condition. A data logger (Agilent-34970A), a climate chamber controller and a PC were among materials used. The temperature data logger was used to record the data in one-minute intervals. The climate chamber for this experiment is an insulated room designed to maintain the required temperature in the experimental laboratory.

The experimental work provides a liquid solidification in a rectangular space under the influence of free convection for a one-day operation. The evaporator surface temperature was varied by controlling the refrigerant compressor power input (not shown here) and the surrounding ambient temperature. The heating system controls the climate chamber temperature to be maintained at 25, 35 and 45℃. The ice- storage system worked for 24 hours at each setting of ambient temperature and compressor speed after initiating the phase change process.

3.3.1 Determining the cold side boundary condition

The evaporator surface temperature, which is the cold side boundary condition of the phase change process, was measured at a representative location along the ice thickness measuring line, as shown in Fig.3.5. It varies with variation of refrigerant flow rate and the condenser pressure that vary with compressor speed and surrounding ambient.

3.3.2 Evaluation of the vertical water temperature

The time necessary for sensible cooling depends on the amount of water in the ice storage system, the initial water temperature, the external ambient temperature and the compressor speed of the refrigeration cycle unit. The main purpose of this vertical temperature measurement was both to mnitor the phase change process and to obtain the liquid side water temperature (phase front boundary condition). The vertical water temperature was measured at locations of 10, 25, 50 and 75 % of the vertical height from the bottom of the ice storage unit as shown in Fig.3.5. The mean value of the four temperatures represents the ice-storage water temperature.

3.3.3 The ice slab thickness measurement

The thickness of the ice on the evaporator surface was measured by placing temperature sensors at different lateral distances from the evaporator surface. After the phase transition stage, while freezing below 0℃, a phase change or solidification of water takes place at nearly 0℃. Therefore, if a temperature sensor shows a reading below 0℃ at any point in the water, it implies that icing has started at that point. Hence, temperature sensors were fixed horizontally at 10mm, 20mm, 40mm, and 60 mm from the evaporator surface as shown in Fig.3.5 to measure the lateral thickness of ice slab being formed. This reading gives a time history of the ice temperature at a fixed space. The measurement also helps to determine sensible energy contained in the solid ice and the lateral temperature profile of ice formed. In the presented work, the measurement taken to determine the thickness of the ice was corresponds to the coldest surface temperature and did not show the relation of ice thickness with total mass. Even though it could be typical for the system developed in this research, the evaporator surface covered by the ice varies with the operating condition, and it was not uniform.

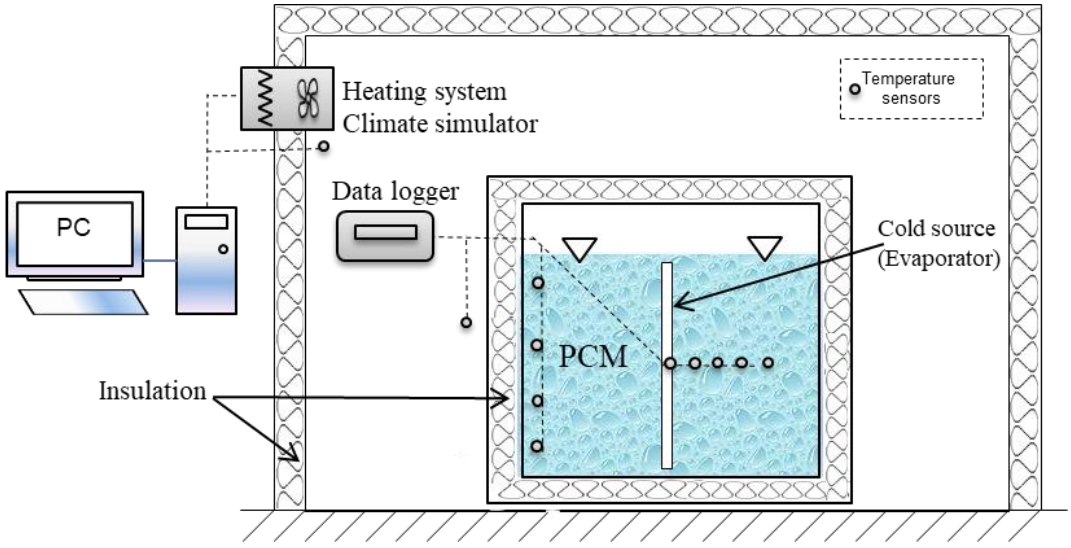

Figure 3. 5 Schematic of the experimental set-up for phase-change model (sectional view of the ice storage)

3.4 The milk cooling and preservation

Fig. 3.6 shows the proposed system schematic of ice-storage for milk cooling application. In the system proposed, the energy transfer between ice-storage and milk-cooler was by means of chilled water recirculation. Varying the chilled water recirculation rate and time of operation

enables the need to cool variable milk volume using the same system developed. The rate of chilled water recirculation also affects the rate of cooling the milk, ice melting and pump power consumption. The proportion of ice to water inside ice-storage was also another important factor affecting the rate of milk cooling. Thus, ice fraction in the ice-storage and chilled water recirculation rate were varied to evaluate the performance of the milk-cooler in this experiment.

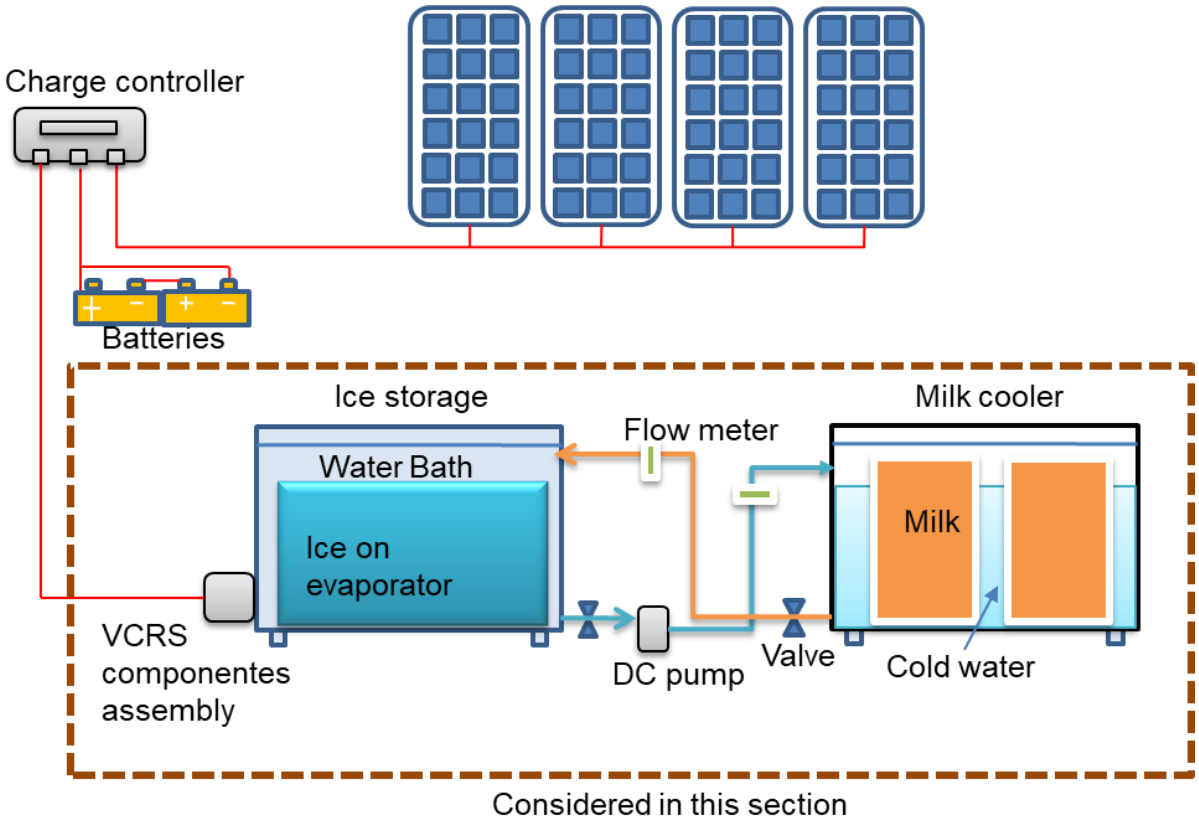

Figure 3. 6 Proposed solar milk cooling schematic

Experimental work was performed to characterize the cooling performance of milk-cooler with chilled water from the ice-storage. Both ice-storage and milk-cooler were insulated metal boxes of 105 and 195 gross litter capacity respectively. The milk-cooler holds two milk-cans of 40 litres each immersed in 75 litres of water-bath. The internal box dimensions were 55 x 32 x 60 cm (LxDxH) and 75 x 40 x 65 cm (LxDxH) respectively for the ice-storage and the milk cooler. A 1.5 mm thick stainless steel, styrofoam of 10 cm thickness with a 0.04 $W.m^{-1}$ K^{-1} thermal conductivity, and a wooden box were used. A 25 kg ice in 70 L water, a 50 kg ice in 45 L water, a data logger (Agilent-34970A), thermocouples (Type-K), a digital measuring balance, a climate chamber controller and a PC were among the materials used. The hydraulic circuit consists of

insulated plastic pipes, a DC pump of 28 W, a control valve, a stop valve and digital flow meter. Hot water (a substitute of milk) at a milking temperature of 35℃ was also part of the materials used. Cost and handling issue for repeated experiments were among the main reasons for using water as a milk substitute.

The experiment was performed for the different scenario by varying the ice fraction in the ice-storage and the rate of chilled water recirculation as a main cooling rate affecting parameters. A 100-litre capacity ice-storage was filled with a 95 litre of water to avoid spillage and overflow during recirculation. An ice mass of 25 kg and 50 kg were produced in respective experiments as representatives for an average daily output of ice from ice-storage using one and two refrigeration cycle units respectively. 80-litre water in the milk cooler was heated to 35℃ as a substitute of fresh milk right after milking. The initial temperature of water-bath inside milk-cooler that surrounds the milk-cans as a heat transfer fluid was at around 10℃, which is the temperature that a milk-cooler attains after 24 hours of milk preservation. After covering the top insulation material for both milk-cooler and ice-storage, a DC pump circulates the chilled water between ice-storage and milk-cooler. Chilled water circulation and flow rate were monitored by using a control valve and a digital flow meter. A stop valve was used to close the chilled water recirculation at the end of each milk-cooling experiment. Fig.3.7 shows the overall schematic of the experimental set up both for ice formation and milk cooling.

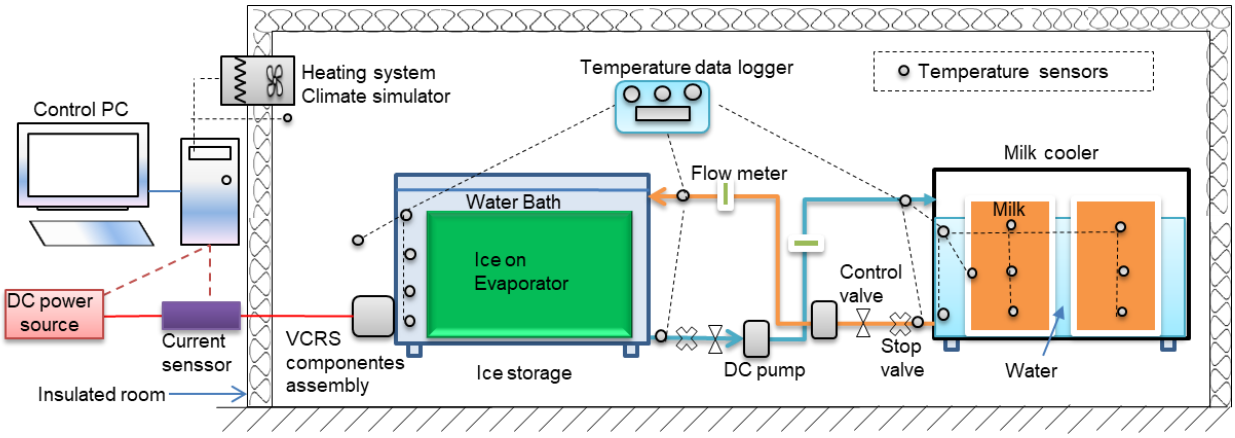

Figure 3. 7 Schematic of milk cooling experimental setup

3.4.1 Recirculating water temperature

The recirculating chilled water temperature at a given time indicates the minimum possible temperature limit of cooling the milk with this setup. In addition to this, the temperature history of a heat transfer fluid (water) in both the ice-storage and the milk-cooler is a useful parameter for modelling, design and control purpose. The forced recirculation between the ice-storage and the milk-cooler assures uniformity in internal temperature distribution, making the exit points to have the same temperature as the internal one. It was also observed from a preliminary test that the recirculating water temperature difference between the exit point of the ice-storage and inlet of the milk-cooler were negligible since the pipes were well insulated and shorter in length. The same is also true for the exit-inlet temperature relations of milk-cooler to ice-storage. Hence, the chilled water temperature measurements were taken from inlet-exit points and at the representative middle locations to measure the ice-storage and milk-cooler water-bath temperatures during recirculation.

3.4.2 Milk cooling curves

A temperature vs time curve indicates how fast the cooling was and the minimum milk temperature attained by the system investigated. The milk-cooling curve will be affected by the chilled water recirculation rate and ice fraction. The agitation mechanism assures the uniformity in milk-temperature while cooling. Nevertheless, it was not included in the system proposed by this research. Hence, temperatures were measured at the top, middle, and bottom points of the milk-can centre as shown in Fig.3.7 to obtain a representative temperature.

3.4.3 Evaluating the milk-cooler preservation performance

The proposed milk-cooler preserves milk after cooling it to the required temperature. The cooler preservation performance was evaluated by measuring the average milk-temperature increase for daily storage at 35℃ surrounding ambient temperature. Thus, the milk-temperature measurement was taken at the respective top, middle, and bottom points in the same way as for the cooling process.

3.4.4 Determination of milk to energy ratio based on actual and theoretical consumptions

The milk to energy ratio is an important cooling system design parameter to relate the milk volume with the ice-storage system. The theoretical energy required by the milk-cooler is the

sum of energy removed from the milk itself, the energy in water-bath surrounding the milk-cans, and heat gain from the external ambient. The energy supplied from the ice storage during recirculation together with the pump power was considered as the actual energy input. However, the pump power contributes a small portion of the energy supplied and can be negligible. Eq (3.11) was used to quantify the actual energy input to the milk cooler from the ice storage. A weigh balance was used to measure the remaining ice mass after respective recirculation time to determine the latent portion of energy from the ice storage.

$$Q_{ice-stoarage} = V_{ice-storage}.\Delta E_{storage} + P_{pump}.\Delta t \quad (3.11)$$

The storage capacity, $\Delta E_{storage}$ depends on the density and specific heat of water and ice, the latent heat of melting the ice ($\Delta h_{fusion,ice}$), the temperature difference across the storage, $\Delta T_{storage}$, and the Packing Factor (PF) as shown in Eqs. (3.12), (3.13) and (3.14).

$$\Delta E_{ice} = \rho_{ice}.(\Delta h_{fusion,ice} + C_{P,ice}\Delta T_{ice}) \quad (3.12)$$

$$\Delta E_{water} = \rho_{water}.\ C_{P,water}.\Delta T_{storage} \quad (3.13)$$

$$\Delta E_{storage} = PF.\Delta E_{ice} + \varepsilon.\Delta E_{water} \quad (3.14)$$

Where,

$\varepsilon = 1 - PF$, if the water temperature inside the ice-storage remains at 0 ℃ after melting of ice $and\ \varepsilon = 1,$ if the water temperature inside ice storage increases above 0 ℃. The packing factor (PF) represents the volume fraction of ice in the ice-storage, ΔT_{ice} is the difference between ice temperature and its melting point.

A known mass together with monitored temperature was implemented to calculate the theoretical energy required by the milk cooler, as shown in Eq. (3.15). Since the milk cooling time was relatively shorter, the heat loss through the wall could be negligible. The milk to energy ratio was calculated to cool 80 L milk from 35℃ to required final temperatures. Eqs. (3.16) and (3.17) show the experimental and theoretical milk to energy ratio, respectively. Finally, a comparison was made between experimental and theoretical energy demand per litre of milk.

$$Q_{milk-cooler} = (m_{milk}.C_{P,milk}.\Delta T_{milk} + m_{wb}.C_{P,wb}.\Delta T_{wb} + UA.\Delta t.\Delta T_{ambt\_cooler}) \quad (3.15)$$

$$(L/E)_{experimental} = \frac{V_{milk}}{Q_{ice-storage}} \quad (3.16)$$

$$(L/E)_{theoretical} = \frac{V_{milk}}{Q_{milk-cooler}} \quad (3.17)$$

3.4.5 Estimation of the milk cooling system capacity with respect to ambient condition and required milk temperatures

The daily energy stored with the ice-storage will vary based on available energy input and other ambient conditions. The instantaneous energy demand for cooling a known volume of milk varies based on required final temperature. On the other hand, cooling to lower temperatures consume more energy not only because of increased temperature gradient but also due to lower heat transfer rates at low temperature gradients. The ice-storage performance parameters together with experimental energy to milk ratio were implemented to determine the milk cooler capacity range with respect to operating ambient.

3.5 External-melt ice discharge with a fan-coil unit as an end-use device

For a known mass of ice-slab in a water-bath as the case for an ice-storage design shown in Fig.3.8, the water temperature and flow rate over the ice-surface are among major factors that affect melting rate (ice discharge rate). The ice-melting rate, on the other hand, affects the rate of energy transfer from the ice-storage to the end-use device (application). The main objective of this experiment was to investigate the effect of chilled water recirculation rate and fan speed variation on the ice-slab melting rate. In addition to this, the range of air temperature drops across FCU, and recirculating water temperature history was evaluated.

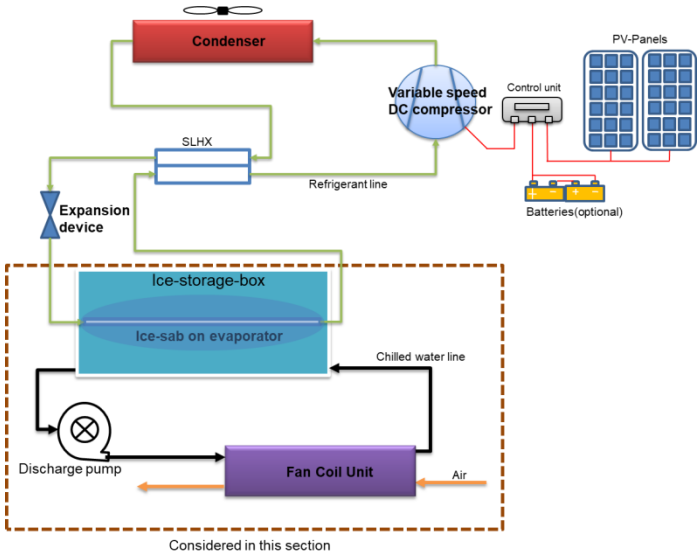

Figure 3. 8 Schematic of ice-storage as applied to cold room/pick load application

The enthalpy- temperature relationship curve is shown in Fig. 3.9. Here T_{melt} is the melting point of ice, H_{sm} and H_{lm} represent the enthalpy associated with the ice and water at the melting point, respectively.

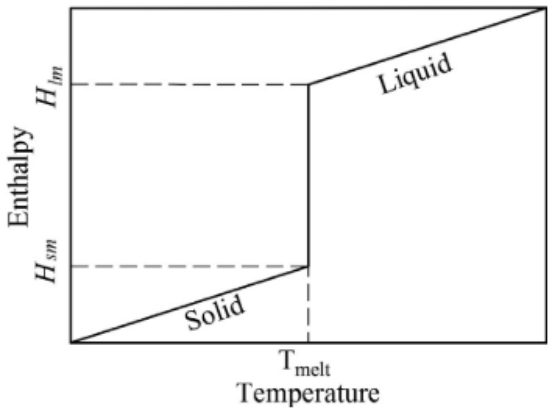

Figure 3. 9 Enthalpy-Temperature relationship graph [66]

$$T = \begin{cases} {}^{H}/_{C_{ps}} & H < H_{sm} \\ T_{melt} & H_{sm} < H < H_{lm} \\ T_{melt} + (H - H_{lm}) \Big/ C_{pl} & H > H_{lm} \end{cases} \quad (3.18)$$

where $H_{sm} = C_{ps} T_{melt}$ *and* $H_{lm} = C_{ps} T_{melt} + L$

Eq.(3.18) indicates that the temperature measurement at a centre location in the ice-slab can be used to estimate the total time taken to melt a given mass of ice which is the approach followed in this research.

For the experimental set-up, conditioned space simulator of an 8 m^3 insulated room was used as an experimental space with a defined cooling load. A 2x2x2 m in dimension room with 4 cm thick styrofoam insulation, automatic space heater, a variable speed fan-coil-unit (FCU), and a control unit were major components of conditioned space simulator. An ice-storage with 25 kg of ice inside 70 L of water at 0 ℃ was used as a source of the chilled water. The hydraulic circuit consists of a flow control valve, a DC pump (Max.900 $L.h^{-1}$), a digital flow meter and insulated plastic pipes. A data logger (Agilent-34970A) and Type-K thermocouples were used to monitor temperatures at different locations.

The aim of the experiment was to characterize the external melt ice-on-flat surface for the application of the ice-storage in the cold room. The first step was setting and configuring of the experiment. A DC-powered vapour compression refrigeration unit, not shown here, was used to produce an ice mass of 25 kg per day before starting the discharge operation. After fixing and connecting the FCU with the ice-storage through chilled water lines, as shown in Fig. 3.10, the control system was switched on to maintain the space temperature at 35℃. The control valve and digital flow meter were used to adjust the flow rate under the constraint of pump capacity and system pressure loss. The air volume flow rate across the FCU was varied using the fan speed control tab. For this experimental campaign, a minimum and maximum design fan speeds and two different chilled water flow rates (2.7 $L.min^{-1}$ and 5.4 $L.min^{-1}$) were selected as parameters that affect ice melting rate in the cold room/air conditioning application. After setting the fan speed and chilled water recirculation rate, the DC pump was operated to maintain the continuous circulation of chilled water.

Temperature measurements were taken at a one-minute interval at the final melting location of the ice-slab. The chilled water temperature was measured at inlet-exit points of both the ice-storage and an FCU. The air temperature at both inlet and outlet points of the FCU was also measured. Finally, the effects of chilled water flow rate variation and airflow rate variation across the FCU on ice-discharge and degree of cold room temperature differential were evaluated. Besides the final melting point temperature, the slop change of both the air and the water temperatures within the four hours discharge time was used to estimate the time taken for complete melting of the ice. A picture from the experimental platform was shown in Fig.3.11 to provide descriptive information on the material and method.

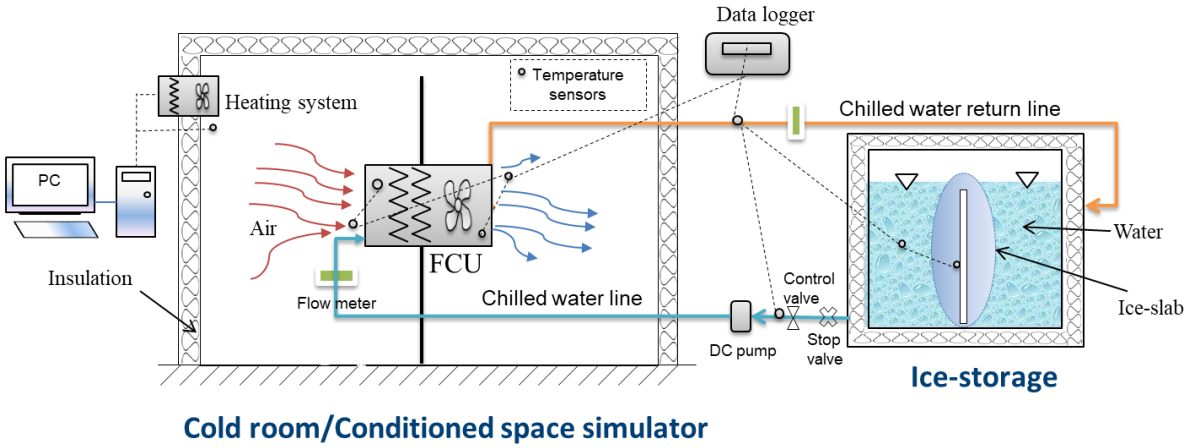

Figure 3. 10 Schematic of the experimental set-up of ice-storage for cold room application

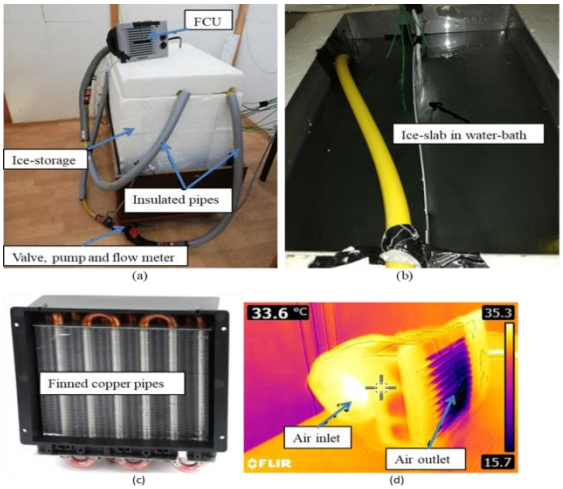

Figure 3. 11 Pictures from the experiment (a) Ice-storage FCU assembly (b) Internal part of ice-storage (c) Internal section of FCU (d) Representative air temperature profile taken by the infrared camera

3.6 Conclusions

Detailed experimental setups for the ice making process, evaluation of the lateral ice thickness development, the ice-based milk cooling and ice discharge characterization with fan-coil-unit were presented. A climate chamber, a room heater, an ice storage system, a milk cooler, a fan-coil-unit, a DC-power source, a data logger, temperature sensors, current sensors, pure water, digital measuring balance, DC-pumps, a hydraulic circuit, flow meter, flow control valves were among materials used for the experiments. After setting and configuring the setups, several experiments were carried out. With the appropriate data and plots from the experimental campaign, the results were presented and analyzed in chapter four.

Chapter 4
Results Analysis and Discussion

4.1 Introduction

In chapter three, detail experimental setups were presented for the small-scale cooling system with the ice storage using a DC-powered refrigeration unit. Based on the experimental setups, materials were prepared, measurements were taken, and data collection was performed. The ice storage system performance characterization was carried out by evaluating the range of daily ice mass production, the system energy demand and corresponding system COPs under varying operational parameters. The system COPs were compared to identify the best efficiency point. The temperature distribution on evaporator surface and prediction of annual energy demand were also among activities performed under performance characterization. The vertical water temperature variation in the ice storage and effects of parameter variation on the degree of sub-cooling before phase transition during ice formation were analyzed. Range of daily ice thickness development on evaporator surface was evaluated as a means to define a spacing of multiple VCRC units in parallel to scale up the system's energy storage capacity.

The ice storage was introduced in the small general scale cooling system set up to shift continuous small capacity electrical load in order to satisfy the instantaneous cooling demand. To this end, an 80 L capacity milk cooling system based on an ice-storage was experimentally analyzed. Moreover, the energy stored through the continuous operation of the ice-storage system must be discharged in a reasonably shorter period to maximize the ice production cycle. For the system set-up considered, the chilled water recirculation rate affects the external convection heat transfer coefficient for both the ice-storage system and milk-cooler. Hence, the effects of chilled water recirculation rate and ice storage energy density on the milk cooling curves, milk preservation, the energy transferred, minimum attainable milk temperatures and recirculating water temperatures were evaluated. The milk to energy ratio was evaluated, and the ranges of milk volumes to cool with respect to the varying ambient condition were evaluated.

The applications of the ice-storage developed in this research can be diversified for cold rooms to preserve fruits and vegetables with the same external melt ice-on-surface approach. Load side management in cold room applications could be affected by controlling the chilled water

recirculation rate and airflow across the end-use device. On the other hand, varying air flow rate across the FCU affects the water temperature entering the ice-storage besides its effect on the air temperature inside the cold room. Therefore, an ice discharge characterization with heat simulated room was performed.

In this chapter, the results for ice storage performance characterization, ice thickness development, evaluations of ice-based milk cooling and cold room application were presented, analyzed and discussed.

4.2 Performance of the ice-storage system for varying operating points

The refrigeration cycle unit was optimized for the best operating point at 3500 rpm and the ambient temperature of 30℃, as indicated in chapter two. In this section, a performance characterization was carried out by varying operational parameters as two compressor speeds at 2000 rpm and 3500 rpm and three ambient temperatures of 25℃, 35℃, and 45℃. The results for temperature distribution on evaporator surface, the daily mass of ice production, energy demand and system COP was analyzed. Performance comparisons against different operating points were carried out. Monthly and annual energy demands were also predicted based on measured values.

4.2.1 Temperature distribution on the evaporator surface

Fig. 4.1 shows the temperature distribution on the evaporator surface at a lower compressor speed limit of 2000 rpm and different ambient temperatures. The evaporator surface temperatures varied between 0.3℃ and -4.2℃ during the phase change process at a compressor speed of 2000 rpm. The minimum temperature of -5℃ on the evaporator surface was achieved at a compressor speed of 3500 rpm as shown in Fig.4.2. The figure also shows that the rate of the temperature drop at all representative sensor locations is higher at a higher compressor speed. The local temperature variation across the evaporator surface for a specific case was an indicator of off-design operational characteristics of an ice-storage. Thus, the temperature curves obtained in this experiment represents a non-uniform cold side boundary condition of a phase change process.

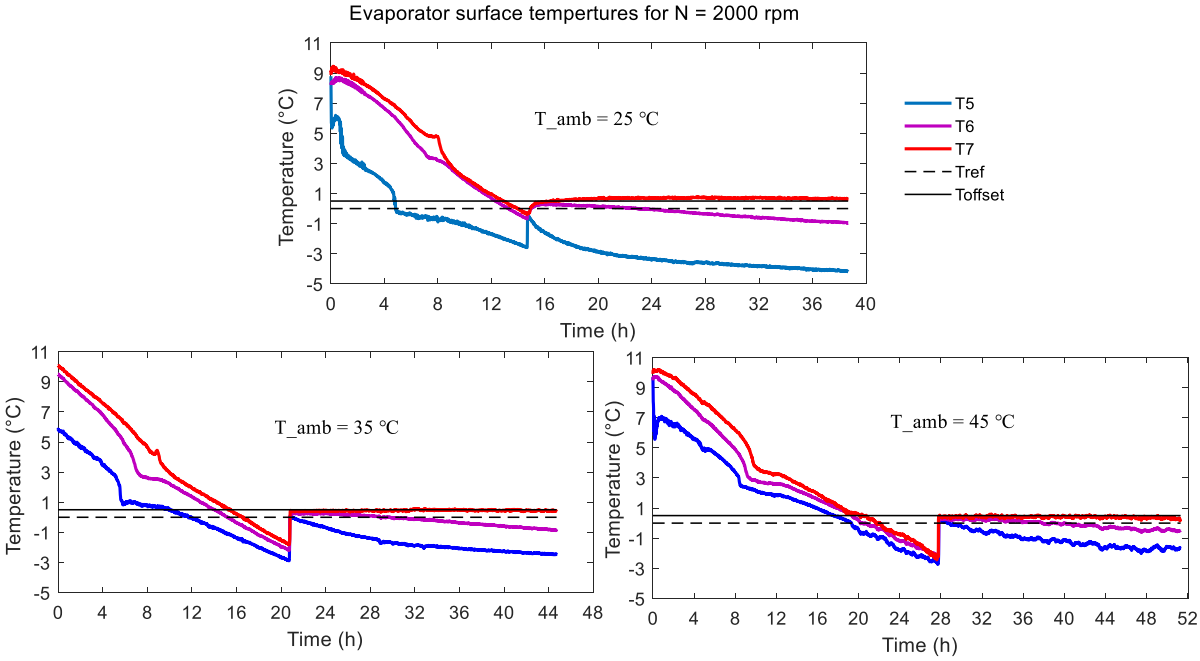

Figure 4. 1 Evaporator surface temperatures vs time at representative locations for lower compressor speed and different ambient temperatures

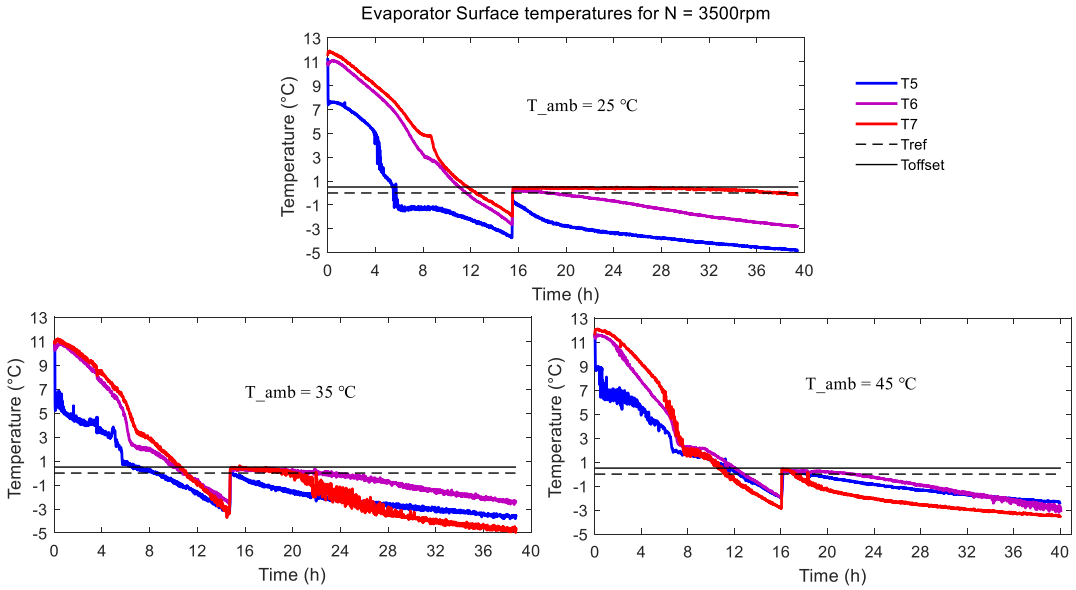

Figure 4. 2 Effect of ambient temperatures on evaporator surface temperatures at representative locations at higher compressor speed

4.2.2 Daily ice mass-produced and the energy stored

Fig. 4.3 shows the ice profile formed on a flat evaporator surface in water-bath configuration for different operating conditions. The shape of the ice formed is not rectangular like the surface of

the evaporator as all the edges of the evaporator have clearance to the channel of the refrigerant tube. The temperature distribution within the ice block also affects the shape of the ice. At a compressor speed of 2000 rpm, the daily mass of ice produced is 19.7 kg, 17.71kg and 13.96 kg for 25℃, 35℃, and 45℃ ambient temperatures, respectively. The daily mass of ice produced is 26.28kg, 25.27kg and 21kg in continuous operations at 25℃, 35℃, and 45℃ ambient temperatures, respectively at a compressor speed of 3500rpm.

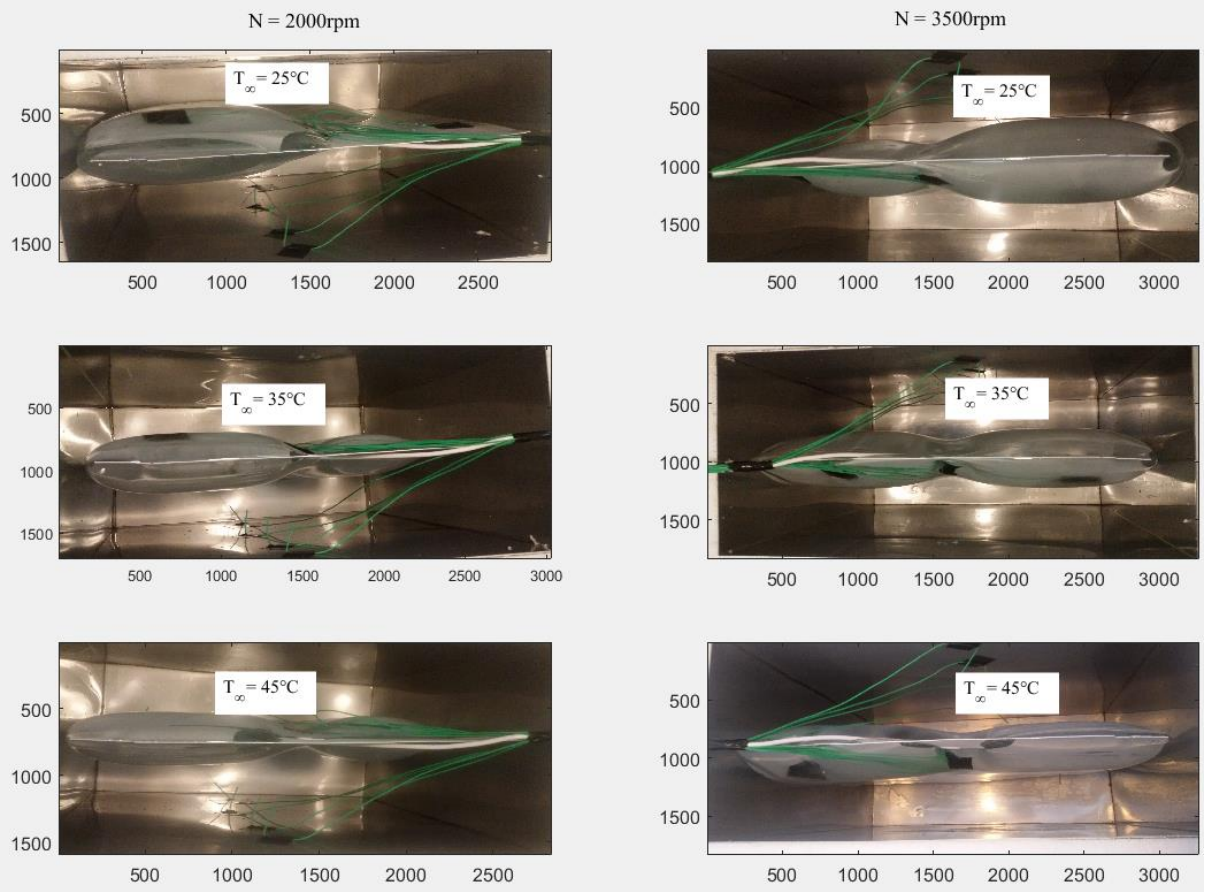

Figure 4. 3 Picture of ice profile on the evaporator surface at different ambient temperatures and compressor speeds at the end of the daily operation

4.2.3 System energy demand

The specific energy demand for a given system is an important design parameter. In this research, the energy demand for the production of ice was experimentally determined for a varying scenario. Fig. 4.4 shows a typical range of power corresponding for minimum and maximum compressor speeds of 2000 and 3500 rpm respectively. As can be seen from the

figure, the energy consumption was higher at the initial stage of sensible cooling while it remains nearly in steady-state form during the phase change process.

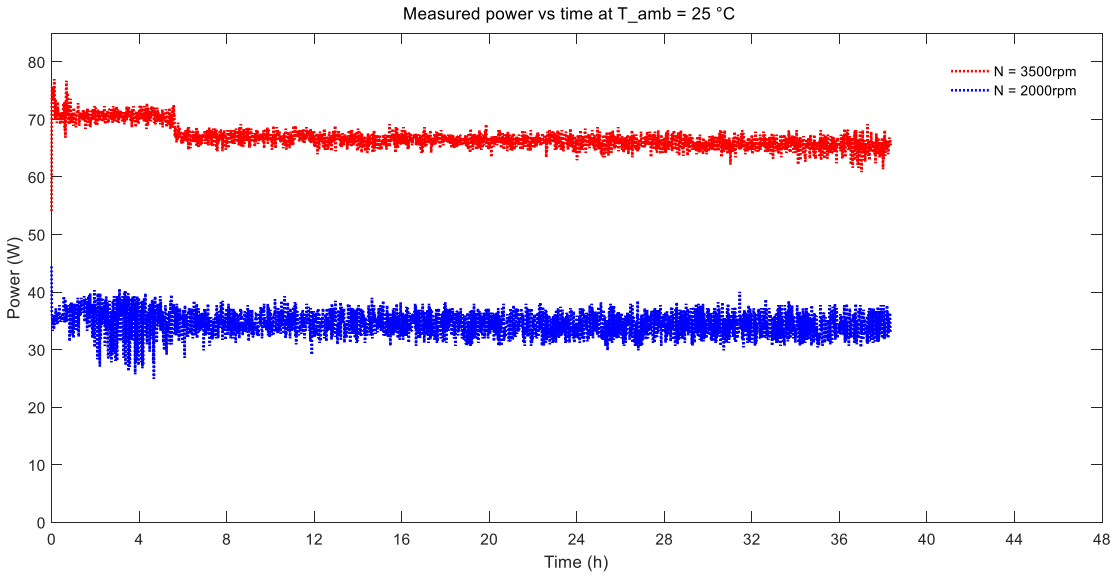

Figure 4. 4 Typical system power consumption for corresponding compressor speeds

The effect of ambient temperature on system energy consumption at different compressor speeds was shown in Fig. 4.5. It can be observed from the figure that the effect of ambient temperature on system power requirement was not significant. By varying the ambient from 25℃ to 45℃, the power requirement varied from 68 W to 72W at a compressor speed of 3500 rpm. Similarly, the system power requirement varied between 36 W and 38.5 W for operation at a compressor speed of 2000 rpm. During the compressor start-up and the sensible cooling stage, the power requirement is relatively higher. But the magnitude of electrical power requirement during the phase change process was relatively lower and nearly constant.

Varying the compressor speed brings a significant change in energy consumption. There is an increase in electrical power requirement, even for a fixed compressor speed, with an increase in the ambient temperature as shown in Fig.4.5. Nevertheless, the rise in energy consumption for temperature intervals of 25 to 35 ℃ is higher than for 35 to 45 ℃ as can be seen from the figure. The reason of difference in energy consumption for similar temperature intervals of 25 to 35℃ and 35 to 45 ℃ would be the possible difference on the degree of refrigerant superheat as well as the degree of irreversibility associated with ambient temperature. Besides this, the refrigeration unit utilized was optimized for operation at 3500 rpm and 30°C ambient temperature.

The electrical energy consumption of a compressor depends on the degree of superheat at evaporator exit and the heat released due to a non-isentropic process. Part of the compressor component heat absorbed by the refrigerant at different temperatures also has an effect on a refrigerant thermodynamic property variation, which have an impact on the compressor energy consumption.

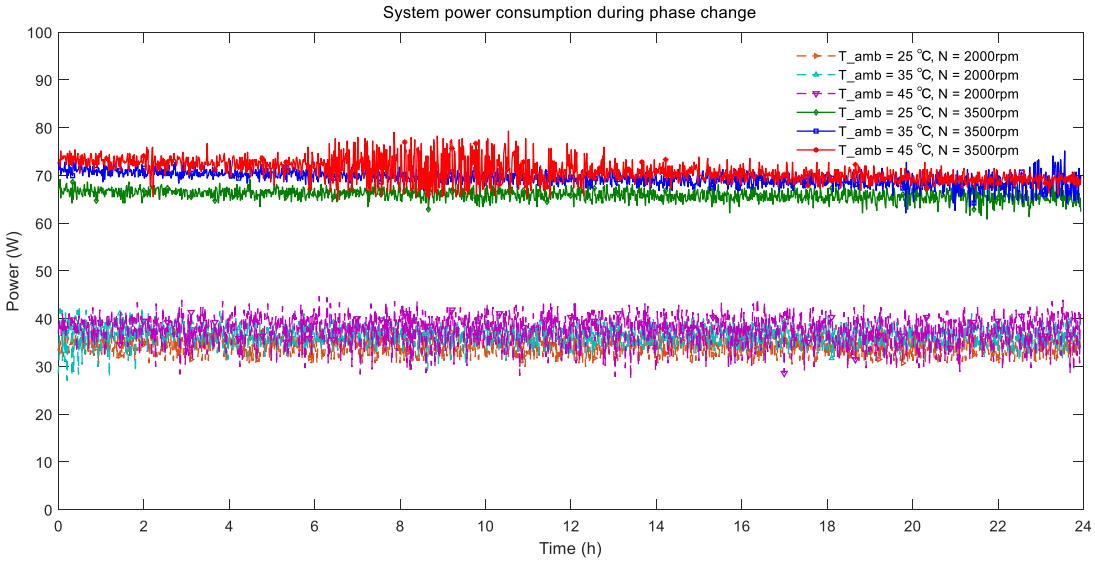

Figure 4. 5 Effect of ambient temperature and compressor speed on the system power requirement

The daily energy demand of the system under varying ambient temperatures and compressor speed was shown in Fig. 4.6. The demand was in the range of 1.59 to 1.71 kWh.day^{-1} for higher compressor speed as ambient varies from 25 to 45℃. At the lower compressor speed of 2000 rpm, the daily energy demand varies between 0.83 and 0.91 kWh.day^{-1} for a similar range in ambient temperatures. The change in daily energy consumption per ambient temperature remains constant for both compressor speeds at a higher ambient, as shown in Table 4.1. Therefore, it can be said that the change in daily energy consumption per ambient temperature was between 3 and 9 Wh°C^{-1}.day^{-1} for the system considered in this research.

Table 4. 1 Effect of ambient temperature on daily energy demand

Compressor speed (rpm)	Change in daily energy consumption per ambient temperature ($Wh.°C^{-1}.day^{-1}$)	
	Ambient temperature range (℃)	
	25-35	35-45
2000	5	3
3500	9	3

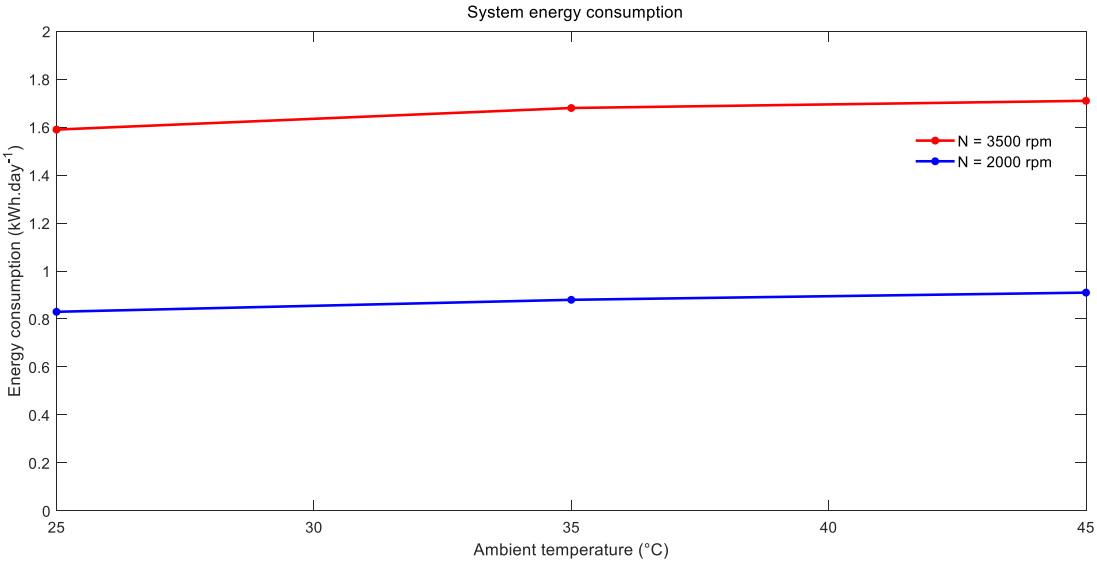

Figure 4. 6 Daily energy demands vs ambient temperature

Based on the measurements for daily energy consumption, the monthly and annual energy demands of the system were projected. Table 4.2 shows the system energy demand for varying compressor speed and ambient temperature. The annual energy demand of the system would vary between 302.95kWh.year^{-1} and 624.15kWh.year^{-1} for the compressor speed ranges of 2000 to 3500 rpm and varying ambient.

Table 4. 2 Monthly and annual energy demand of the ice-storage system

Energy demand	T_amb (℃)	N = 2000 rpm			N = 3500 rpm		
		25	35	45	25	35	45
Daily	kWh.day^{-1}	0.83	0.88	0.91	1.59	1.68	1.71
Monthly	kWh.month^{-1}	24.90	26.40	27.30	47.70	50.40	51.30
Annually	kWh.year^{-1}	302.95	321.20	332.15	580.35	613.20	624.15

By assuming frequent discharge after a daily operation, the annual energy storage in the form of ice would vary between 478.15kWh.year^{-1} and 897.9kWh.year$^{-1,}$ as shown in Table 4.3. The minimum value corresponds for 2000 rpm at 45 ℃ ambient whereas the maximum value was for operation under 3500 rpm and 25 ℃ ambient temperatures.

Table 4. 3 Monthly and annual energy storage capacity in the form of ice under different operation

Stored energy	T_amb (℃)	N = 2000 rpm			N = 3500 rpm		
		25	35	45	25	35	45
Daily	kWh.day^{-1}	1.84	1.66	1.31	2.46	2.37	1.97
Monthly	kWh.month^{-1}	55.2	49.8	39.3	73.8	71.1	59.1
Annually	kWh.year^{-1}	671.6	605.9	478.15	897.9	865.05	719.05

The refrigeration effect is the amount of energy removed from the space to be cooled by the refrigeration system. This load is the sum of the energy stored in the form of heat and corresponding heat loss from the system. Table 4.4 shows the system's refrigeration effect measured and projected based on experimental data. Accordingly, the system has the annual refrigeration capacity in the range of 697.15kWh.year^{-1} to 1036.6kWh.year^{-1}.

Table 4. 4 Refrigeration effect under the different operation modes

Refrigeration effect	T_amb (℃)	N = 2000 rpm			N = 3500 rpm		
		25	35	45	25	35	45
Daily	kWh.day^{-1}	2.18	2.13	1.91	2.8	2.84	2.57
Monthly	kWh.month^{-1}	65.4	63.9	57.3	84	85.2	77.1
Annually	kWh.year^{-1}	795.7	777.45	697.15	1022	1036.6	938.05

4.2.4 Coefficient of performance for the ice storage system

Fig. 4.7 shows the ice storage system COP and the general energy flow. The energy consumption of the compressor and the system's thermal loss increase as the ambient temperature increases for a given compressor speed. Since heat loss from the compressor is not accounted for in this experiment, the thermal loss remains constant for a given ambient temperature and different compressor speeds. For all ambient temperatures, the COP is higher at lower compressor speeds.

Nevertheless, the variation of the compressor speed significantly affects the useful energy delivered and the corresponding system COP. This figure also shows that a higher system COP does not guarantee more useful energy from a given system. With the current system set-up, operating the system at a higher compressor speed and a lower ambient temperature achieves a better output in terms of useful energy delivered.

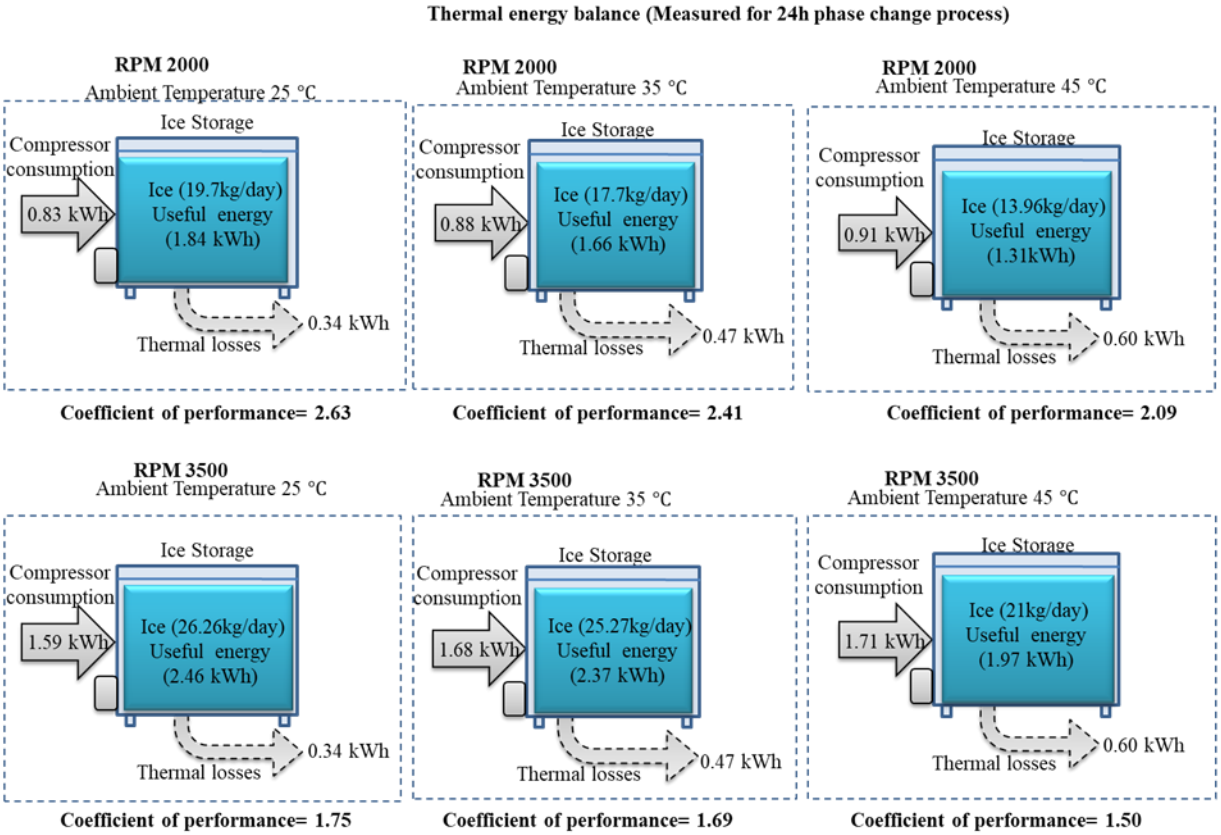

Figure 4. 7 Ice-storage system performance summaries

Table 4. 5 Performance drop with changing ambient temperature operating point

Operating point variation			COP drop (%)
Compressor speed (rpm)	Ambient temperature(℃)		
	From	to	
3500	25	35	3.4
		45	14.3
2000	25	35	8.4
		45	20.5

Table 4.5 shows a relative percentage change in performance with reference to operation at 25 ℃ ambient conditions. A smaller COP drop of 3.4 % was achieved for operation at 3500 rpm and ambient temperature change of 10 ℃ from reference. When an optimum operation point of the refrigeration system is determined at higher ambient temperature, increasing the ambient temperature causes increased drop in performance. Table 4.6 also indicates that changing operating points for both the compressor speed and ambient temperature at a time highly affects the system performance.

The compressor speed operating point change on COP and useful energy change was shown in Table 4.6. A higher percentage increase in COP was observed for compressor speed change at lower ambient temperature. However, the COP increases as compressor speed decrease regardless of ambient temperature. This implies that optimizing the variable speed drive refrigeration cycle unit at its maximum speed would result in an energy-efficient operation at lower speeds. On the other hand, useful energy loss could be higher if the compressor is operated at lower speed and higher ambient temperature. Therefore, for the condition of power input from solar energy, the compressor should be operated at full capacity, especially during day time for a better output. The efficiency mode operation during the night time would be a complimentary option with comparative advantage on energy consumption to reduce the required battery capacity.

Table 4. 6 COP vs useful energy for compressor speed operating point change at a fixed ambient temperature

Operating point change due to compressor speed (rpm)		Ambient temperature(℃)	COP increase (%)	Useful energy decrease (%)
from	to			
3500	2000	25	50.3	25.2
		35	42.6	30.0
		45	39.3	33.5

4.3 Water-ice phase change and ice thickness development

In this section, the ice growth boundaries and ice layer development were presented and discussed. Besides, the ice layer growth rate was compared for different ambient, and the potential relationship of the ice slab thickness with the ice storage sizing was discussed.

4.3.1 Phase front boundary condition temperature range

The vertical water temperature distribution during phase change was shown in Fig.4.8 and Fig.4.9. The discontinuities represented by the vertical line in all cases were a phase transition period, which was significantly shorter. In this transition region, the latent heat of freezing causes an increase in the bulk temperature until it reaches the phase change temperature point. Except for one scenario shown in Fig.4.8, the water inside the ice-storage attained a uniform phase change temperature during starting of solidification right after transition. As the ice formation on the evaporator surface continues, the water temperature remains nearly at around a phase change value of 0℃. This shows that the liquid mass was sufficient to avoid temperature fluctuations inside the ice storage due to sensible heat addition from ambient during the phase change process. The maximum vertical water temperature difference between the top and the bottom layers was not more than 0.5℃ for all the cases. Moreover, changing the compressor speed did not affect the uniformity of the vertical water temperature significantly. It was also observed that the increased thermal stratification of the vertical water layer at later stages was due to the increase of the ice layer on the evaporator surface.

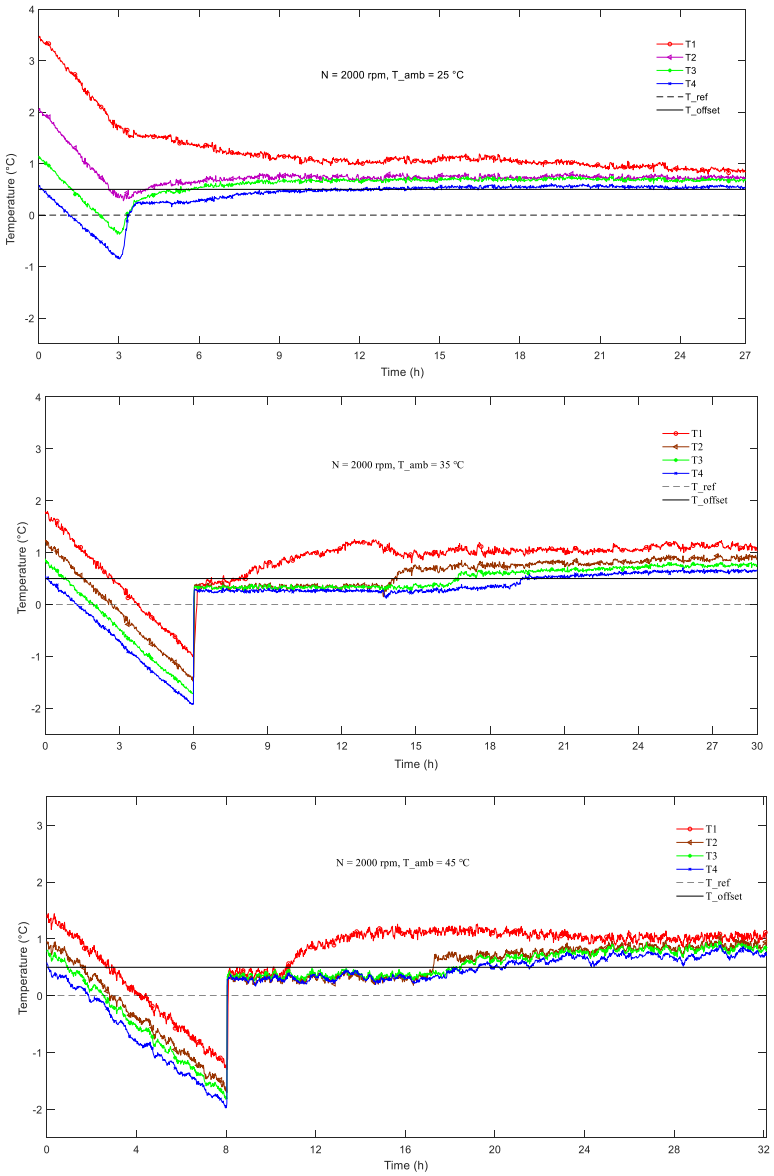

Figure 4. 8 Vertical water temperature (Sub-cooling and phase front boundary condition) vs time in the ice storage for lower compressor speed and different ambient temperatures

4.3.2 Effect of ambient temperature on sub-cooling before the phase transition

At lower compressor speed as seen from Fig.4.8, the sub-cooling time taken before the start of a phase transition process increases with the increase of the ambient temperature. It takes 3, 6, and 8 hours respectively at 25, 35, and 45℃ ambient temperatures. For a higher compressor speed, the sub-cooling time taken was relatively shorter, and it shows a decreasing trend with increasing ambient, as shown in Fig.4.9. The corresponding time taken at 25, 35, and 45℃ ambient temperatures are 4.8, 4.0, and 3.42 hours respectively. The sub-cooling time depends on the mass

of water considered and the net heat removal rate from the water. Since the water mass used was constant in all cases, the net heat removal rate from the water by the refrigeration cycle was mainly responsible for an increase or a decrease in the sub-cooling time observed in this experiment.

The net heat removal rate depends on the compressor power input, condenser pressure, system heat loss, and the thermodynamic and thermo-physical property variations among others during operation. For the experimental set-up used in this research, the heat loss through the ice-storage surface to the surrounding ambient was similar for operation at different compressor speeds. However, the heat loss from the compressor surface and motor winding loss may vary due to refrigerant flow rate variation with compressor speeds. The sub-cooling time variation trend implies that the net heat removal rate from the water decreases with increasing ambient temperatures at lower rpm. This phenomenon was different for operation at a higher compressor speed that gives a shorter time and a decreasing trend.

Considering the magnitudes of sub-cooling temperature limits, -2.8℃ at 3500rpm and -1.4℃ at 2000rpm were the corresponding minimum, and maximum values obtained considering a 0.5℃ thermocouple-reading offset and an ambient temperature of 25℃. The magnitude of sub-cooling temperature increases with increasing ambient for lower compressor speed, but it did not show a significant change for a higher rpm case. However, lower ambient and lower rpm case shows a significant difference in the degree of sub-cooling compared with other cases. This indicates that the rate of cooling the water and the surrounding ambient can affect the magnitude of sub-cooling needed for a water-to-ice phase change process.

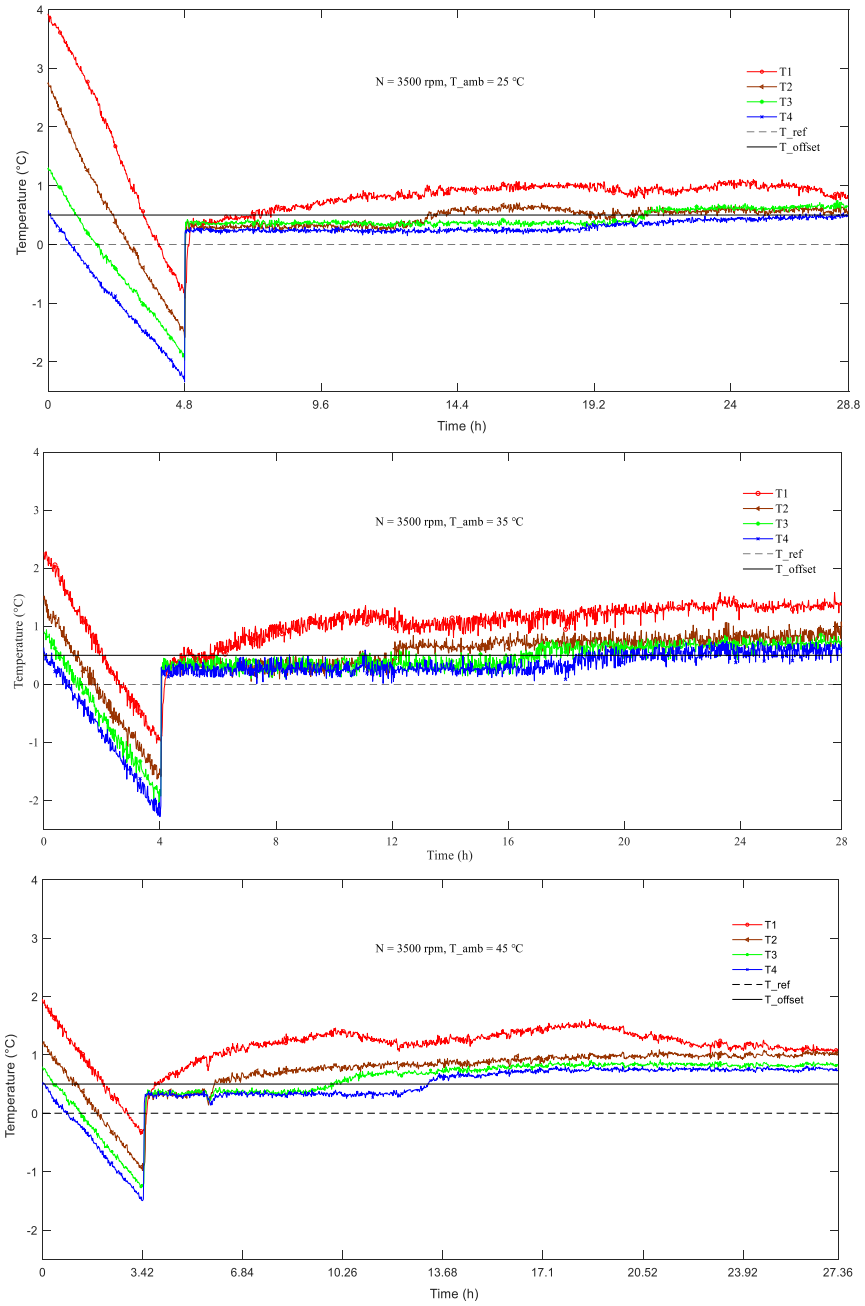

Figure 4. 9 Vertical water temperature (Super-cooling and phase front boundary condition) vs time in ice storage for higher compressor speed and different ambient temperatures

4.3.3 Cold side phase change boundary condition temperature range

The evaporator surface temperature serves as a boundary condition in phase change problem modelling of ice production. Due to thermodynamic and thermos-physical property variation during the phase change process, the evaporator surface temperature across the coil surface becomes non-uniform. Fig.4.10a shows the temperature variation at a point for cold side

boundary condition when the compressor operates at its lowest speed of 2000 rpm. The temperature-time curve was more parabolic for the first 12 hours of operation after initiation of phase change at lower ambient case than higher ambient temperatures. The increased pressure ratio across the compressor could be the reason for increased refrigerant flow rate, which in turn produces a relatively warmer and uniform temperature distribution across the evaporator surface at higher ambient temperature. Hence, less parabolic and relatively higher cold side boundary temperatures at a point were responsible for smaller ice thickness at increased ambient temperature.

A similar cold side boundary temperature curves for increased compressor speed of 3500 rpm were shown in Fig.4.10b. In this case, the parabolic nature of the temperature-time curve was reduced to the first 8 hours of operations. The magnitude of the cold side boundary temperature at a point was also relatively lower for higher compressor speed case. This lower temperature could have a positive impact on ice-slab layer thickness growth. It was also observed that increasing both the compressor speed and ambient temperature increased the linear range of boundary temperature-time profile. This linear temperature-time profile, on the other hand, is associated with the lower rate of ice thickness development.

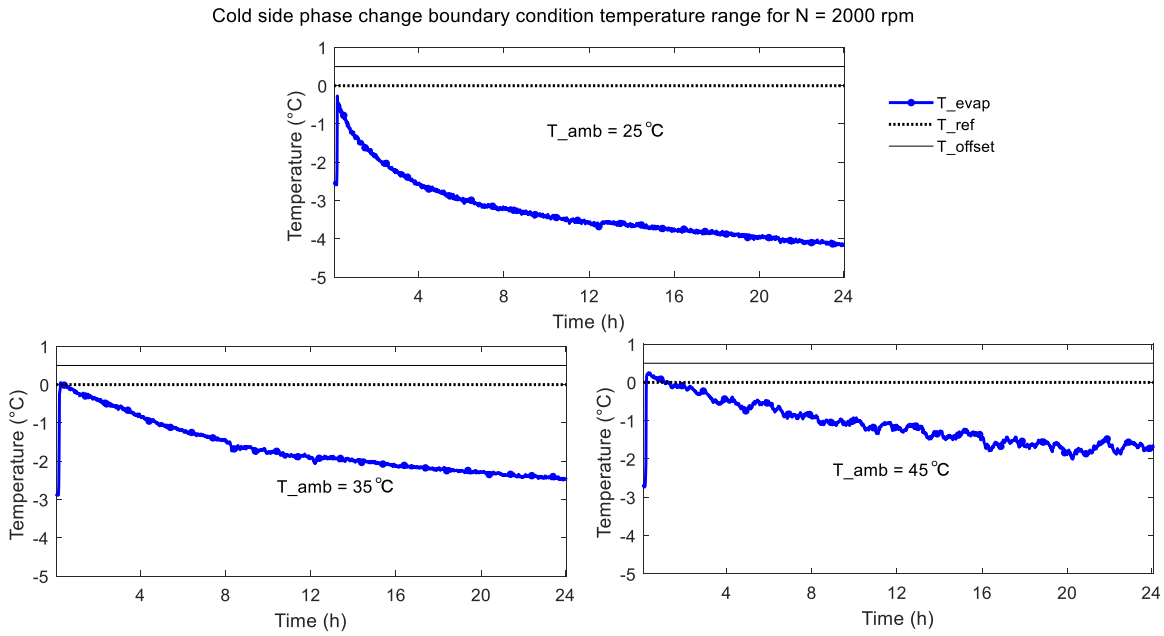

(a)

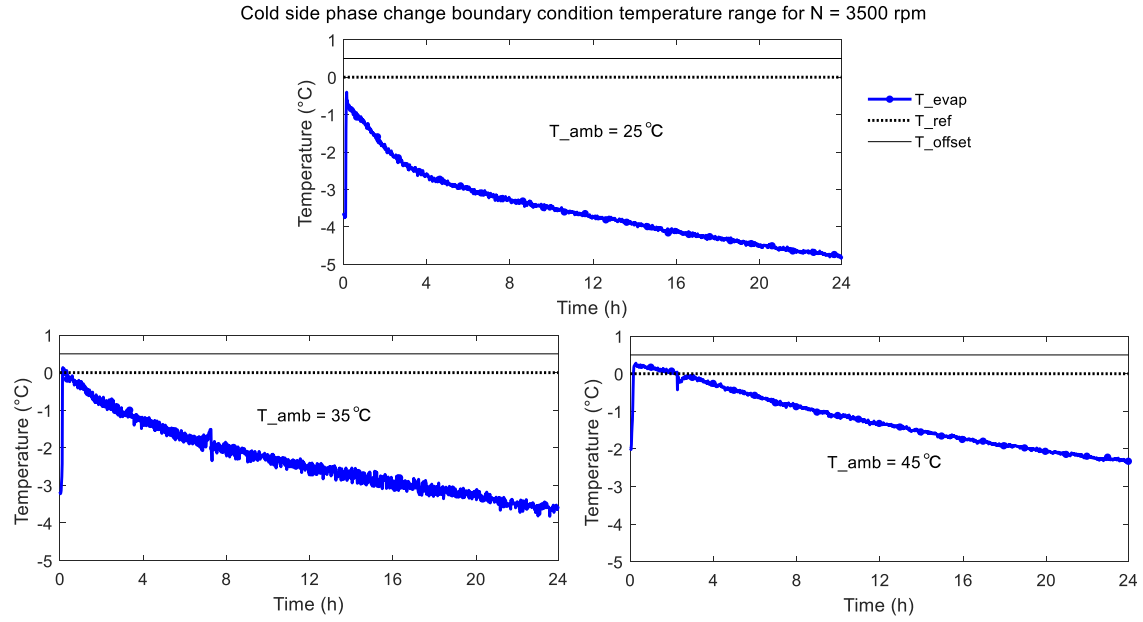

(b)

Figure 4. 10 Cold side surface temperature variations vs time for different ambient temperatures (a) lower compressor speed (b) higher compressor speed

4.3.4 Spatial ice slab temperature distribution indicating the lateral thickness change

The results of maximum ice thickness development on the evaporator surface were shown in Fig.4.11 and Fig.4.12 respectively for lower and higher compressor speeds. The total thickness of ice formed on both sides of the evaporator at a compressor speed of 2000 rpm is 12.6 cm, 9 cm, and 7 cm at 25℃, 35℃, and 45℃ ambient temperatures, respectively. At a compressor speed of 3500 rpm for ambient temperatures of 25℃, 35℃, and 45℃ the respective total ice thickness developed on the evaporator surface is 12.5 cm, 9 cm, and 9 cm. The figure also shows faster solidification at an early stage of the phase change process in all cases, indicating the lower rate of ice thickness development at the later stages.

The ice thickness developed for the two different compressor speeds at the same ambient temperature was equivalent as seen from the figures. However, this was a local phenomenon since the temperature distribution on the evaporator surface and the corresponding width covered by the ice layer differs for each scenario. In general, the ice thickness was non-uniform across the vertical evaporator due to non-uniform surface temperature. Hence, the equivalence in the ice thickness developed in this case does not show the equivalence of the total ice-mass production per day.

In most cases, the rate of ice layer thickness development decreases after a value of 4 cm. However, the lower rate of ice-thickness development at a later stage was compensated with an increased surface area due to the elliptic shape of the ice-slab in this experimental set-up. Hence, one can’t conclude that the decrease in the ice layer thickness due to increased thermal resistance will reduce the hourly and daily ice production rates. On the other hand similar, ice thicknesses were obtained for differing COP values. Hence, the ice layer thickness was not correlated with system COP because of non-uniformity in its profile.

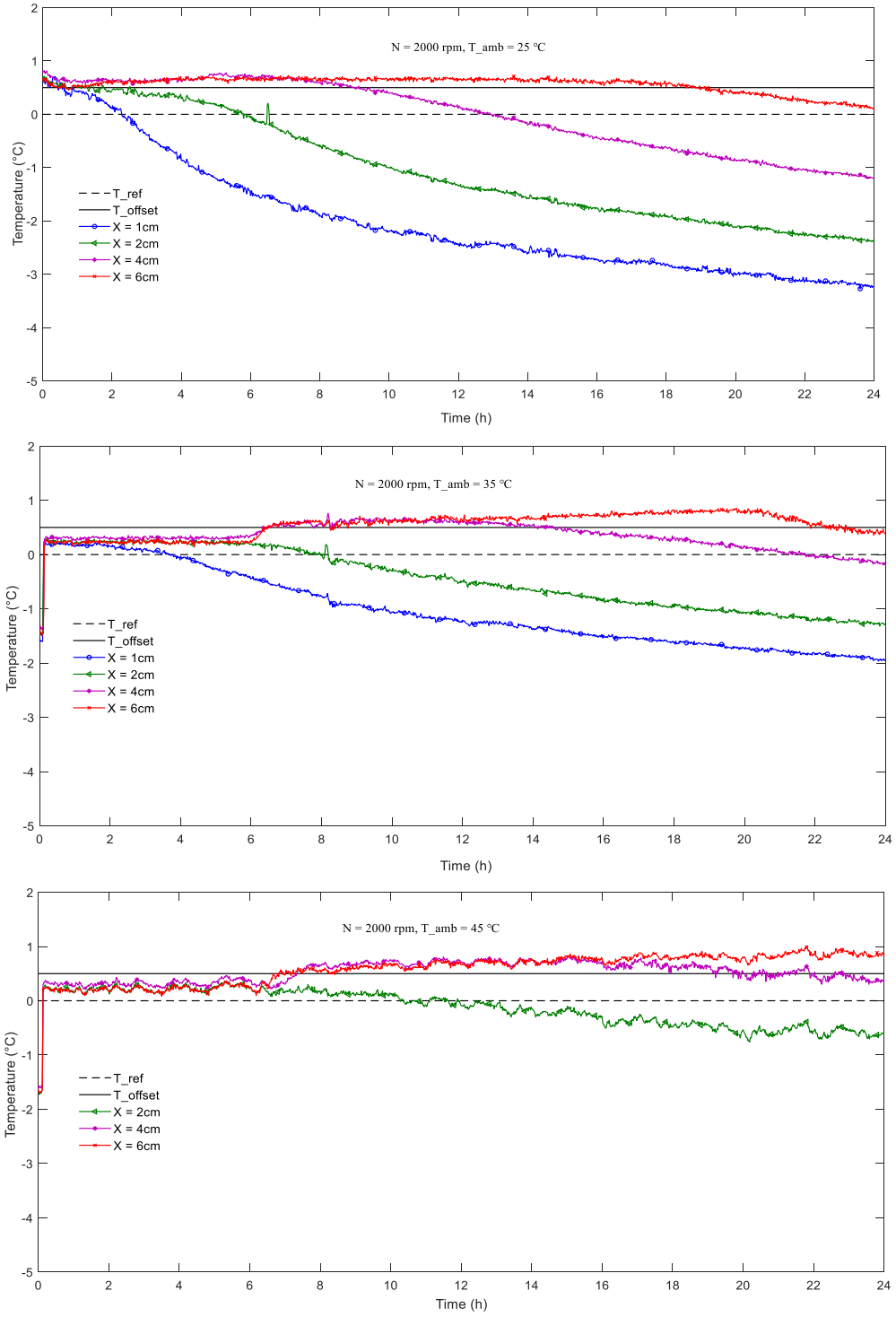

Figure 4. 11 Temperature distributions across the ice block vs time for different ambient temperatures and lower compressor speed showing ice thickness on the evaporator surface

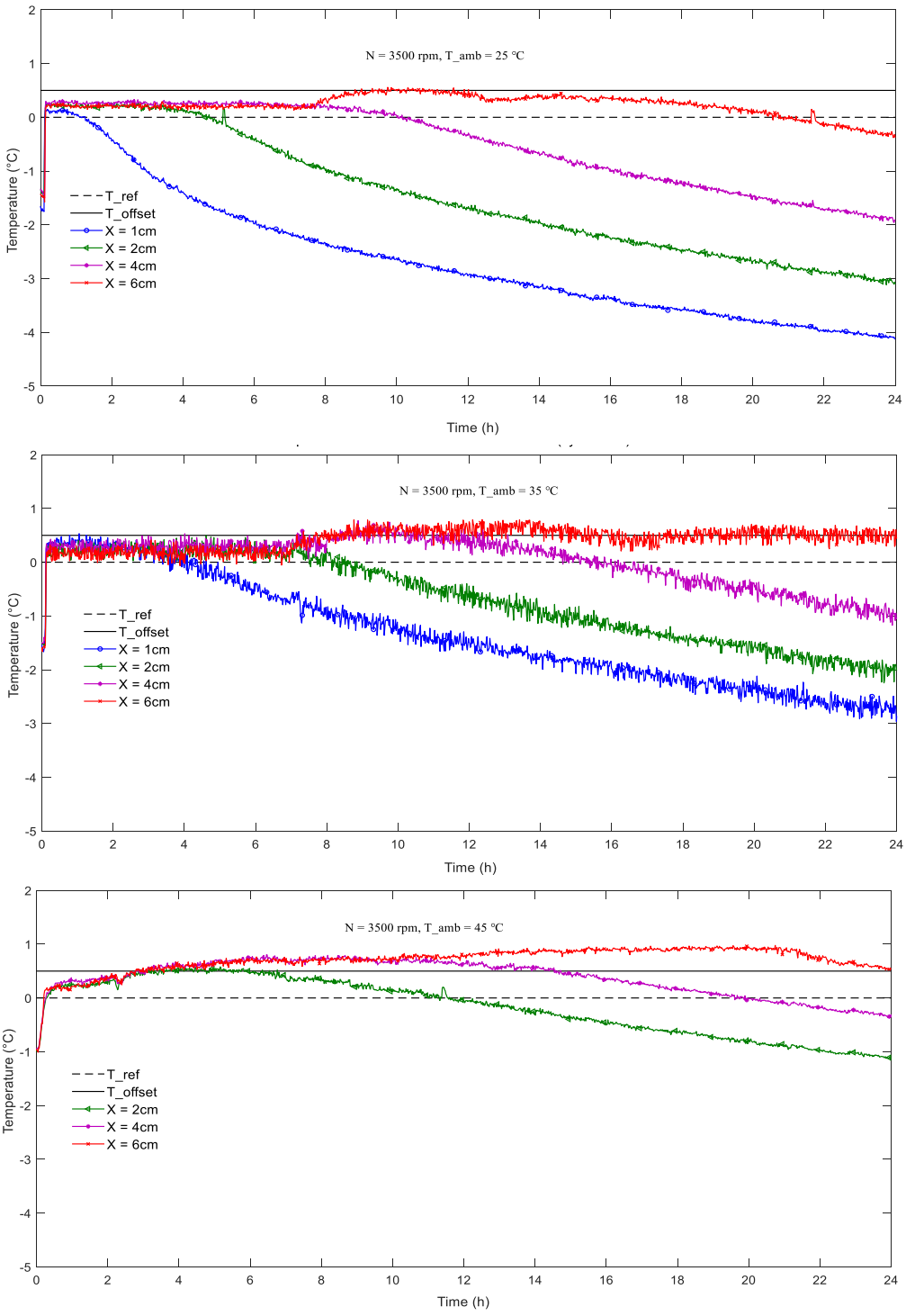

Figure 4. 12 Temperature distributions across the ice block vs time for different ambient temperatures and higher compressor speed showing ice thickness on the evaporator surface

4.3.5 Relevance of lateral thickness of with ice storage sizing and scale-up

Fig.4.13 shows the proposed ice-storage system with the parallel installation of several small capacity refrigeration cycle units (modular units) to satisfy the demand-based load requirement. With the minimum spacing of about 12.5 cm (2X) between two evaporator plates, a single ice-storage capacity can be scaled up to 150 kg ice production per day using six modular units. Thus, such ice-storage system can be used for medium scale milk cooling and smaller capacity cold room applications.

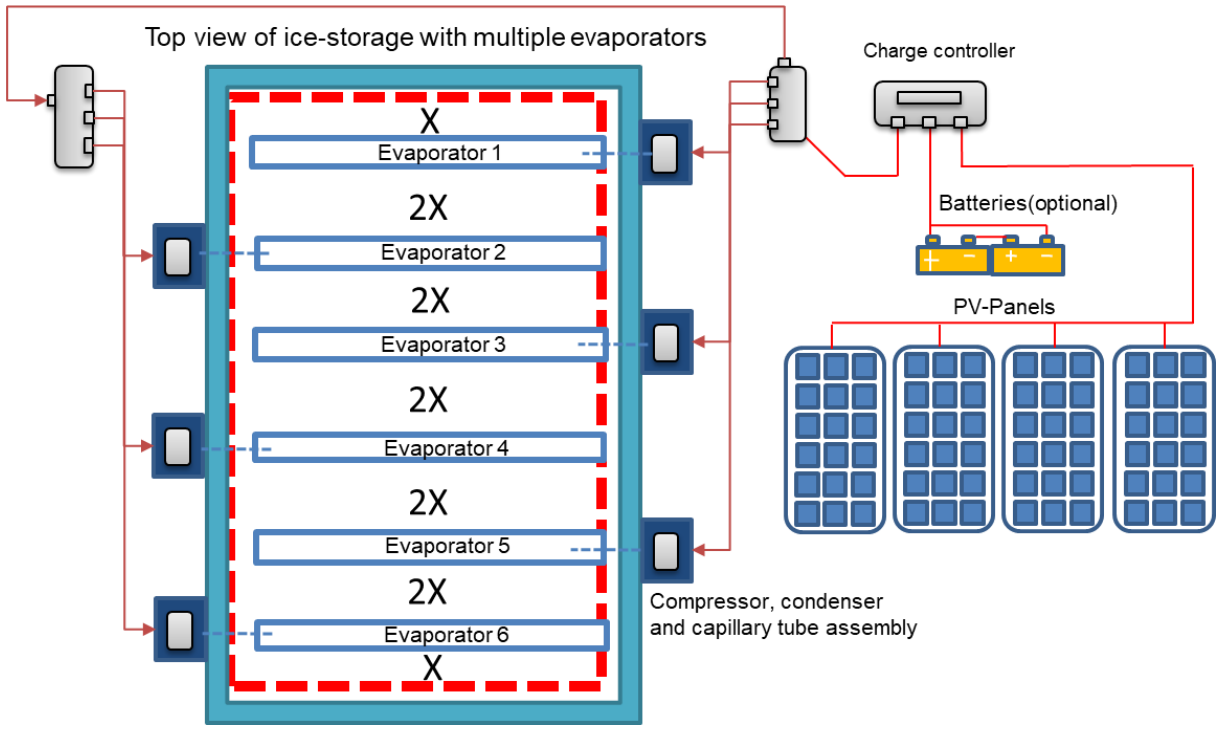

Figure 4. 13 Proposed Schematic of evaporator configuration inside ice storage for scalability concept

For the operation of the ice-storage beyond one day without discharging, the lateral thickness increase continuous in the slower rate than the first day. However, the daily mass of ice will not be affected significantly for two days of continuous operation. A 50 kg of ice with 18 cm ice slab thickness was observed for a 48 h continuous operation in a 35℃ ambient. The ice storage with one modular unit was also tested for more than nine days of continuous operation of the compressor at its maximum speed. During this lengthy operation at a 35℃ ambient, the minimum evaporator surface temperature observed was -10.74 °C. By changing the ambient temperature to 20 °C after 9th day while the ice storage system kept running for five additional

hours, the evaporator surface temperatures of -12.8 °C were achieved. A 100 kg of ice slab with 32cm thickness, as shown in Fig. 4.14 was formed in five and half days of continuous operation after phase transition state. Sensible cooling of the ice-slab was limited by the evaporator temperature and hence operation after complete solidification will not be energy efficient. The compressor suction-line temperature was around ambient, no suction line frost was observed, and thus the system is suitable for continuous operation.

Figure 4. 14 Picture of ice formed showing complete freezing in a 100-litter capacity insulated box and a single modular unit

4.4 Ice based milk cooling performance

This section presents the performance study of the milk cooling systems using ice-storage as the source of cold. A packing factor (PF) of 0.26 and 0.52 in a 95 L total ice-storage volume at 0℃ were considered as ice-storage energy density variables for milk cooling experiment. A forced recirculation of chilled water at flow rates of 300 and 600 Lh^{-1} was implemented. Cooling an 80 L of milk from 35 to 4℃ in less than 4 h was considered as a basic requirement of the system

4.4.1 Effect of WRR and PF on milk cooling curves

The milk cooling curves at the bottom, middle and top of the milk-can along the central axis were shown in Fig.4.15. The figure shows that the milk temperature along the vertical tends to be uniform as cooling proceeds. The milk temperature for each scenario attained less than a 1℃ difference along vertical after a 2.5 h cooling. The curves also show that the average milk

temperature drops to below 15 ℃ in 1 h and below 10 ℃ in 2 h in all cases so that the cooling rate is sufficient to prohibit bacterial growth after milking.

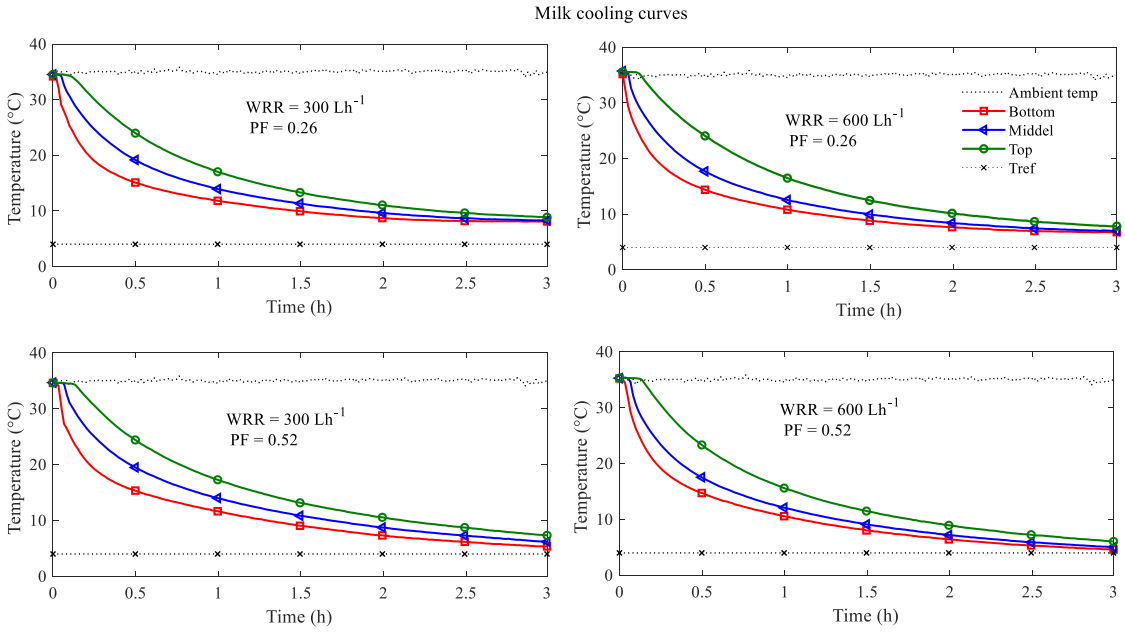

Figure 4. 15 Transient temperature distribution of milk along vertical axis at milk-can center for different packing factors and chilled water recirculation rates

For lower energy density in the ice-storage, the average milk temperature attained at the end of a 3 h cooling was 8.4 ℃ for a 300 Lh^{-1} and 7.2 ℃ for a 600 L h^{-1} recirculation rate. For higher energy density corresponding to a PF of 0.52 considered, the average milk temperatures at the end of a three h cooling were 6.3 and 5.2 ℃ respectively for 300 and 600 L h^{-1} recirculation rates. From the milk cooling curves shown, a PF of 0.52 at a chilled water recirculation rate of 600 L h^{-1} gives a better milk-cooling rate towards a reference temperature.

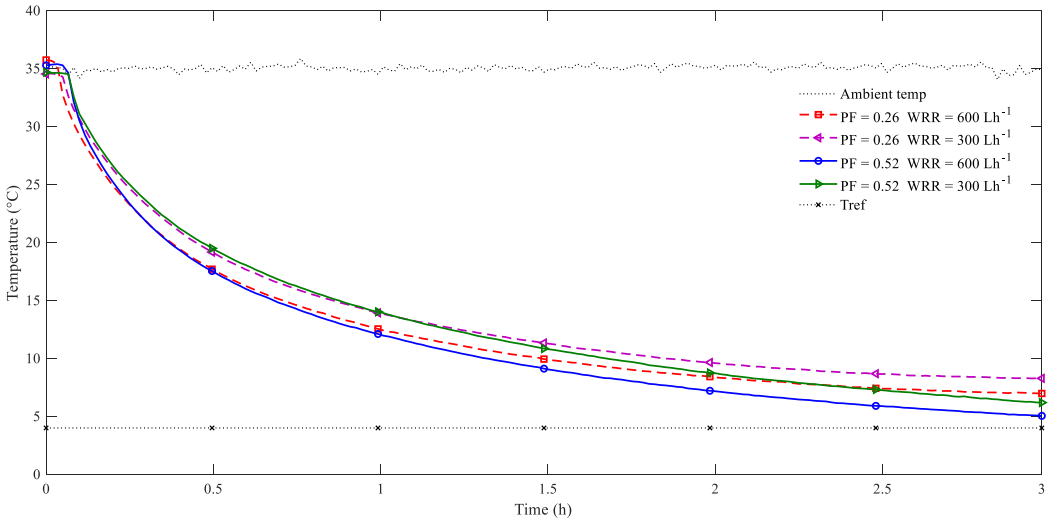

Figure 4. 16 Effect of packing factor and chilled water recirculation rate on average milk temperatures

The milk cooling curves coincide for different packing factors but the same recirculation rate during the first 1 and 1.5 hours respectively at recirculation rates of 600 and 300 Lh^{-1} as shown in Fig.4.16. The difference in milk cooling curves due to packing factor was observed after the first 1 and 1.5 hours, respectively, for the flow rates indicated on the figure. Decreasing the chilled water recirculation rate introduces a time lag on milk cooling rate, whereas varying the PF mainly affects the minimum attainable milk temperature. At a later stage of recirculation when the milk temperature reaches 5-6℃, it takes about one hour to get a temperature drop of 1℃. Therefore, by increasing the recirculation rate we can decrease the milk cooling time taken. This is because; transporting a given amount of energy takes longer time at lower recirculation rate. Hence, a packing factor of 0.52 and above at chilled water recirculation rate of 600 L h^{-1} would be a better design option for the milk cooling system in the range of 100 Ld^{-1} capacities.

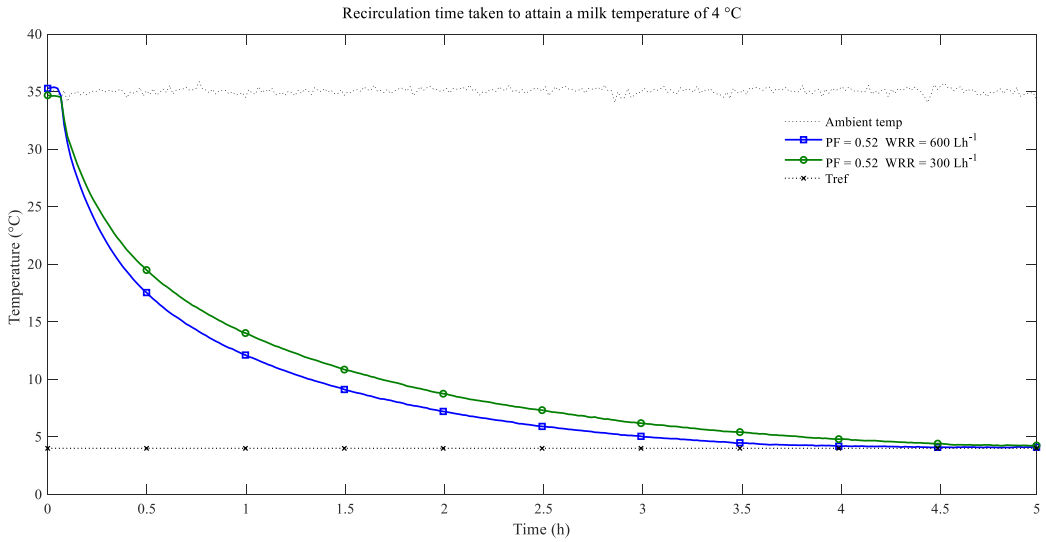

Figure 4. 17 Milk cooling time taken for a fixed packing factor and varying chilled water recirculation rate

The case of 0.26 packing factor was not sufficient to cool an 80 litre of milk below 7 ℃, and hence the PF of 0.52 was considered for cooling time evaluation in this case. The milk-cooling rate was faster at an early stage, and it decreases with decreasing the temperature difference between the milk and heat transfer fluid (water bath) as shown in Fig.4.17. A significant decrease in the rate of milk cooling was observed after the milk temperature of 10 ℃ or two hours of cooling time. A milk temperature drop ranges from 26 to 28 ℃ during the first two hours of cooling whereas it was not more than 3 to 4 ℃ for the same duration afterwards as can be seen from Table 4.7. However, the milk was cooled to 4 ℃ in 4 hours at a chilled water recirculation rate of 600 L h^{-1}, and it takes 5 hours to reach a 4 ℃ temperature if the chilled water recirculation rate is reduced to 300 L h^{-1}.

Table 4. 7 Final milk Temperatures at different packing factor and recirculation rate

Cooling time (h)	**Packing factor**			
	0.52		0.26	
	Chilled water recirculation rate (Lh^{-1})			
	300	600	300	600
	Milk temperature (℃)			
0	34.74	35.27	34.53	35.18
1	14.18	12.61	14.15	13.75
2	8.82	7.48	9.76	8.67
3	6.29	5.22	8.41	7.18

4	4.88	4.39	-	-
5	4.36	3.76	-	-

4.4.2 Milk-cooler preservation performance

After cooling the milk to 4℃, the system preserves milk for about 12 hours without a significant increase in temperature. The average milk temperatures after 24 hours of storage, including the cooling time, was 5.5, 7, 9, and 11 ℃ respectively for conditions indicated in Fig.4.18. The insulation of milk-cooler has a more significant role in reducing heat gain from ambient. Moreover, the water bath available at a lower temperature after the end of cooling helps in maintaining the milk temperature without significant response to higher external ambient. The average milk-temperature increase observed after one-day preservation was in the range of 1.5-3℃.

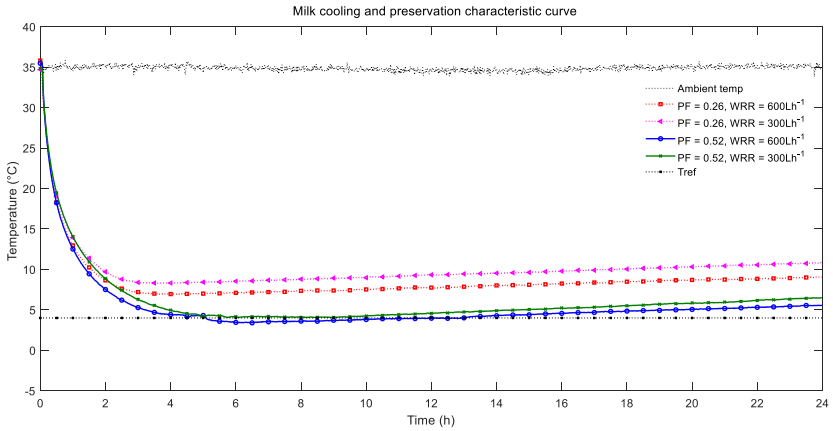

Figure 4. 18 Milk cooling and preservation characteristics for different packing factors and chilled water recirculation rates

4.4.3 Recirculating water temperature variation

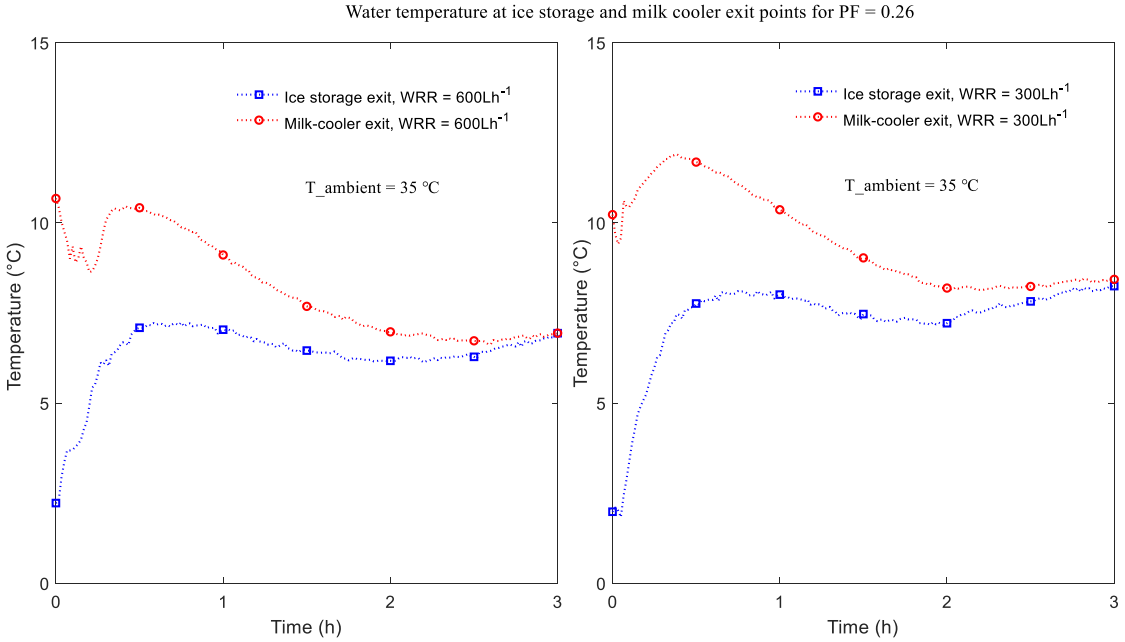

a)

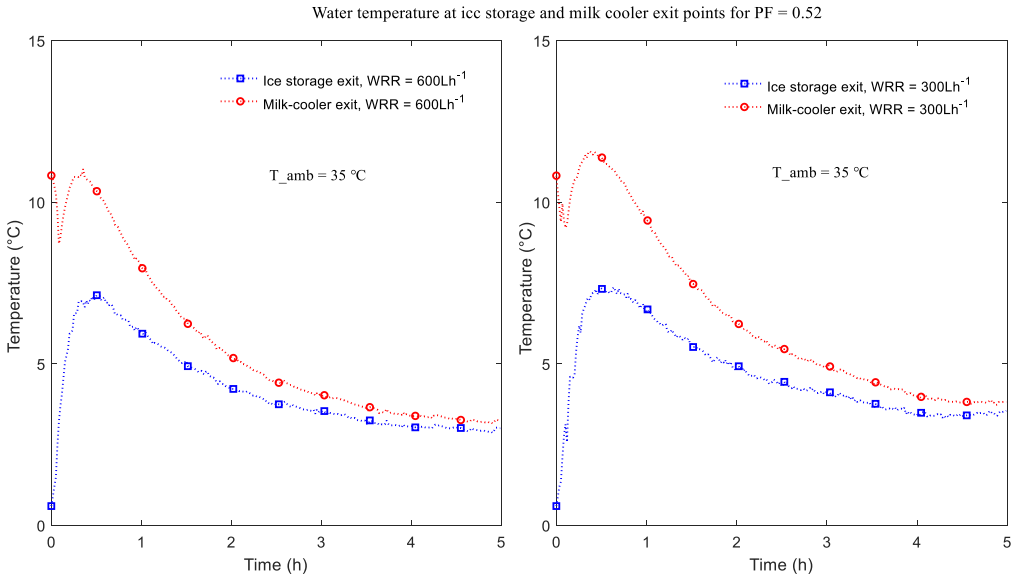

b)

Figure 4. 19 Recirculating water temperature variations at the ice-storage and milk-cooler exit points

The ice-storage and milk-cooler exit-inlet temperature variation for PF of 0.26 was shown in Fig. 4.19a. The milk-cooler exit temperature determines the minimum possible temperature that milk in the storage can have with ideal heat exchange. The exit water temperatures after two hours of recirculation were towards a common focus point indicating that the ice was completely melted

in two hours and the sensible heat exchange takes place afterwards. Up on recirculation for three hours, the ice-storage and milk-cooler exit temperatures reached a common point. Recirculation after 3 h will not decrease the milk temperature in this case. For a 600 L h^{-1} recirculation rate, the ice-storage exit temperature increased from 6.2 to 6.9 ℃ during the last one hour of recirculation, giving only milk temperature drop of 1.5℃. For the case of 300 L h^{-1} recirculation rates, an ice-storage exit temperature increased from 7.21 to 8.25 ℃ in the last one hour of recirculation for the same milk temperature drop of 1.5℃. In both cases, the system could cool milk to a temperature below 10 ℃ in 2 h. However, the ice fraction was not sufficient to further cool down the milk. Therefore increased ice fraction in the ice-storage should be considered for this scenario.

Fig.4.19b shows the temperature history of recirculating water at both ice-storage and milk-cooler exit points for a PF of 0.52. The water temperature in the ice-storage follows an increasing trend for the first 0.5 h, and then it decreased. This was because of the heat interaction with water bath that was initially at about 10 ℃ and continuously absorbing heat from the milk. After a 0.5 h of recirculation, the heat from ice melting became dominant over the water bath temperature inside the milk-cooler so that both ice-storage and milk-cooler temperatures continued decreasing. The initial mixing of chilled water with a water bath in milk cooler (HTF) resulted in an instantaneous temperature drop on HTF during startup. By decreasing the initial temperature of the water-bath inside milk-cooler, it is possible to reduce the initial temperature transients and increase rate of milk cooling. Nevertheless, decreasing the water-bath temperature below10 ℃ needs additional cooling mechanism, which adds cost and complexity on the overall system.

Another important observation from Fig.4.19b was that the temperature difference between ice-storage exit and inlet approach equilibrium points after 3.5 h for 600 L h^{-1} and after 4.5 h of cooling for 300 Lh^{-1} recirculation rates. The temperature differences between the ice-storage inlet and outlet were changed from only 0.4 to 0.2 ℃ during recirculation after the mentioned equilibrium points. The ice-storage exit temperature was changed from 3.25 to 3.01 ℃ whereas the milk-cooler exit temperature was changed from 3.66 to 3.24 ℃ during the last 1.5 h of recirculation at a rate of 600 L h^{-1}. For the case of 300 L h^{-1} recirculation rates, the ice-storage exit temperature changes from 3.77 to 3.54 ℃ and the milk-cooler exit temperature showed a

decrease from 4.43 to 3.7 ℃ during the last 1.5 h. During recirculation between 3.5 to 5 h, the average milk temperature decreased from 4.7 to 3.76 ℃ for 600 Lh^{-1} and from 5.51 to 4.36 ℃ for 300 Lh^{-1}. This implies that a four-hour chilled water recirculation could be sufficient to cool the milk to the required temperature of 4 ℃ for forced circulation milk cooling system developed in this research.

4.4.4 Energy to milk ratio and the energy transfer effectiveness

The energy transferred to both the milk and the HTF (water-bath in the milk-cooler) was shown in Fig.4.20. The result presented was for a 3 h cooling at a PF of 0.26 and a 5 h cooling at a PF of 0.52. According to the results, it took 2 h to transfer a 2.44 kWh of energy at a recirculation rate of 600 Lh^{-1} and 3 h at 300 Lh^{-1} for a PF of 0.26. For milk cooling with a higher PF, transferring a 2.83kWh of energy took 3 h at 600 L $h^{-1,}$ but it needed 5 h to transfer the same amount of energy at 300 L h^{-1} recirculation rates. In general, a maximum of 2.94 and 2.83 kWh of energy removal from milk was possible at higher and lower recirculation rates, respectively. Another observation was that doubling the PF doubles the energy absorbed by the heat transfer fluid. The figure also shows that the recirculation rate did not affect the storage of energy by HTF. It is also important to mention that the sensible heat absorbed by the HTF plays a positive role in milk preservation after cooling.

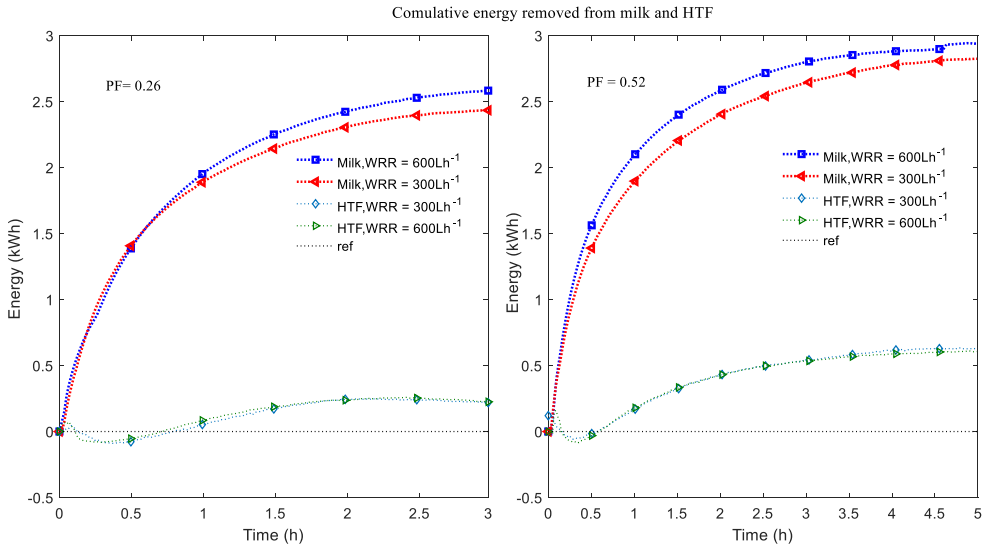

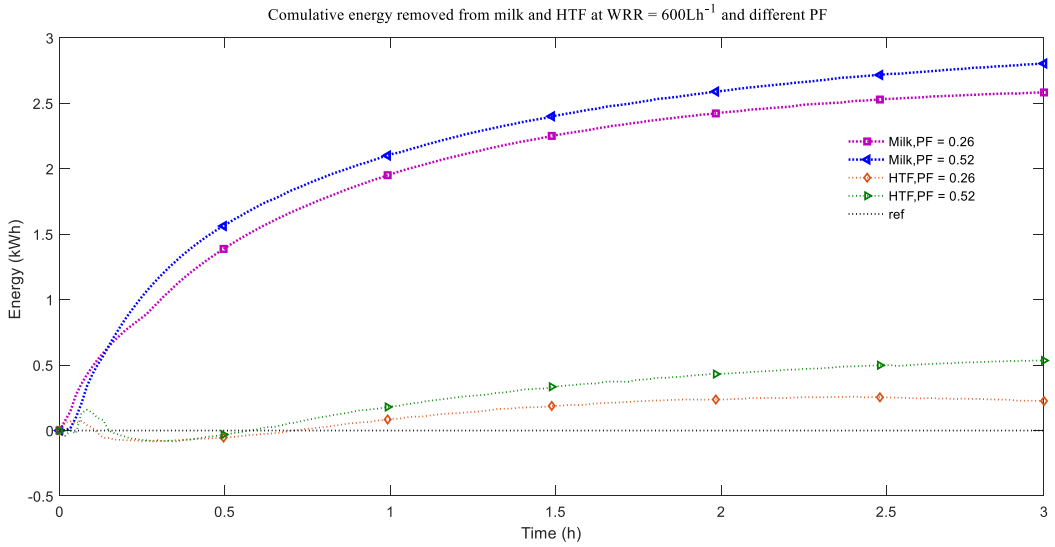

Figure 4. 20 Cumulative energy transferred to the milk-cooler vs recirculation time

4.4.5 The milk cooling system capacity range under varying parameters

The milk cooling system developed in this research was required to meet a condition of 4℃ in 4 h. However, pre-cooling to below 15℃ could be another potential application of the technology both in milk collection centers and small scale processing firms in developing countries. The final milk temperature requirement also varies based on the intended use of milk either for the process, short term storage before transportation, or a standard regulation of a given country for the bacteriological count. Besides this, the ice-storage energy production capacity variation with compressor power input and surrounding ambient could also affect the milk volume to cool. Therefore, the system's capacity in terms of milk volume to cool with respect to varying ambient and final milk temperatures of 15, 10, and 4 ℃ were analyzed in this section.

4.4.5.1 Comparisons of experimental and theoretical energy demand of the milk

The measured energy supplied to the milk cooler is the sum of the latent heat of melted ice and sensible heat within the ice storage. The theoretical energy for milk cooling was calculated based on the sensible energy demand to cool 80 L milk at 35 ℃ and a 75 L of water-bath at 10℃ surrounding the milk-cans. Table 4.8 shows the experimental and theoretical energy demand to cool 80 L milk to different temperatures. The variation between experimental and theoretical energy demand increases as milk temperature decreases in all cases. This is because, at lower milk temperature, the heat exchange with the surrounding water-bath becomes smaller due to the

lower temperature difference between the two fluids. On the other hand, the ice continues melting due to convection by recirculating fluid. The heat losses to the surrounding ambient also increase relative to the initial recirculation time. Even though the pumping power and heat loss due to recirculation remain constant under a given scenario, the milk temperature drop at a lower temperature is smaller, causing an increase in loss fraction. In addition to this, to cool milk below 10℃ with the current set-up, energy is consumed by the HTF (water-bath) that disproportionally affects the energy demand. Hence, it can be said that the proposed milk cooling set-up would be energy efficient option for final milk temperature requirements in the range of 10℃ and attaining a 4℃ is an energy intensive option.

Table 4. 8 Experimental and theoretical milk cooling and preservation energy demand

PF = 0.52							
WRR = 300 L.h^{-1}				WRR = 600 L.h^{-1}			
Milk temperature (℃)	Energy required (kWh)			Milk temperature (℃)	Energy required (kWh)		
	Exp.	Theoretical	difference %		Exp.	Theoretical	difference %
14.2	2.49	2.05	6.83	12.6	2.41	2.3	4.78
8.8	3.29	2.82	9.93	7.5	3.26	3.02	7.95
6.3	3.61	3.19	13.17	5.2	3.66	3.35	9.25
4.9	4.04	3.41	18.48	4.2	4.02	3.48	15.52
PF = 0.26							
WRR = 300 L.h-1				WRR = 600 L.h-1			
14.2	2.24	1.94	9.28	13.4	2.25	2.08	4.81
9.8	2.83	2.55	10.98	8.6	2.82	2.70	5.19
8.4	3.17	2.66	19.17	7.2	3.04	2.79	8.96

The milk to energy ratio that relates the volume of milk with the energy demand was an important parameter which can be used for general calculations. A tabular relation for milk volume per kWh input shown in Table 4.9 was established based on the experimental and theoretical data. Since the water was used as a substitute for milk, an increase in energy requirement due to specific heat capacity difference and other physical property variation could be expected in real situations on field. This could also affect both experimental and theoretical value of the milk volume per energy input presented in this work.

Table 4. 9 The milk volume per energy input with respect to final temperature requirements

Cooled milk temperature (℃)	Energy required (kWh)		Milk volume per energy input L.(kWh)$^{-1}$	
	Exp.	Theoretical	Exp.	Theoretical
15	2.08	1.98	38	40
10	2.93	2.66	27	30
4	4.2	3.50	19	23

4.4.5.2 The milk cooler capacity variation with final milk temperatures

The climatic condition affects both the energy production and the heat loss from the cooling system. Variation in compressor power input and the ambient temperatures were considered as representations of basic climatic condition parameters affecting the milk cooling system developed in this research. The proposed milk cooling system was evaluated for the operation of two modular units in parallel within the ice storage to get sufficient energy for cooling. Using the ice storage performance parameters from Fig.4.7 of this chapter, the daily capacities could be projected for two units in parallel operation and shown in Table 4.10.

Table 4. 10 Daily energy output under varying climatic conditions

Compressor power (W)	2*40			2*70		
Ambient temperature (℃)	25	35	45	25	35	45
Daily energy output (kWh)	3.68	3.32	2.62	4.92	4.74	3.94

Using Tables 4.9 and 4.10, the amount of milk to be cooled with respect to the ambient condition could be estimated. Tables 4.11 and 4.12 show the capacity range of the milk cooling system based on theoretical and actual energy demands, respectively. Some additional energy requirement needs to be assessed to maintain the continuous operation of the ice storage and possible additional losses incurred at field level. With this aspect, a reasonable amount of ice should always be there to avoid super-cooling of water before the start phase change process. For compressor operation at 2*70 W and an ambient temperature of 25℃, the experimental system capacity over theoretical would vary in the range of 10 to 18 L based on final milk temperature required. For the range of experimental energy input and ambient temperatures considered, the capacity of the milk cooling system could vary from 50 L to 94 L for standard milk temperature

of 4℃. However, the system can handle a milk volume in the range of 189 L if the milk temperature of 15℃ is a final requirement.

Table 4. 11 Milk cooler capacity based on theoretical energy demand

Daily capacity (milk volume in litre)						
Required milk temperature (℃)	2*40 W compressor power input			2*70 W compressor power input		
	Operating ambient temperature (℃)			Operating ambient temperature (℃)		
	25	35	45	25	35	45
15	149	134	106	199	192	159
10	111	100	79	148	143	118
4	84	76	60	112	108	90

Table 4. 12 Milk cooler capacity based on experimental energy input

Daily capacity (milk volume in litre)						
Required milk temperature (℃)	2*40 W compressor power input			2*70 W compressor power input		
	Operating ambient temperature (℃)			Operating ambient temperature (℃)		
	25	35	45	25	35	45
15	142	128	101	189	182	152
10	101	91	72	135	130	108
4	70	63	50	94	90	75

4.5 Ice discharge characteristics with fan-coil-unit as end-use device

An insulated room with constant heating to simulate the cooling load was used during ice discharge. A known mass of ice from a daily operation of the ice-storage was used as an input for each scenario. A fan-coil-unit (FCU) with variable cooling load capacity was used to cool the air in an insulated room with a climate simulator. For the external melt ice-in-water-bath configuration, the chilled water recirculation rate was varied together with an FCU load to characterize the ice discharge performance. The effects of varying operational parameters both on the ice discharge rate and the range of air temperature drop across an FCU were experimentally analyzed, and the results are presented below.

4.5.1 Effect of fan speed on room air temperature variation

The hot air entering the Fan-Coil-Unit (FCU) was maintained at a constant temperature of 35℃ in all scenarios. Fig.4.21 shows the effect of varying air flow rate across FCU on room air temperature. A minimum and maximum fan speeds were used together with chilled water flow rate variation. For WRR of 2.7 L.min^{-1}, the FCU exit air temperature varies between 12 and 16 ℃ during a discharge period of 2.5 h. With the average temperature being 15℃, a 20 ℃ temperature drop across an FCU was obtained. On the other hand, increasing the fan speed to a maximum airflow rate level brings the average FCU exit air temperature to 20℃, making the temperature drop across FCU to be 15℃. At an increased WRR of 5.4 L.min^{-1}, the FCU exit temperature becomes lower. A lower fan speed, in this case, gives a temperature range of 9 to 13.6℃. With the average exit temperature of 12.5℃ during a 2.5 h discharge period, an air temperature drop across FCU of 22.5℃ was obtained. A higher fan speed, in this case, gives an FCU outlet temperature range of 14 to 20℃. This scenario provides a temperature drop across the FCU to be 17.5℃.

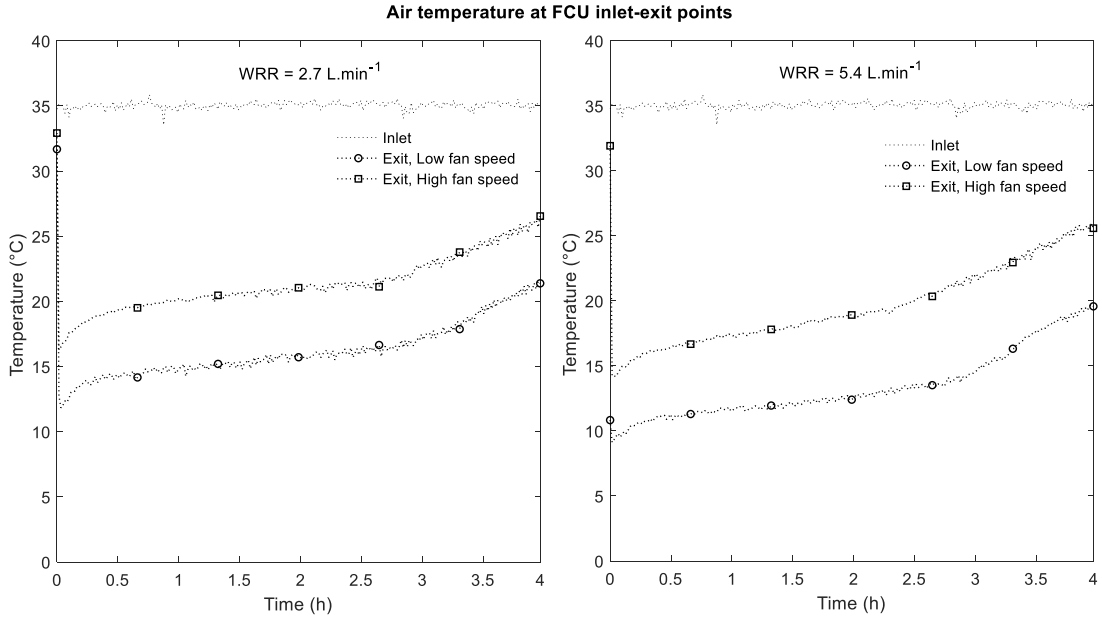

Figure 4. 21 Range of air temperature drop across FCU showing the effect of varying fan speed

In general, a temperature drop across an FCU of 15 to 20 ℃ was observed by varying a fan speed at a lower water recirculation rate of 2.7 L.min^{-1}. Doubling the chilled water recirculation rate gives a temperature drop across an FCU in the range of 17.5 to 22.5℃ respectively for higher

and lower fan speeds considered. Lower fan speed resulted in lower exit air temperature in both flow rate cases. This is because, at lower fan speed, the lesser air volume and relatively longer residence time allow more heat to be transferred to the colder fluid (chilled water). An increased chilled water recirculation rate also helps to extract more heat from hot air at a given time so that it was possible to get lower exit air temperatures for both fan speeds considered. The result obtained could be used as an important input to evaluate the UA parameter of the FCU to model a cold room application.

4.5.2 Effect of chilled water recirculation rate on FCU exit air temperature

Fig.4.22 shows the effect of varying the chilled water recirculation rate on FCU exit air temperature for a given fan speed. As can be seen from the figure, chilled water recirculation effect on FCU exit air temperature was observed during ice melting. The room air temperature gradient will be more affected by airflow variation along with FCU than the change in recirculation rate. Hence, a variable flow fan with fixed pump flow rate would be a better control option for ice storage in cold room application.

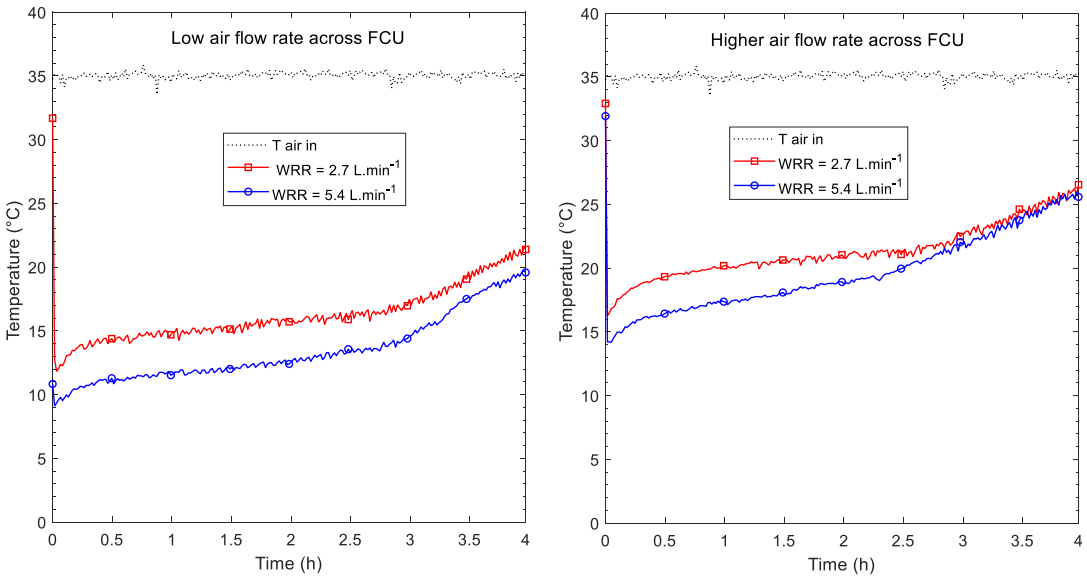

Figure 4. 22 Effect of chilled water recirculation rate on air temperature drop across FCU

4.5.3 Effect of chilled water recirculation rate on water temperature inside ice-storage

The ice-to-water fraction inside the ice-storage affects the water temperature during discharge and the corresponding rate of ice-melting inside. The effect of recirculation for the water was

basically to create a uniform temperature along vertical, whereas it enhances the bulk convection coefficient on liquid-solid interface region. Fig.4.23 shows water temperature variation inside ice-storage for different chilled water recirculation rates (WRR) and fan speeds. The ice-storage temperature variation was not affected by the recirculation rate for water below 4℃ as can be seen from the figure. For both fan speeds considered, lower WRR resulted in higher ice-storage water temperature as long as there is stored energy due to ice. However, the rate of water temperature increase was higher for higher fan speed. A time lag of 30 minutes was observed on temperature reading at a lower fan speed case when compared with higher fan speed. Moreover, doubling the chilled water recirculation rate resulted in a temperature difference of 1℃. In general, lower fan speed and higher WRR (5.4 L.min^{-1}) gives minimum storage water temperature.

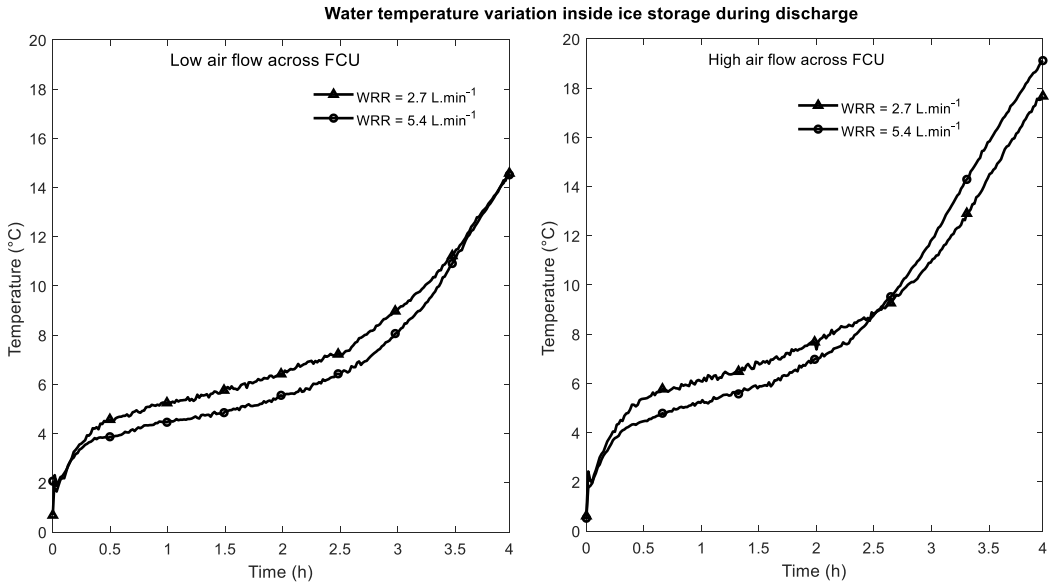

Figure 4. 23 Effect of chilled water recirculation rate on water-bath temperature in the ice-storage

4.5.4 Effect of fan speed and WRR on water temperature across FCU

Fig.4.24 shows the variation of water temperatures at inlet and exit points for the FCU used in this experiment. As the figure shows, the water temperature change was more affected by the water recirculation rate than the airflow variation across FCU. A water temperature change of 3.5℃ was obtained at a WRR of 2.7 L.min-1 and higher airflow across the FCU. For an increased WRR of 5.4 L min^{-1}, the water temperature change across the FCU was reduced to 2℃ regardless of the change in airflow across the FCU. This implies that a chilled water recirculation

rate in the range of 5.4 L min^{-1} would be required when the ice storage is implemented for cold room application.

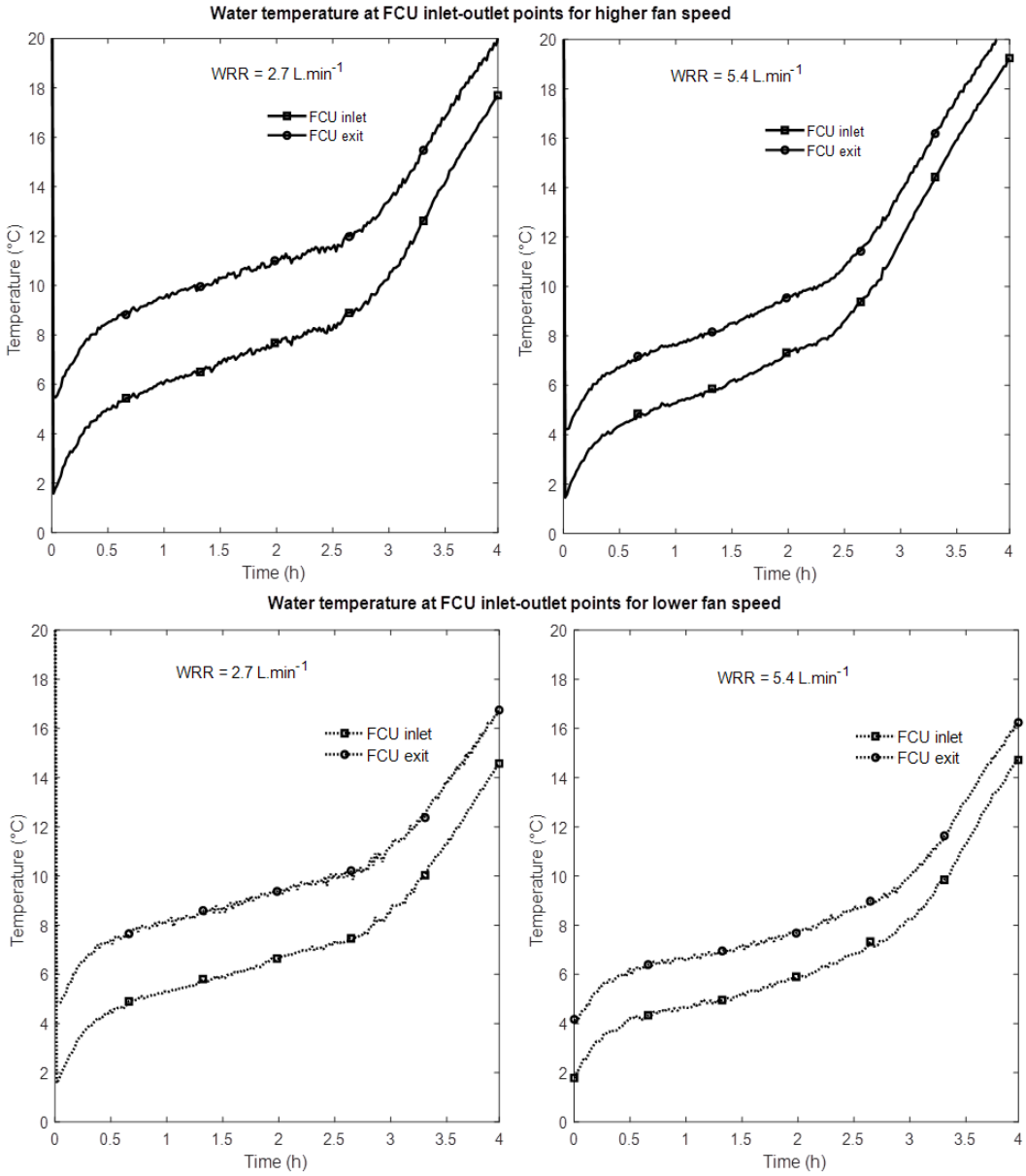

Figure 4. 24 Water temperature variations across FCU during ice discharge

4.5.5 Overall ice-melting/discharge time

Knowing the melting rate of ice-slab on flat evaporator surface helps to manage the cooling load of a system. In the ice-storage system proposed in this research, the time taken to discharge a daily ice produced is one of an important design factor to be determined. Range of chilled water

flow rates and fan speeds considered were based on practical application of the system for small scale cooling. Due to the constraint of the available experimental set-up, total time taken for complete melting was evaluated even though it gives general information rather than specific time-based phenomena. The slop change in temperature measurements for conditioned air, chilled water circulating through the FCU and water inside the ice-storage can be considered as indicators of complete melting of ice provided that there is no further energy addition to the ice-storage. Fig.4.25 shows the temperature history with time inside the ice-storage for varying chilled water recirculation rate (WRR) and fan speeds. At a WRR of 2.7 L.min^{-1} and both low and high fan speeds considered, the line slope change was at 2.5 h. For the case of WRR = 5.4 L.min^{-1}, melting was completed at 2.33 h and 2.67 h respectively at higher and lower fan speeds. Increasing the air volume across the FCU by increasing the fan speed resulted in higher water temperature in the ice-storage due to more heat extraction from the circulating water. The effect of increased water recirculation rate was observed by decreasing the melting time. In general, it takes 2.5 hours on average to completely discharge the 25 kg of an ice-slab with the current configuration.

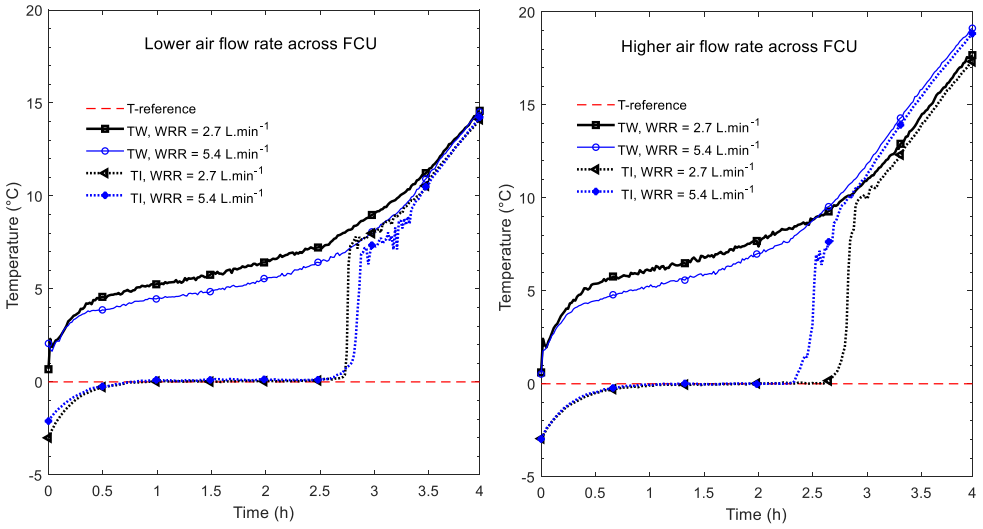

Figure 4. 25 Ice and water temperature variations inside ice-storage during discharge

4.6 Highlights of major findings

The ice production technique implemented in this research was shown in Fig.4.26 with the evaporator in the water bath configuration. There was a direct heat exchange between the refrigerant and the water during the energy storage process in the form of ice. In the conventional

approach of small scale, ice making process as used by Torres-Toledo et al. [57], the refrigerant evaporating temperature was in between -20℃ and -10℃ since the air was the heat transfer medium. However, an evaporating temperature of around -5℃ was maintained in a daily operation for the ice storage system developed in this research. Torres-Toledo et al. also reported a system COP in the range of 1.1 to 1.63 for smart ice maker of 12kg daily maximum ice mass output. Axaopoulos et al. [22] reported a daily ice mass in the range of 4.5-17 kg using 440 W_p solar panel by operating four small DC compressors at a time. The researchers designed the ice storage system for battery-free operations so that the refrigeration cycle units operate below design capacity during most of the day and remain idle during the night time. However, developing an ice storage system that works at its maximum capacity during the day time and with minimum power input required during the night time will increase the daily ice mass output.

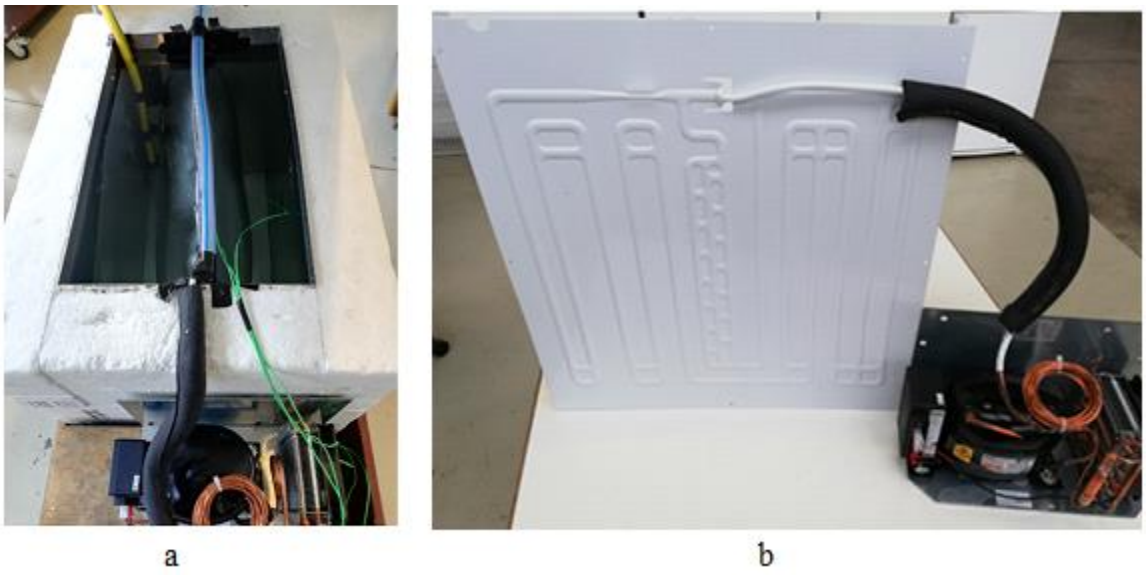

Figure 4. 26 Pictures from experimental campaign (a) Experimental ice storage system developed (b) DC-powered refrigeration cycle unit fabricated

Therefore, the current system was designed to operate at full load capacity during the day time and supposed to work at lower capacity during the night time with the help of a battery bank. In the experimental system, the higher and lower compressor speeds were used as representatives for respective day and night modes. Since the purpose of the system developed is to store energy in the form of ice, a battery-free configuration is still possible with solar PV but a reduced daily energy storage capacity. A daily ice mass production of 13.96 kg - 26.28 kg was obtained from the system developed in this research. The compressor energy consumption was between

0.83kWh and 1.71kWh for the COP values in the range of 2.63 and 1.5. A system configuration with a maximum and minimum daily ice production tends to have a COP value of 1.75 and 2.09 respectively. Accordingly, the system COP improvement and increase in the daily ice mass production was achieved with the technique used in this research when compared with literature values.

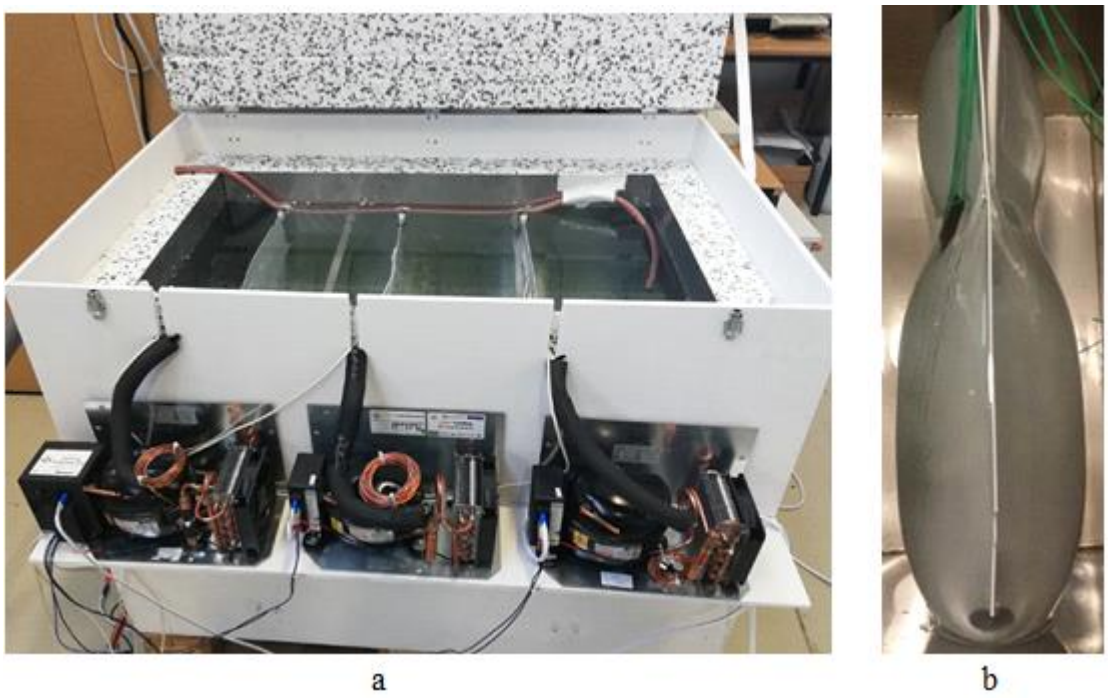

Figure 4. 27 Scaled up ice storage system (a) Arrangement of multiple units in parallel (b) Ice profile on a single evaporator surface within the ice storage

Fig.4.27 shows an ice storage system fabricated for an increased energy storage capacity by arranging independent refrigeration cycle units in parallel. Modular units were assembled in a single insulated compartment with evaporator spacing recommendations of 12.5 cm each. This configuration can also be used for a battery-free operation where several units will operate either at a time or sequentially based on the availability of solar energy. Most ice makers based on commercial refrigerators were not suitable for such an approach of capacity improvement since the refrigerator compartments are designed for specific load requirements. Moreover, the local manufacturing of the ice storage system can be realized elsewhere by using modular units from a specialized company. This modular unit based ice storage system development approach will also minimize the total system cost and improve local manufacturing skill.

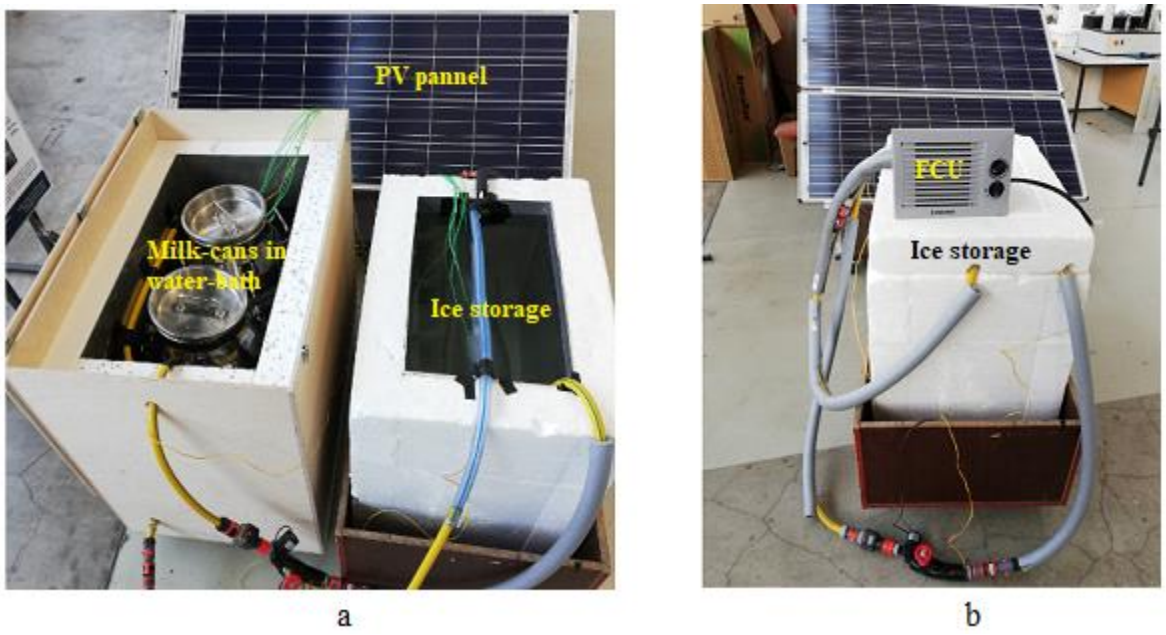

Figure 4. 28 Application setup of the PV powered ice storage system (a) Milk cooling by chilled water recirculation (b) FCU as end-use device for cold room

Foster et al. [50] used brine bags around milk-can to cool the milk down to 4℃ with ice blocks around the internal walls of a PV refrigerator. With the energy interaction set-up of ice – air– brine – milk container – milk, the researchers reported a rapid cooling of milk to 4℃ in a shorter time even though the milk cooling curve was not provided. The effectiveness of the heat exchange and the milk to ice ratio were not also reported by researchers to have a quantitative comparison of their system with others. Torres-Toledo et al. [45] used an ice compartment inside milk-can to cool the milk down to 10℃ in 3 h. Even though the energy interaction was ice –ice compartment – milk, which is a more effective approach for energy transfer, cooling of milk down to 4℃ was not achieved due to a lower heat transfer area between milk and ice block. Milk temperature control, handling of variable milk volume, diversification of the ice storage application to the cold room were among common limitations the systems had.

The ice production technique together with energy transfer approach modifications were the main contributions of this work. Recirculating water as a heat transfer fluid between the milk-cooler and the ice storage was utilized in this research making the energy interaction to be ice – water – milk container – milk as shown in Fig.4.28a. This set-up gives a better option for the handling of a variable milk volume and corresponding milk temperature control by means of the recirculating water flow rate. The water to water heat exchange together with a forced circulation

due to pumping will enhance the rate of ice melting and corresponding energy transfer to the milk. This approach also provides flexibility in ice storage application diversification by switching the product load to a fan-coil-unit as shown in Fig.4.28b.

4.7 Conclusions

The result has been presented and analyzed for performance characterization of the ice storage system, the ice phase change process, the ice-based milk cooling performance and ice discharge test using FCU as an end-user device. Accordingly, the following conclusions were made:

The minimum evaporator surface temperature attained at the end of each experiment was -5℃, which has a positive impact on performance improvement. Besides this; changing the compressor speed has a significant effect on the uniformity of the temperature distribution on the evaporator surface, which may be due to related changes in refrigerant flow rates, and a pressure drop inside the tubes.

According to the results from the experimental work, it was possible to produce a 26.28 kg of ice from water at 0℃ in a one-day operation by using a DC power of 70 W. Moreover, the ice production rate is highly affected by the compressor speed than ambient temperatures. The system has a better COP at lower compressor speeds but a higher ice production rate at higher compressor speeds. The ice storage system analyzed achieved a COP value in the range of 1.5 to 2.63. However, a COP value of 1.75 at 1.59 kWh of system energy consumption gives a better ice production compared with other scenarios. For the annual energy demand in the range between 303kWh.year^{-1} and 624.15kWh.year^{-1}, the system can achieve a refrigeration capacity of 697kWh.year^{-1} to 1036.6kWh.year^{-1}. However, the useful annual energy stored would be between 478kWh.year^{-1} and 897.9kWh.year^{-1} considering the heat lost to the ambient.

Both cold side and phase front boundary conditions for water-ice phase change process were quantified and characterized. Effect of ambient temperature and compressor power input variations on the degree of sub-cooling before phase transition was also analyzed. The ice-slab layer development on the evaporator surface for small capacity refrigeration cycle unit was characterized for varying operating conditions. The sub-cooling time taken before phase transition was higher at lower compressor speed and higher ambient temperatures. Higher compressor speed resulted in shorter sub-cooling time before transition regardless of ambient

temperature variations. The phase change temperature was maintained at nearly 0℃ during the phase change process for all cases with only 0.5℃ temperature difference between the top and bottom layers of the water inside the ice-storage. A lateral ice-slab thickness varied between 7 and 12.6 cm depending on the compressor power input and ambient temperatures for a continuous daily operation. A minimum evaporator plate spacing of 12.5 cm was recommended for a modular arrangement of independent refrigeration cycle units in parallel in order to scale-up the load requirement.

Small-scale milk cooling system based on ice-storage to shift continuous available electrical load to satisfy instantaneous heat demand was also analyzed. The result showed that the rate of cooling was faster during the early hours of recirculation while it takes a longer time to get a smaller temperature drop for the milk below 10℃. Besides this, longer recirculation time negatively affects the effectiveness of a heat exchange process as observed from the experiment. The milk to energy relation indicates that milk volume could be varied from 94 L to 1135 L by varying final temperature requirement from 4℃ to 10℃. Hence, it was possible to infer from the experimental result that an ice packing factor of 0.52 in a 100 L volume ice-storage with a chilled water recirculation rate of 600 Lh^{-1} would be an appropriate design parameter for a 100 Ld^{-1} capacity milk cooling system.

In the experiment with heat simulated room, the maximum air temperature drop across an FCU of 22.5℃ was obtained for a chilled water recirculation rate (WRR) of 5.4 $L.min^{-1}$ and lower FCU load. By increasing the airflow across an FCU to the maximum (120 $L.h^{-1}$) and decreasing the WRR by half to 2.7 $L.min^{-1}$, the air temperature gradient was changed to 15℃. The effect of WRR on the ice discharge rate was significant at higher FCU load, whereas at lower FCU load, water recirculation rate only affects the air temperature gradient. Moreover, the complete melting of a 25kg ice in the range of 2.33 h to 2.67 h implies that the ice storage system with multiple modular units would be suitable for a 2 - 3 h pick load supplement application.

Chapter 5
General Conclusions and Future Work

5.1 General conclusion

The dominance of smallholder farms (large population, small quantities), lack of access to modern energy, and low levels of technology are among challenges to address in improving the cold value chain in developing countries. The agricultural engineering institute of Hohenheim University in Germany implemented a commercial DC-freezer as smart ice-maker for on-farm milk cooling technology that implements PV as the electrical energy source. However, further investigation was needed on the improvement of ice production technique and minimum attainable milk temperature of the system. So that developing an ice-storage system with a flow controlled cooling loop is a key factor to make the ice-based cooling technology more diverse and competitive. Two possible solutions have been proposed in this thesis to improve the technique of ice-based cooling technology using solar PV as the electrical energy source.

The first solution was on ice production technique which aims at the development of a general-purpose ice-storage system by using evaporators in water-bath configuration. The use of roll-bond plate evaporators directly in water-bath reduces the thermal resistance between the refrigerant and the water by avoiding the air space as used in a conventional freezer. Using ice-on-surface approach would also improve the thermodynamic cycle performance by increasing the evaporating temperature of the refrigerant during the water-ice phase change process. The proposed approach also provides an opportunity to scale-up the ice production capacity by connecting modular units in parallel to satisfy the demand-driven cooling load. The second solution proposed was the introduction of a hydraulic circuit between the ice-storage and the product to be cooled. This mechanism has the advantage of controlling the product temperature as required as well as suitable for the diversified application.

The following conclusions can be taken from this research work:

- During the refrigeration system design process, a suitable combination of refrigerant charge and capillary tube dimensions should be selected for the condition that maximizes the system performance and avoids the suction line temperature drop. The refrigerant overcharge could lead to frost formation at the suction side of the compressor by creating a lower suction line temperature.
- For a variable speed compressor, an optimum refrigerant charge at higher rpm could be an overcharged condition for operation at lower rpm, but the system would operate in stable condition without condensation at the suction line.
- For the ice storage system considered, COP increases as compressor speed decreases regardless of ambient temperature. This implies that optimizing the operating point of variable speed drive refrigeration cycle unit at its maximum speed would result in energy-efficient operation at lower speeds.
- The optimum operating point is an important design parameter in the refrigeration system. The COP drop of 3.4% observed for operational point change from 25 ℃ to 35 ℃ at 3500 rpm suggests that best operating point for the ice storage system developed was at maximum compressor speed and ambient temperatures between 25 ℃ and 35℃.
- Through the experimental campaign, it was observed that operation at a lower energy input gives a better performance, whereas an increase in energy input improves the useful energy output besides a corresponding decrease in system performance. This implies that choice has to be made between the best efficiency point and best operating point based on the available power input and required cooling capacity.
    - The experimental system developed in this research achieved a COP value in the range of 1.5 to 2.63.
    - The range of COP obtained here has improved over the reported smart ice maker COP range of 1.1 to 1.6.
- The refrigerant evaporating temperature could remain above -5℃ for a continuous daily operation regardless of varying compressor power input and surrounding ambient temperature. However, if the ice formation process continuous without melting daily, the evaporating temperature could go up to -10℃ within 48 h of continuous operation. Besides this; changing the compressor speed affected the uniformity of the temperature distribution

on the evaporator surface, which may be due to related changes in refrigerant flow rates, and a pressure drop inside the tubes.

- A comparative increase in mass ice output with increased compressor energy input implies that when using a solar PV system as a source of power for an ice-storage storage system developed, the amount of solar radiation at a given location is a more influencing factor on cooling capacity than ambient temperatures.
- Scalability of the ice storage system can be achieved by parallel operation of multiple refrigeration cycle units (modules). In such a process, the roll-bond plate evaporators should be arranged sequentially inside the water-bath, and the minimum recommended spacing would be in the range of 12.5 cm.
- The cold side phase change boundary temperature showed a faster temperature drop with time at the early stages of the ice formation process when compared with a later stage. This implies that the ice-layer development at a point was faster at an early stage with a slower growth rate at a later stage. However, this slower rate of ice-layer development at a later stage does not necessarily indicate a decrease in the rate of ice mass due to thermal resistance increase. An increase in the perimeter of an elliptic ice-layer profile could compensate the radial ice-layer decreasing effect.
- Moreover, it can be inferred from the range of system performance values achieved that ice accumulation on evaporator surface would be a suitable option to store energy from solar for small scale cooling applications.
- Varying the chilled water recirculation rate and the ice-storage energy density had an impact on milk cooling rate and final attainable milk temperatures. Lower recirculation rate introduces significant time lag on milk cooling rate, which is not recommended from the bacterial growth control point of view. Hence, a packing factor of 0.52 and above in a 100 L capacity ice-storage at a chilled water recirculation rate of 600 Lh^{-1} would be a better design option for the milk cooling system in the range of 100 L d^{-1} capacities.
- The required milk temperature is an important factor to decide on the volume of milk to cool besides the quality aspect since milk cooling to lower temperature requires more energy input. At the optimum operating condition, the ice storage system with two modular units could cool 94 L of milk per day to 4℃. However, the milk volume could increase to 135 L and 189 L if the milk temperatures required are 10 ℃ and 15 ℃, respectively.

  - Milk volume per energy input of 38, 27, and 19 L.(kWh)$^{-1}$ were achieved while cooling milk from 35℃ to 15, 10, and 4 ℃ respectively.
  - The respective theoretical values were 40, 30, and 23 L.(kWh)$^{-1}$ for the same setup.
- For the small-scale milk cooling system developed, the heat exchange at a lower temperature gives a smaller temperature gradient which is in the range of 1℃ drop in 1 h. The maximum milk temperature drop observed was during an early stage of cooling, which has a positive impact on prohibiting bacterial growth in milk.
- Regarding the milk preservation performance, the average milk-temperature increase observed after one-day storage without chilled water recirculation was in the range of 1.5-3℃. Hence, the system developed could also serve for milk preservation.
- In the ice melting performance test with a fan-coil-unit and a heat simulated room, a relatively faster ice discharge rate was obtained at a lower storage temperature and increased water recirculation rate. This implies that bulk convection could be a dominant mode of heat transfer for ice on the surface external melting process.
- Increased airflow across an FCU and a decreased chilled water recirculation rate causes a high water temperature difference across an FCU which will consequently have an effect of increasing the ice-storage water temperature. Such a condition would add a cool down load on ice-formation stage. Besides this, air volume variation can result in relatively higher room temperature gradient over recirculating water volume variation. Hence, a variable volume fan with a fixed speed pump would be better control parameters to implement.
- Finally, the developed cooling system using the ice-storage was demonstrated to be scalable, multifunctional and adaptable for local production using key components from specialized companies. In addition to this, the proposed ice production technique also achieved a higher system COP and increased daily mass of ice production compared with smart ice maker using a conventional approach.

5.2 Future work

The start-up company solar cooling engineering-UG (http://solar-cooling-engineering.com/) in Germany has introduced the key components of the small scale ice storage system developed in this research to the market since early 2019. Having this as a major success on application and

commercialization of the research findings, suggestions and recommendations for further research directions are listed below:

- The presented ice-storage system needs further investigation when using several refrigeration cycle units connected in parallel to increase the capacity. The effect of reduction in exposed surface area for heat loss against an increase of daily ice production per cooling unit needs to be investigated.
- The roll-bond plate evaporator in water-bath configuration was used for the ice-storage system. The large mass accumulated on the surface on a daily basis may cause a component failure in the long run. Hence, fatigue load and thermal stress analysis on the evaporator surface should be performed.
- A control strategy for multiple compressor operation to optimize available solar energy with time is an important research aspect to scale up and diversify the application of the ice-storage system developed.
- The milk cooling system was developed with a recirculation pump between the ice-storage and milk cooler. Control of milk temperature and water recirculation rate are important parameters to implement the system. Therefore, an automated control system for both ice formation and discharge process is an essential aspect to consider.
- The cooling system studied is multifunctional and modular, which is suitable for various small scale applications. Cold rooms and milk cooling are proposed functionalities analyzed by the experimental work. Development of a simulation model that includes the solar field, ice formation process, multiple end-user applications and control strategies will help to identify further system improvement strategies.
- Design and optimization of the refrigeration cycle unit by using different refrigerants like R134a and R290 to compare with performance and efficiency with R600a used in this research
- Investigate availability and techno-economic feasibility of local insulation materials in remote areas to implement the result obtained from this research in developing countries. Characterization and thermo-physical property evaluation is an important aspect to consider.
- Evaluate the battery-free configuration and compare with systems of different battery capacity.

- Carry out field performance testing of solar PV integrated ice-storage system. Potential application in tropical areas and partnering with African countries is recommended.
- Investigate the hybrid electrical energy sources as an alternative to solar PV to diversify application range to air conditioning pick load supplement.

References

[1] International Institute of Refrigeration, "5 th IIR Informatory Note on Refrigeration and Food," pp. 4–7, 2007.

[2] International Institute of Refrigeration, "5th Informatory Note on Refrigeration and Food," *Iifiir*, pp. 9–11, 2009.

[3] Food and Agriculture Organization of the United Nations, "Global Food losses and Food Waste," 2011.

[4] Food and Agriculture Organization of the United Nations, "How Access to Energy can Influence Food Losses: A brief overview," 2016.

[5] S. B. Murmu and H. N. Mishra, "Post-harvest shelf-life of banana and guava : Mechanisms of common degradation problems and emerging counteracting strategies," *Innov. Food Sci. Emerg. Technol.*, vol. 49, no. July, pp. 20–30, 2018.

[6] B. B. Gardas, R. D. Raut, and B. Narkhede, "Modeling causal factors of post-harvesting losses in vegetable and fruit supply chain : An Indian perspective," *Renew. Sustain. Energy Rev.*, vol. 80, no. August, pp. 1355–1371, 2017.

[7] International Institute of Refrigeration, "38th Note on Refrigeration Technologies: The Role of Refrigeration in the Global Economy," *IIR*, p. 12 pp, 2019.

[8] R. Muhumuza, A. Zacharopoulos, J. D. Mondol, M. Smyth, and A. Pugsley, "Energy consumption levels and technical approaches for supporting development of alternative energy technologies for rural sectors of developing countries," *Renew. Sustain. Energy Rev.*, vol. 97, no. November 2017, pp. 90–102, 2018.

[9] E. J. Ivan Katic, Per Henrik Pedersen, "Standalone Cool/Freeze Cluster Driven by Solar Photovoltaic Energy," 2010.

[10] Simply Solar Technology Consulting Group, "Solar Milk Cooling." [Online]. Available: https://www.simply-solar.de/index.php/projects/7-projects/42-batteryless-milk-cooling. [Accessed: 10-May-2020].

[11] J. K. Jensen, C. Busk, C. Cording, P. H. Pedersen, and W. B. Markussen, "Extending the autonomy time of an icelined solar powered vaccine cooler," *Refrig. Sci. Technol.*, vol. 2019-Augus, pp. 3460–3467, 2019.

[12] K. V. Dinesh Chawla, Anil Jat, Rahul Garjola, Subham Srivastava, Kunwar Kaushal, "A

Review on the Refrigeration System Powered By Photvoltaic (PV) Energy," *IIOABJ*, vol. 10, pp. 22–26, 2019.

[13] A. A. M. El-Bahloul, A. H. H. Ali, and S. Ookawara, "Performance and Sizing of Solar Driven dc Motor Vapor Compression Refrigerator with Thermal Storage in Hot Arid Remote Areas," *Energy Procedia*, vol. 70, pp. 634–643, 2015.

[14] F. Agyenim, N. Hewitt, P. Eames, and M. Smyth, "A review of materials, heat transfer and phase change problem formulation for latent heat thermal energy storage systems (LHTESS)," *Renew. Sustain. Energy Rev.*, vol. 14, no. 2, pp. 615–628, 2010.

[15] A. López-Navarro *et al.*, "Experimental investigation of the temperatures and performance of a commercial ice-storage tank," *Int. J. Refrig.*, vol. 36, no. 4, pp. 1310–1318, 2013.

[16] M. Hoseini, M. Heidari, A. Ataei, and J. Choi, "Modeling and optimization of R-717 and R-134a ice thermal energy storage air conditioning systems using NSGA-II and MOPSO algorithms," *Appl. Therm. Eng.*, vol. 96, pp. 217–227, 2016.

[17] Z. Kang, R. Wang, X. Zhou, and G. Feng, "Research Status of Ice-storage Air-conditioning System," *Procedia Eng.*, vol. 205, pp. 1741–1747, 2017.

[18] D. MacPhee and I. Dincer, "Performance assessment of some ice TES systems," *Int. J. Therm. Sci.*, vol. 48, no. 12, pp. 2288–2299, 2009.

[19] M. A. Ezan, A. Erek, and I. Dincer, "Energy and exergy analyses of an ice-on-coil thermal energy storage system," *Energy*, vol. 36, no. 11, pp. 6375–6386, 2011.

[20] E. Oró, A. de Gracia, A. Castell, M. M. Farid, and L. F. Cabeza, "Review on phase change materials (PCMs) for cold thermal energy storage applications," *Appl. Energy*, vol. 99, no. Supplement C, pp. 513–533, 2012.

[21] M. Bilgili, "Hourly simulation and performance of solar electric-vapor compression refrigeration system," *Sol. Energy*, vol. 85, no. 11, pp. 2720–2731, 2011.

[22] P. J. Axaopoulos and M. P. Theodoridis, "Design and experimental performance of a PV Ice-maker without battery," *Sol. Energy*, vol. 83, no. 8, pp. 1360–1369, 2009.

[23] C. Yu, X. Zhang, X. Chen, C. Zhang, and Y. Chen, "Melting performance enhancement of a latent heat storage unit using gradient fins," *Int. J. Heat Mass Transf.*, vol. 150, p. 119330, 2020.

[24] Y. Huang, Q. Sun, F. Yao, and C. Zhang, "Performance optimization of a finned shell-and-tube ice storage unit," *Appl. Therm. Eng.*, vol. 167, no. November 2019, p. 114788,

2020.

[25] S. Wang *et al.*, "Discharging performance of a forced-circulation ice thermal storage system for a permanent refuge chamber in an underground mine," *Appl. Therm. Eng.*, vol. 110, pp. 703–709, 2017.

[26] S. Wu, G. Fang, and Z. Chen, "Discharging characteristics modeling of cool thermal energy storage system with coil pipes using n-tetradecane as phase change material," *Appl. Therm. Eng.*, vol. 37, pp. 336–343, 2012.

[27] A. K. Raul, P. Bhavsar, and S. K. Saha, "Experimental study on discharging performance of vertical multitube shell and tube latent heat thermal energy storage," *J. Energy Storage*, vol. 20, no. June, pp. 279–288, 2018.

[28] E. Osterman, K. Hagel, C. Rathgeber, V. Butala, and U. Stritih, "Parametrical analysis of latent heat and cold storage for heating and cooling of rooms," *Appl. Therm. Eng.*, vol. 84, pp. 138–149, 2015.

[29] Z. Khan, "An experimental investigation of discharge / solidi fication cycle of paraffin in novel shell and tube with longitudinal fins based latent heat storage system," *Energy Convers. Manag.*, vol. 154, no. November, pp. 157–167, 2017.

[30] A. H. Mosaffa, F. Talati, H. B. Tabrizi, and M. A. Rosen, "Analytical modeling of PCM solidification in a shell and tube finned thermal storage for air conditioning systems," *Energy Build.*, vol. 49, pp. 356–361, 2012.

[31] X. Zhao, B. Dong, W. Li, and B. Dou, "An improved enthalpy-based lattice Boltzmann model for heat and mass transfer of the freezing process," *Appl. Therm. Eng.*, vol. 111, pp. 1477–1486, 2017.

[32] S. Liu, L. Hao, Z. Rao, and X. Zhang, "Experimental study on crystallization process and prediction for the latent heat of ice slurry generation based sodium chloride solution," *Appl. Energy*, vol. 185, pp. 1948–1953, 2017.

[33] X. Yun *et al.*, "Ice formation in the subcooled brine environment," *Int. J. Heat Mass Transf.*, vol. 95, pp. 198–205, 2016.

[34] J. Sun, J. Gong, and G. Li, "A lattice Boltzmann model for solidification of water droplet on cold flat plate," *Int. J. Refrig.*, vol. 59, pp. 53–64, 2015.

[35] D. Clausse, E. Y. Wardhono, and J. L. Lanoiselle, "Formation and determination of the amount of ice formed in water dispersed in various materials," *Colloids Surfaces A*

Physicochem. Eng. Asp., vol. 460, pp. 519–526, 2014.

[36] G. Chaudhary and R. Li, "Freezing of water droplets on solid surfaces: An experimental and numerical study," *Exp. Therm. Fluid Sci.*, vol. 57, pp. 86–93, 2014.

[37] Z. Jin, X. Cheng, and Z. Yang, "Experimental investigation of the successive freezing processes of water droplets on an ice surface," *Int. J. Heat Mass Transf.*, vol. 107, pp. 906–915, 2017.

[38] N. Li, Y. Tuo, Y. Deng, J. Li, R. Liang, and R. An, "Heat transfer at ice-water interface under conditions of low flow velocities," *J. Hydrodyn. Ser. B*, vol. 28, no. 4, pp. 603–609, 2016.

[39] R. I. ElGhnam, R. A. Abdelaziz, M. H. Sakr, and H. E. Abdelrhman, "An experimental study of freezing and melting of water inside spherical capsules used in thermal energy storage systems," *Ain Shams Eng. J.*, vol. 3, no. 1, pp. 33–48, 2012.

[40] Y. Zhang, K. Du, J. P. He, L. Yang, and Y. J. Li, "Impact factors analysis of the enthalpy method and the effective heat capacity method on the transient nonlinear heat transfer in phase change materials (pcms)," *Numer. Heat Transf. Part A Appl.*, vol. 65, no. 1, pp. 66–83, 2014.

[41] H. Hu and S. A. Argyropoulos, "Mathematical modelling of solidification and melting: A review," *Model. Simul. Mater. Sci. Eng.*, vol. 4, no. 4, pp. 371–396, 1996.

[42] M. Muhieddine, E. Canot, and R. March, "Various Approaches for Solving Problems in Heat Conduction with Phase Change," *Int. J. Finite Vol.*, p. 19, 2009.

[43] Z. Lipnicki, D. Sasse, and B. Weigand, "Experimental and analytical investigation of the solidification around cooled cylinders subjected to free convection," *Int. J. Heat Mass Transf.*, vol. 78, pp. 321–329, 2014.

[44] Food and Agriculture Organization of the United Nations, "Benefits and Potential Risks of the Lactoperoxidase system of Raw Milk Preservation," Rome, 2005.

[45] V. Torres-Toledo, A. Hack, F. Mrabet, A. Salvatierra-Rojas, and J. Müller, "On-farm milk cooling solution based on insulated cans with integrated ice compartment," *Int. J. Refrig.*, vol. 90, pp. 22–31, 2018.

[46] G. Bylund, *Dairy processing handbook*. Sweden: Tetra Pak Processing Systems, 1995.

[47] K. Ndyabawe and W. S. Kisaalita, "Diffusion of an evaporative cooler innovation among smallholder dairy farmers of Western Uganda," *Technol. Soc.*, vol. 38, pp. 1–10, 2014.

[48] M. Edwin and S. J. Sekhar, "Thermal performance of milk chilling units in remote villages working with the combination of biomass , biogas and solar energies," *Energy*, vol. 91, pp. 842–851, 2015.

[49] R. G. Charles, M. L. Davies, P. Douglas, and I. L. Hallin, "5 - Sustainable Solar Energy Collection and Storage for Rural Sub-Saharan Africa," in *A Comprehensive Guide to Solar Energy Systems*, T. M. Letcher and V. M. Fthenakis, Eds. Academic Press, 2018, pp. 81–107.

[50] R. Foster *et al.*, "Direct drive photovoltaic milk chilling: Two years of field experience in Kenya," *ISES Sol. World Congr. 2017 - IEA SHC Int. Conf. Sol. Heat. Cool. Build. Ind. 2017, Proc.*, no. June, pp. 932–941, 2017.

[51] K. S. Khan, W. Amjad, A. Munir, and O. Hensel, "Improved solar milk chilling system using variable refrigerant flow technology (VRF)," *Sol. Energy*, vol. 197, no. January, pp. 317–325, 2020.

[52] S. Kalogirou, *Solar energy engineering : processes and systems*. Elsevier Inc., 2009.

[53] International Energy Agency, "Tracking Clean Energy Progress," 2019.

[54] F. S. Fabiani Appavou, Adam Brown, Bärbel Epp, Duncan Gibb, Bozhil Kondev, Angus McCrone, Hannah E. Murdock, Evan Musolino, Lea Ranalder, Janet L. Sawin, Kristin Seyboth, Jonathan Skeen, *REN21 - 2019 Global Status Report*. 2019.

[55] International Energy Agency, "World Energy Outlook 2019," 2019.

[56] V. Torres-Toledo, K. Meissner, A. Coronas, and J. Müller, "Performance characterisation of a small milk cooling system with ice storage for PV applications," *Int. J. Refrig.*, vol. 60, pp. 81–91, 2015.

[57] V. Torres-Toledo, K. Meissner, P. Täschner, S. Martınez-Ballester, and J. Müller, "Design and performance of a small-scale solar ice-maker based on a DC-freezer and an adaptive control unit," *Sol. Energy*, vol. 139, pp. 433–443, 2016.

[58] V. Tores-Toledo, "Design , simulation and validation of small-scale solar milk cooling systems," University of Hohenheim, 2018. Doctoral Thesis

[59] D. Poelhekke, "Biogas-Powered Milk Chiller for Small-Scale Dairy Farmers in Eastern Africa," 2016.

[60] M. A. B. Yunus A. Cengel, *Thermodynamics, An Engineering Approach*, Fifth Edit. New York.: McGraw-Hill, 2006.

[61] SECOP, “Secop Heat Load Calculation Software.” .

[62] SECOP, “BD35K Direct Current Compressor for Solar Applications R600a, 10-45V DC.”

[63] TM Technischer Gerätebau GmbH, “TM products catalogue: Cool boxes and accessories.” Neu-Ulm, Germany, p. 21.

[64] A. Pisano, S. Martínez-Ballester, J. M. Corberán, and A. W. Mauro, “Optimal design of a light commercial freezer through the analysis of the combined effects of capillary tube diameter and refrigerant charge on the performance,” *Int. J. Refrig.*, vol. 52, pp. 1–10, 2015.

[65] American Society of Heating Refrigerating and Air-Conditioning Engineers, *ASHRAE Handbook : Refrigeration*, SI Edition. Atlanta: ASHRAE, 2014.

[66] G. L. Lei, W. Dong, M. Zheng, Z. Q. Guo, and Y. Z. Liu, “Numerical investigation on heat transfer and melting process of ice with different porosities,” *Int. J. Heat Mass Transf.*, vol. 107, pp. 934–944, 2017.